

Florida International University
FIU Digital Commons

FIU Electronic Theses and Dissertations

University Graduate School

7-29-2014

Synthesis of a PbTx-2 photoaffinity and fluorescent probe and an alternative synthetic route to photoaffinity probes

Ryan T. Cassell

doctoral student, rcass004@fiu.edu

Follow this and additional works at: <http://digitalcommons.fiu.edu/etd>

 Part of the [Organic Chemistry Commons](#)

Recommended Citation

Cassell, Ryan T., "Synthesis of a PbTx-2 photoaffinity and fluorescent probe and an alternative synthetic route to photoaffinity probes" (2014). *FIU Electronic Theses and Dissertations*. Paper 1612.
<http://digitalcommons.fiu.edu/etd/1612>

This work is brought to you for free and open access by the University Graduate School at FIU Digital Commons. It has been accepted for inclusion in FIU Electronic Theses and Dissertations by an authorized administrator of FIU Digital Commons. For more information, please contact dcc@fiu.edu.

FLORIDA INTERNATIONAL UNIVERSITY

Miami, Florida

SYNTHESIS OF PBTX-2 PHOTOAFFINITY AND FLUORESCENT PROBES AND
AN ALTERNATIVE SYNTHETIC ROUTE TO PHOTOAFFINITY LABELS

A dissertation submitted in partial fulfillment of

the requirements for the degree of

DOCTOR OF PHILOSOPHY

in

CHEMISTRY

by

Ryan T. Cassell

2014

To: Interim Dean Michael R. Heithaus
College of Arts and Sciences

This dissertation, written by Ryan T. Cassell, and entitled Synthesis of PbTx-2 Photoaffinity and Fluorescent Probes and an Alternative Synthetic Route to Photoaffinity Labels, having been approved in respect to style and intellectual content, is referred to you for judgment.

We have read this dissertation and recommend that it be approved.

Kevin O'Shea

Watson Lees

Xiaotang Wang

John Makemson

Kathleen Rein, Major Professor

Date of Defense: July 29, 2014

The dissertation of Ryan T. Cassell is approved.

Interim Dean Michael R. Heithaus
College of Arts and Sciences

Dean Lakshmi N. Reddi
University Graduate School

Florida International University, 2014

© Copyright 2014 by Ryan T. Cassell

All rights reserved.

DEDICATION

This dissertation is dedicated to my family. To my Mother and Grandparents Art and Ann Rebman for their endless love, support, and encouragement to pursue my desires. To my Father whose passing away was very difficult for me but unintentionally provided the drive and ambition for me to pursue college. To Allen Hamann who helped in raising me by providing the love, guidance, and structure that was critical in my youth.

Last but not least, to all my friends that believed in me along the way.

ACKNOWLEDGMENTS

I am very grateful to the numerous people who have been supportive during the journey and pursuit of this Ph.D. degree. I would like to express gratitude to my advisor Dr. Kathleen Rein for her support and guidance during the entire degree process. Lord knows the frustration she felt and the patience that was needed as my advisor. I would also like to thank my other committee members for their suggestions and guidance throughout the years.

I would like to thank all of my labmates and people who I had the pleasure of working with throughout the years at FIU. A special thanks to Wentian Wang and Li Liu for their friendship and motivational words of wisdom and encouragement when frustration and insanity was getting the best of me. I would like to acknowledge all the other graduate students at FIU that shared their time, knowledge, and friendship with me. I hope to continue nourishing these relationships that were built during my time as a graduate student.

ABSTRACT OF THE DISSERTATION
SYNTHESIS OF PbTx-2 PHOTOAFFINITY AND FLUORESCENT PROBES AND AN
ALTERNATIVE SYNTHETIC ROUTE TO PHOTOAFFINITY LABELS

by

Ryan T. Cassell

Florida International University, 2014

Miami, Florida

Professor Kathleen Rein, Major Professor

A natural phenomenon characterized by dense aggregations of unicellular photosynthetic marine organisms has been termed colloquially as red tides because of the vivid discoloration of the water. The dinoflagellate *Karenia brevis* is the cause of the Florida red tide bloom.

K. brevis produces the brevetoxins, a potent suite of neurotoxins responsible for substantial amounts of marine mammal and fish mortalities. When consumed by humans, the toxin causes Neurotoxic Shellfish Poisoning (NSP). The native function of brevetoxin within the organism has remained mysterious since its discovery. There is a need to identify factors which contribute to and regulate toxin production within *K. brevis*. These toxins are produced and retained within the cell implicating a significant cellular role for their presence.

Localization of brevetoxin and identification of a native receptor may provide insight into its native role as well as other polyether ladder type toxins such as the ciguatoxins, maitotoxins, and yessotoxins. In higher organisms these polyether ladder

molecules bind to transmembrane proteins with high affinity. We anticipated the native brevetoxin receptor would also be a transmembrane protein.

Photoaffinity labeling has become increasingly popular for identifying ligand receptors. By attaching ligands to these photophors, one is able to activate the molecule after the ligand binds to its receptor to obtain a permanent linkage between the two. Subsequent purification provides the protein with the ligand directly attached.

A molecule that is capable of fluorescence is a fluorophore, which upon excitation is capable of re-emitting light. Fluorescent labeling uses fluorophores by attaching them covalently to biologically active compounds.

The synthesis of a brevetoxin photoaffinity probe and its application in identifying a native brevetoxin receptor will be described. The preparation of a fluorescent derivative of brevetoxin will be described and its use in localizing the toxin to an organelle within *K. brevis*. In addition, the general utility of a synthesized photoaffinity label with other toxins having similar functionality will be described.

An alternative synthetic approach to a general photoaffinity label will also be discussed whose goal was to accelerate the preparation and improve the overall synthetic yields of a multifunctional label.

TABLE OF CONTENTS

CHAPTER	PAGE
1. Introduction.....	1
1.1 Florida red tides and harmful algae blooms (HAB).....	1
1.2 Economic impacts of HAB's	2
1.3 Neurotoxic shellfish poisoning	2
1.4 Brevetoxins and other polyether ladder toxins	3
1.5 Voltage-gated Na ⁺ channels and brevetoxin activity	6
1.6 Brevenal	7
1.7 Osmoregulation and dinoflagellates	8
1.8 Native function of brevetoxins and osmoregulation possibilities.....	9
1.9 Vertical migration behavior	12
1.10 Nutrient limitation in growth rate and brevetoxin production	12
1.11 Photoaffinity labeling.....	13
1.12 Brevetoxin photoaffinity labeling.....	16
1.13 Diazirines	17
1.14 General synthesis of diazirines	20
1.15 Biotin.....	21
1.16 Click chemistry	22
1.17 Cyanobacteria and their toxins.....	24
1.18 Fluorescent dyes.....	26
1.19 Objectives	28
2. Experimental design of PbTx-2 photoaffinity probes.....	29
2.1 Photoaffinity labels 1 and 2 and placement on PbTx-2	29
2.2 Synthetic schemes for attachment of 1 and 2 to the A, H, and K rings	30
2.3 Attachment of azide-biotin to the alkyne of PbTx-2 photoaffinity label derivatives	32
2.4 Synthesis of photoaffinity label 1 and 2	33
2.5 Undesirable formation of a geminal dibromo diazirine.....	36
2.6 Synthesis of 6-bromohexyne from 5-hexyn-1-ol.....	37
3. Synthesis of photoaffinity probes and a fluorescent probe.....	38
3.1 Brevetoxin photoaffinity probes	38
3.2 Synthesis of K-ring photoaffinity label.....	39
3.3 Thiol-Michael addition at the α , β -unsaturated aldehyde side chain of PbTx-2	40
3.4 Model studies on the thiol-Michael addition to PbTx-2	41
3.5 Thiol incorporation into photoprobe 1 and the attachment of biotin through a click reaction.....	43
3.6 Reduction of 24 with DTT and subsequent Michael addition to the K-ring side chain of PbTx-2	47
3.7 Attachment of Alexa fluor 488 to PbTx-2	49

3.8 Incubation of <i>Karenia brevis</i> cells with PbTx-2 fluorescent probe and PbTx-2 photoaffinity probe	52
3.9 Synthesis of alternative thiol azide linker	53
3.10 Synthesis of microcystin LR photoaffinity probes	54
3.11 Synthesis of nodularin photoaffinity probes	55
4. Alternative synthetic route to photoaffinity labels.....	56
4.1 Proposed alternate synthesis to desired photoaffinity labels	56
4.2 Alternate synthesis of photoaffinity labels	58
4.3 Exploring photoaffinity label synthesis with compound 42	60
5. Experimental procedures	63
References.....	87
VITA.....	96

LIST OF FIGURES

FIGURE	PAGE
1. Brevetoxin backbones A & B and the major derivatives.....	4
2. Structure of the brevetoxin antagonist brevenal	8
3. Nitrene formation from photolysis of azides and the thermolysis of isocyanates	14
4. Binding of brevetoxin to its receptor and labeling after photolysis.....	15
5. Tritiated phenyl azide PbTx-3 photoaffinity probe used by Trainer and Catteral	16
6. Representative alkyl and aryl diazirines	17
7. Generation of single and triplet carbenes from a diazine	18
8. Photolysis of diazirines to yield carbenes and covalent insertion into C-H bonds.....	19
9. General synthesis of a diazine ring from a carbonyl	20
10. Synthesis of 3-aryl-3-(trifluoromethyl)diazirine from bromobenzene	21
11. Biotin and modified biotin with a terminal alkyne	22
12. General dipolar cycloadditions between 1, 3 dipoles and a dipolarophile	22
13. Huisgen cycloadditions between an azide and terminal alkyne click reaction.....	23
14. Structure of microcystin LR.....	25
15. Structure of nodularin	26
16. Fluorescein, Rhodamine, and Alexa fluor 488	27
17. Photoaffinity labels 1 & 2 and brevetoxin PbTx-2 & PbTx-3	29
18. Proposed photoaffinity probes attached to brevetoxin rinds A, K, and H	30
19. General thiol-yne reaction.....	44
20. ¹ NMR comparisons of PbTx-2, 23, and PbTx-2 photoaffinity probe 25	49

21. HPLC trace of PbTx-2 fluorescent probe vs. Alexa fluor 488	51
22. <i>Karenia brevis</i> cells incubated with PbTx-2 fluorescent probe and Alexa fluor 488..	52
23. Proposed alternative synthesis to photoaffinity labels.....	57

LIST OF SCHEMES

SCHEME	PAGE
1. PbTx-2 A-ring reduction and attachment to photoaffinity label 2.....	30
2. PbTx-2 K-ring side chain attachment to photoaffinity label 1	31
3. PbTx-2 H-ring diol formation and attachment to photoaffinity label 1	32
4. Example of biotin attachment to the PbTx-2 A-ring derivative	33
5. Synthesis of photoaffinity label 1	34
6. Oxidation of photoaffinity label 1 to 2 using Jones reagent	36
7. Formation of geminal dibromo diazirine and its reverse reaction	37
8. Synthesis of 6-bromohexyne from 5-hexyn-1-ol.....	37
9. Proposed products of thiol-Michael addition between cysteamine and PbTx-2.....	41
10. Thiol-Michael click reaction between 19 and PbTx-2.....	43
11. Unsuccessful synthesis of thiol 1 due to competing thiol-yne reaction.....	44
12. Synthesis of diazirine 21 with azide linker.....	45
13. Attempted reductive amination between 21 and cysteamine.....	46
14. Synthesis of biotin linked diazirine 23.....	46
15. Reductive amination of 23 with cysteamine to yield disulfide 24.....	47
16. Disulfide reduction of 24 with DTT and Michael addition to PbTx-2	48
17. Synthesis of thiol linkers 26 and 27	50
18. Synthesis of PbTx-2 fluorescent probe using Alexa fluor 488 and 28	50
19. Synthesis of alternative thiol azide linker.....	53
20. Synthesis of microcystin LR photoaffinity probe.....	54
21. Synthesis of nodularin photoaffinity probe.....	55

22. Alternate synthesis to photoaffinity label with multiple functionality	59
23. Diazirine synthesis using unprotected oxime 42	61

1. Introduction

1.1 Florida red tides and harmful algae blooms (HAB)

A natural phenomenon characterized by dense aggregations of single cell or several species of unicellular photosynthetic marine organisms has been termed colloquially as red tides because of the vivid discoloration of the water which can appear red, green, and brown or darkened in general. A more accepted term scientifically for this algae proliferation is a harmful algae bloom (HAB) with coastal waters around the world experiencing a general increase in the frequency and types of these blooms. Phenomena such as global climate change including changing ocean temperatures, currents and general weather patterns, agricultural practices increasing nutrient loading and dispersal and even over fishing have all been implicated in the rise of HAB occurrences around the globe¹.

The dinoflagellate *Karenia brevis* is the cause of the Florida red tide bloom. *K. brevis* produces the brevetoxins, a potent suite of neurotoxins responsible for substantial amounts of marine mammal, seabird, and fish mortalities and which when ingested by humans cause Neurotoxic Shellfish Poisoning (NSP). Blooms of this toxic dinoflagellate can occur annually and occur mainly in late summer and early fall. Dispersal of the blooms usually takes place within a few weeks though in 2006 a bloom persisted for over a year. Increases in the duration and frequency of these blooms have been recently noted².

There have been documented cases of these blooms in the Gulf of Mexico since the 1800's: prior to any significant agricultural or industrial development of the region

and resulting pollution. Even records of Spanish explorer's record conditions similar to red tide in the mid 1500's describing mass fish die offs which they described as "bad air". Blooms have also occurred throughout the Gulf loop from the eastern coast of Mexico to the coast of North Carolina where one of the largest reported NSP outbreaks occurred³.

1.2 Economic impacts of HAB's

Economic impacts of HAB's are notable as a result of the closures of beaches and commercial fisheries affecting the tourism and seafood industries. Florida alone was reported to lose upwards of 20 million dollars a year in tourism revenue because of the closure and subsequent cleanup of beaches⁴. Extensive monitoring programs of shellfish beds are conducted by the Florida Department of Agriculture and Consumer Services with bed closures when *K. brevis* levels exceed 5000 cells/l near or in harvesting areas⁵. These closures severely affect commercial fishing industries whose livelihoods are directly dependent on their harvest.

1.3 Neurotoxic shellfish poisoning

Massive fish kills and marine mammal poisoning are observed as well as significant environmental effects and human health issues ascribed to the toxins produced during *K. brevis* blooms. Toxin vectors such as fish (despite these toxins also killing them) and seagrass contribute to the marine mammal poisoning observed in dolphins and manatees where, despite low water *K. brevis* concentrations, post mortem tissue samples of the affected animals showed very high levels of the toxin⁶.

As filter feeders, molluscan shellfish such as oysters, clams, mussels and coquinas also accumulate and retain toxins produced by microscopic algae even after blooms have dissipated. When brevetoxins are consumed by humans, mainly from eating contaminated seafood, it causes Neurotoxic Shellfish Poisoning (NSP)⁷. Neurotoxic shellfish poisoning is characterized by acute gastrointestinal problems involving vomiting and nausea and a variety of neurological symptoms which normally last multiple days. Neurological symptoms can include slurred speech, dizziness, ataxia, and even partial paralysis. Hospitalization often occurs although no deaths have been reported.

Aerosolization of the toxins and distribution by coastal winds results in respiratory illnesses. The *K. brevis* organism is fragile and lacks a rigid cellulose wall. The organism can be lysed by coastal waves which releases the toxin into the seawater⁸. People with asthma are particularly susceptible to the effects of these aerosolized toxins with exposure resulting in respiratory distress. Marine mammals have also been shown to be effected by aerosolized toxins and in one such event, the lung pathology of 149 manatees which had died off the southwest coast of Florida showed that brevetoxins had been inhaled⁹.

1.4 Brevetoxins and other polyether ladder toxins

Brevetoxins are cyclic polyethers with molecular weights around 900 Da. These polyethers are unique and complex containing 10 *trans*-fused rings designated A through J in brevetoxin A type and 11 *trans*-fused rings designated A through K in brevetoxin B type. Each toxin contains a lactone functional group in the A-ring with the distal ring containing a side chain. Brevetoxins are made of one of the two structural skeletal

backbones termed A and B, which are fairly linear but possess a flexible region in the middle of the molecule (Figure 1). The A-type brevetoxins are the most potent though they are the least abundant. The names and designations of these toxins have changed over time.

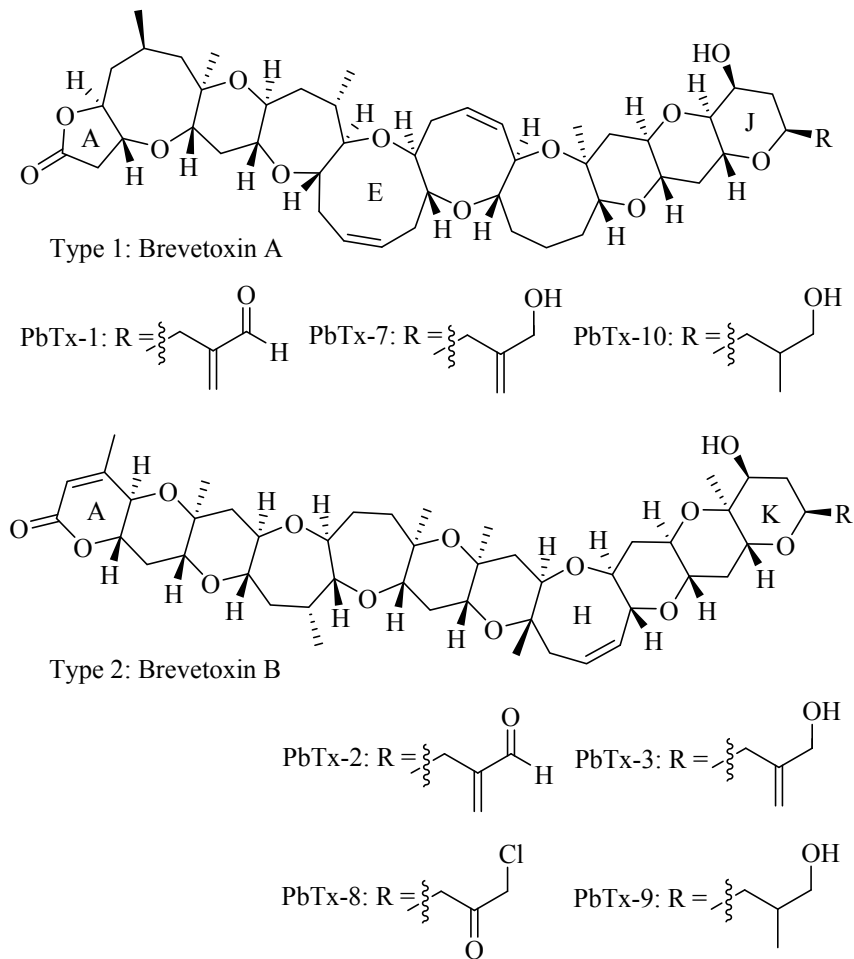


Figure 1: Brevetoxin backbones A & B and the major derivatives

The major brevetoxins produced are PbTx-2 followed by PbTx-3 and PbTx-1 although more than 10 brevetoxins have been isolated during blooms as well as metabolic

derivatives from shellfish and other organisms¹⁰. In vivo, these toxins are active in concentrations from the nanomolar to picomolar range.

Other polyether ladder toxins are known such as the ciguatoxins, maitotoxins, and yessotoxins. Ciguatoxins are produced by the dinoflagellate *Gambierdiscus toxicus* and cause ciguatera fish poisoning. The ciguatoxins are sodium channel activators which have been shown to bind to the same binding site on the sodium channel as the brevetoxins¹¹. Maitotoxins are also produced by *Gambierdiscus toxicus* and are potent neurotoxins containing 32 *trans*-fused rings and an aliphatic chain on both the head and tail of the molecule. In terms of secondary metabolites, it is the largest and most toxic natural product known¹². These toxins have been shown to activate voltage-gated calcium channels though neither the molecular mechanism of action on the channel nor the exact site on the receptor is known¹³. The yessotoxins are produced by the dinoflagellates *Protoceratium reticulatum*, *Lingulodinium polyedrum*, and *Gonyaulax spinifera* and were originally classified as a toxin responsible for diarrhetic shellfish poisoning (DSP) though now they are separated from the DSP group because they don't cause diarrhea nor inhibit protein phosphatases¹⁴. The yessotoxins contain 11 *trans*-fused polyether rings, two sulfate groups on one end and an unsaturated side chain on the opposite end. The number of yessotoxin analogs reported range from 30 to over 90¹⁵. These analogues arise as a result of hydroxylations, carboxylations, desulfations, methylations, oxidations, changes in the length of the carbon side chain and even an absence of the A-ring.

1.5 Voltage-gated Na⁺ channels and brevetoxin activity

Voltage-gated Na⁺ channels are crucial and indispensable for many of life's processes, with at least 10 distinct channels having been identified in mammalian cells¹⁶. These channels are electrical signal generators controlling muscle contraction, hormone secretion, and information processing within the brain. They are comprised of a large heteromeric α -subunit (~260 kDa) and one or two auxiliary β -subunits (~33-36 kDa) which constitute a functional voltage-gated Na⁺ channel with the signaling characteristics of neurons depending on the differences in protein subtypes, their concentration and the spatial distribution of the proteins throughout the membrane. The α -subunits of all sodium channels are structurally similar. An α -subunit is made up of four domains each containing six transmembrane segments designated as S1-S6 and a pore loop.

Several neurotoxins target these voltage-gated channels and disrupt their normal functions. Receptor binding by various toxins has been shown to occur at six different receptor locations with very high specificity. The channel pore is physically blocked and ion conductance prevented with large polypeptide toxins and hydrophilic low molecular mass toxins such as saxitoxin and tetrodotoxin, which bind to extracellular sites on the membrane. Lipid soluble toxins such as brevetoxin and ciguatoxin and the alkaloid toxins bind to intramembranous receptor sites, altering voltage-dependent gating by changing the membrane potential¹⁷.

Brevetoxins are lipid soluble, which is why they pass so readily through cell membranes such as the blood brain barrier and buccal mucosa¹⁸. These toxins are readily absorbed and are metabolized in the liver after distribution throughout the body with metabolites being detected in urine within hours after ingestion. Binding to the voltage

gated sodium channels (VGSC) by these cyclic polyether toxins occurs with high affinity at receptor site 5 on the α -subunit. The VGSC sites 2, 4, 6, and 7 are allosterically linked with site 5. Upon binding, they open the voltage-sensitive sodium ion channels allowing uncontrolled sodium influx into the cell¹⁹ causing nerve membrane depolarization. Interaction between the receptor site 5 and each toxin is thought to be mainly hydrophobic with the A-ring lactone appearing to act as a hydrogen-bond acceptor which stabilizes and enhances the ligand binding affinity. The binding is believed to occur via a “head down” orientation with respect to the channel²⁰.

The effects of brevetoxin have been studied on mice, rats, and frogs with depolarization of membranes and ultimately respiratory failure being the cause of death²¹. A number of derivatives of the natural brevetoxins have been synthesized and their activity studied. Some of the derivatives include, but are not limited, to K-ring side chain benzoyl and naphthoyl derivatives²², a reduction of the A-ring lactone, and a reduction of the H-ring alkene.

1.6 Brevenal

Brevenal was first discovered in 2004 and is a natural inhibitor of brevetoxin. It was isolated and characterized from *K. brevis* Wilson clone cultures. Brevenal is a non-toxic short chain molecule containing 5 cyclic polyether rings with two conjugated side chains, one a dienal side chain, the other a dienyl side chain. Brevenal is a brevetoxin antagonist that binds to sodium channel receptors. It was originally thought to compete against brevetoxin at the active site on the VGSC with the competitive inhibition of brevenal being shown in binding assays²³. Recently though, the terminal aldehyde of

brevenal was reduced using tritiated sodium borohydride to produce the radioactive analog [^3H]-brevenol. The [^3H]-brevenol was shown to bind to a site that is distinct from the other known sites on the channel, including site 5 (the brevetoxin binding site)²⁴. These two binding sites may be allosterically linked.

The use of brevenal as a potential therapeutic against cystic fibrosis, a debilitating lung disorder²⁵ is being investigated. Brevenal alleviates wheezing, clears mucus from the lungs and eases shortness of breath whereas the brevetoxins constrict bronchioles and cause breathing difficulties. Total synthesis of brevenal has been carried out by more than one research group^{26,27,28}. Studies have suggested that in lower salinity waters, more PbTx-1 is produced in relation to PbTx-2 and brevenal production is decreased²⁹. It is not known why *K. brevis* produces both the suite of toxins and simultaneously their antagonist.

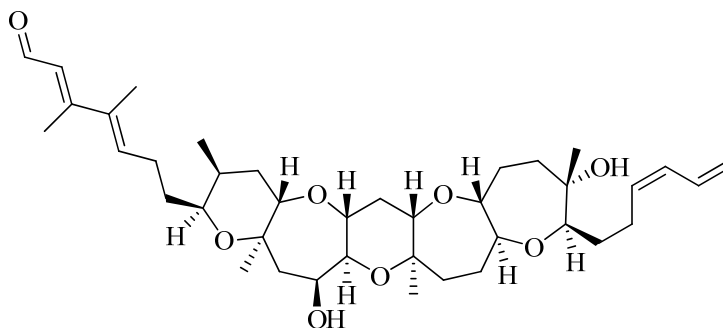


Figure 2: Structure of brevetoxin antagonist brevenal

1.7 Osmoregulation and dinoflagellates

If voltage gated channels are found in dinoflagellates, perhaps a possible role between toxin production during osmotic stress and ion transport could be made. The

mechanism for readjustment of ions for osmoregulation and after osmotic stress by regulating ions through the use of ion pumps has been implied.

Key factors that control phytoplankton growth, abundance and dispersal include changes in salinity, nutrients, light and temperature. As a consequence of being a local parameter, significant variations in salinity occur along coastal waters making a dynamic environment for phytoplankton to contend with. The regulation of the homeostasis of an organism's fluids and osmotic pressure is termed osmoregulation with correct concentrations being very important. Cells must constantly adjust their salt concentration to maintain optimal metabolic functioning. Osmoregulation processes have evolved to allow for the quick regulation of internal water and salt concentrations to various aquatic environments³⁰.

It is unknown whether osmoregulatory control in dinoflagellates proceeds through ion transport or an osmolytic type mechanism. Sodium and calcium voltage-activated channels were recently reported in the marine diatom *Odontella sinensis*³¹. The marine phytoplankton *Coccolithus pelagicus* was also shown using the patch-clamp technique to contain voltage activated channels. A possibility is that brevetoxin may interact with Na⁺ channels allowing for ion adjustment and facilitating osmoregulation.

1.8 Native function of brevetoxins and osmoregulation possibilities

There is a need to identify factors which contribute to and regulate toxin production within *K. brevis* because of the negative impact on coastal regions and human health. These toxins are produced and retained within the cell implicating a significant cellular role for their presence. Brevetoxin production can vary amongst the *Karenia*

species and individual organisms. Variability of toxin content within cell cultures have been seen to fluctuate from 1-69 pg/cell with the reason for such drastic fluctuations unknown²⁹.

The native functions of the brevetoxins within *K. brevis* organism have remained enigmatic since their discovery. It has been reported that toxin levels respond to environmental conditions with an increase in toxin production shown to be triggered from changes in salinity and osmotic stress implicating a role of osmoregulation within the organism. A greater than ten-fold increase in brevetoxin was observed for three *K. brevis* clonal cultures under hypoosmotic stress. The cultured Wilson clone showed a 16-fold increase in toxin production while a different strain (TXB4) showed a 20-fold increase and the SP3 clone a 14-fold increase³². The Wilson clone also showed a toxin increase when exposed to hyperosmotic stress. Little change was observed in the suite of brevetoxin derivatives produced or culture growth rates in comparison to acclimated cultures following the hypoosmotic stress. Brevenal production, though not as pronounced was also increased after hypoosmotic and hyperosmotic stress. These findings led to the hypothesis that brevetoxin facilitates osmoregulation through interactions with sodium channels allowing for intracellular ion adjustment.

The previous study involving *K. brevis* under osmotic stress was challenged by a three laboratory study which found no evidence that low salinity stress in eight *K. brevis* strains showed increased brevetoxin production³³. These research teams were unable to reproduce the results by Errera and Campbell failing to support the hypothesis that osmotic stress or a sudden decrease in salinity triggers the production of brevetoxins. The research teams argued that because the brevetoxins bind to sodium channels and induce

an inward flux of ions as a result of the channels being held open, an increase in cellular toxin content would only allow a greater flow of sodium ions into the cell and would not adjust for the osmotic stress in the correct direction.

Following this, Errera and Campbell challenged the replication protocols which include extraction and analytical methods, *K. brevis* isolates, and culturing conditions differing among the three laboratories attempting to reproduce their observation that toxin levels increase under osmotic stress. Furthermore, Errera and Campbell state that ion movement is directed by the electrical potential induced at the membrane which would cause sodium ions to flow out of the cell while under hypoosmotic stress³⁴. Other functional roles in addition to osmoregulation have not been ruled out and the debate continues between the investigators involved³⁵.

Considerable attention has been focused on understanding mechanisms regulating bloom dynamics and progression such as the vegetative cell cycle and vertical migration behavior which are crucial to surface population development and subsurface cell aggregation. The study of gene regulation and genetic structure are critical to understanding bloom dynamics and the cellular responses that are triggered from the environment.

Some evidence that the brevetoxins serve a defensive role by deterring zooplankton grazing and therefore enhancing survival, has been demonstrated³⁶. Behavioral effects in some copepod species have been observed from sublethal exposure to *K. brevis* cells and brevetoxin. The observed effects include starvation and physiological incapacitation though mortality was generally low. Heightened photosensitivity, and suppressed speed and swimming activity were among the sublethal

effects observed which are consistent with starvation. All species tested showed an accumulation of brevetoxins though some species exhibited severe sensory effects while others showed very little effects.

1.9 Vertical migration behavior

K. brevis cells are not simply passive particles but undergo diel vertical migration behavior. They maximize carbon fixation by vertically migrating during the day and fall to lower depths at night for dissolved nutrients³⁷. It was also found that following a synchronous cell division that 50% migrated to the surface and that major biochemical constituents differed between the mid-water populations and those that had migrated. This suggest an unequal share of the parental resources being delivered to the daughter cells with these nutrient poor cells being more phototactic.

1.10 Nutrient limitation in growth rate and brevetoxin production

The carbon nutrient balance hypothesis (CNBH), applied originally to terrestrial plants, describes an increase in toxin production in response to reduced nutrient availability³⁸. This CNBH model was used to study fluctuating toxin content in *K. brevis* cells which has been shown to differ by greater than fourfold but was typically attributed to genotypic variations among strains. Whether the amount of toxin per cell is a result of genetic differences among strains or strictly environmental factors has been a question asked for some time by researchers. Recently these studies showed that brevetoxin levels within *K. brevis* were elevated when blooming under nitrogen and nutrient limitations³⁹.

An increase in brevetoxin production in *K. brevis* was also reported to occur under phosphate limited growth⁴⁰. Brevetoxin content per cell were 2.3-7.3 fold higher in phosphorous limited cells in comparison to phosphorous replete cells. The study also showed an inverse relationship between the amount of cellular carbon associated with brevetoxins and the specific growth rate which is predicted by the carbon nutrient balance hypothesis.

Other dinoflagellates showed increases in cellular toxin content because of nutrient limitation of growth. Both the cyanobacterium *Nodularia spumigena*, which produces the phosphatase inhibitor nodularin, and the dinoflagellate *Karlodinium veneficum*, which produces karlotoxin, showed increased intracellular levels of their toxins during times of phosphorous limitation^{41, 42}.

1.11 Photoaffinity Labeling

The identification of ligand-binding regions is an important field in biochemistry and enzymology and the use of photoaffinity labeling has become increasingly popular. Photoaffinity labeling is recognized as a powerful methodology for detailed structural analysis of binding domains⁴³. Photoaffinity labeling takes advantage of highly reactive intermediates such as nitrenes or carbenes, which are created from functional groups capable of being activated photochemically⁴⁴. Ideally a photolabel should be chemically inert but become reactive when exposed to UV light. Photoaffinity probes include photolabile functional groups such as azides and isocyanates which form nitrenes upon photolysis and diazirines which form carbenes upon photolysis.

Nitrenes were first proposed by German chemist Ferdinand Tiemann in 1891 in attempt to explain the Lossen rearrangement⁴⁵. Nitrenes can be formed from azides and isocyanates following photolysis or thermolysis.

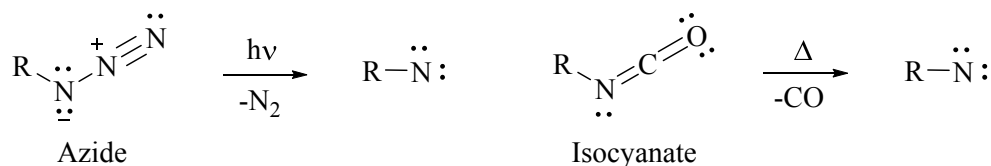


Figure 3: Nitrene formation from photolysis of azides and thermolysis of isocyanates

Azides will react and expel nitrogen gas to form the nitrene whereas isocyanates will react in a similar manner to expel carbon monoxide and form a nitrene. The reactive nitrene intermediate once formed can exist as a singlet or triplet, with the triplet being lower in energy and the more stable of the two. Arylnitrenes have been extensively used for photoaffinity labeling with their precursors being the corresponding aryl azide⁴⁶.

Diazirines which yield carbenes upon photolysis, have become very popular as photoprobes. They have been claimed to be the most valuable photoprobe mainly because of the short irradiation time needed and overall stability and specificity. Aryl azides are less useful as photoprobes because of potential nucleophilic side reactions and the long irradiation times required for nitrene formation⁴⁷. Once formed, carbenes will insert themselves irreversibly into C-H or C-C bonds. By attaching ligands to these photophors, one is able to activate the molecule (generate the carbene by exposure to UV light) after the ligand binds to the ligand-binding region to form a covalent linkage between the two. Subsequent purification will provide the protein or receptor with the ligand directly attached. Figure 4 shows how the interaction of a receptor with ligand covalently linked

to a photoaffinity label. After activation, the entire receptor-ligand-photoaffinity label complex will be linked.

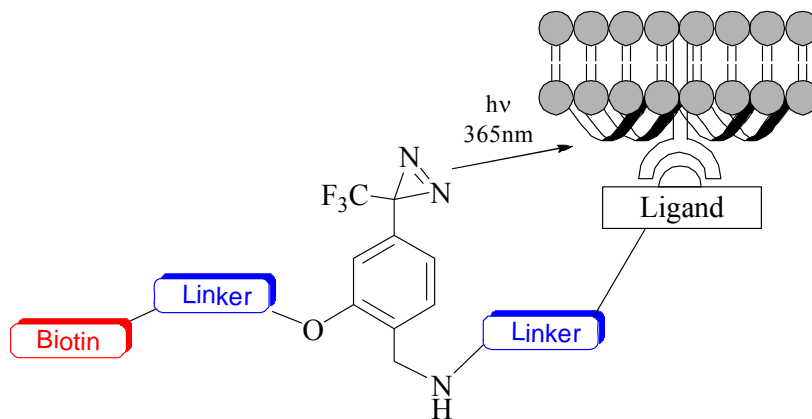


Figure 4: Binding of brevetoxin to its receptor and labeling after photolysis

A recent example of photoaffinity labeling was reported by a Japanese group using maitotoxin. The group attached a photolabel to maitotoxin, a polycyclic ether toxin responsible for ciguatera fish poisoning. The photolabel attached to maitotoxin was biotinylated and used in labeling experiments with blood cells in an attempt to identify binding proteins⁴⁸. The maitotoxin photoaffinity probe was incubated with erythrocytes and subjected to irradiation at 365 nm and binding proteins were isolated using streptavidin beads. The SDS-PAGE showed labeled bands from binding with erythrocyte membrane proteins, though the identification of these proteins was not successfully completed. An interesting note was that the binding of one of the proteins to the maitotoxin photoprobe around 23 kDa was competitively inhibited in the presence of PbTx-2.

1.12 Brevetoxin photoaffinity label

A brevetoxin photoaffinity probe was synthesized previously and used to identify brevetoxin receptors in rat brain synaptosomes⁴⁹ and to localize the binding site with the receptor. A tritiated *p*-azidobenzoate derivative of the brevetoxin side chain was synthesized by treating PbTx-2 with sodium borotritiide to reduce the aldehyde side chain yielding tritiated PbTx-3 which was then coupled with *p*-azidobenzoic acid using carbonyldiimidazole to yield a brevetoxin photoaffinity probe. The probe was then used to identify two distinct and specific sites where the toxin binds in the rat brain synaptosomes. The *p*-azidobenzoate probe formed a nitrene upon activation and specifically labeled a membrane bound protein of 260 kDa. Analysis was performed using SDS-PAGE showing this protein contained the most bound radioactivity. Various neurotoxins were used in competitive binding studies to show that the brevetoxins bind to a unique receptor site. The neurotoxin ciguatoxin was shown to displace brevetoxin from this binding site indicating that it also activates the same site¹¹.

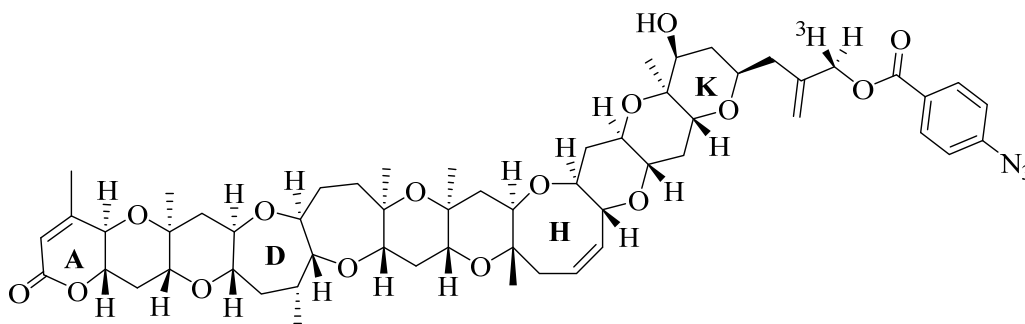


Figure 5: Tritiated phenyl azide PbTx-3 photoaffinity probe used by Trainer and Catterall⁴⁹

1.13 Diazirines

Diazirines are two nitrogen one carbon three-membered rings with a nitrogen-nitrogen double bond⁵⁰ (Figure 6). These functional groups were first synthesized and discovered in 1960⁵¹. Their structure was confirmed in 1962⁵² but it was not until the 1970's that their application as photoprobes were described. Two types of diazirines have been defined, namely aliphatic or aromatic diazirines. Aromatic diazirines have an aromatic ring attached to the carbon of the three-membered diazirine ring whereas the aliphatic diazirine has an aliphatic substituent on the ring carbon. The simplest diazirine synthesized is unsubstituted and exists as a gas. Protein folding mechanisms and states have been probed using this simple photoreactive gas^{53,54}. Aliphatic diazirine use is not as prevalent as the aromatic diazirines due to rearrangements resulting from the intermediate carbenes produced during photolysis often moving from the original site of generation.

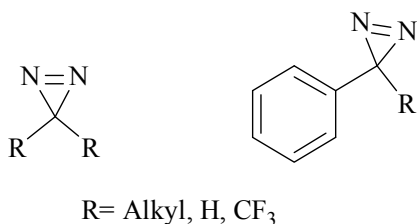


Figure 6: Representative alkyl and aryl diazirines

Diazirines as carbene precursors have steadily gained in popularity and importance since this discovery by Smith and Knowles in 1973⁵⁵. Because of their ability to generate carbenes, they have found widespread use in photoaffinity labeling. Diazirines are activated by long-wave UV light typically within the 330-380 nm range which is very useful as this wavelength range does not damage proteins⁵⁶ and biological

systems as shorter wavelengths do. The molecular environment of the diazirine is the determining factor for UV absorption. The diazirine three-membered ring is unexpectedly stable thermally. It is stable to a wide variety of chemical reagents including oxidizing and reducing reagents and a broad range of pH. Upon photolysis, a diazirine will generate predominately a carbene. The short irradiation times needed and overall stability and specificity make its use as a photoprobe popular. The lifetimes of carbenes are in the nanosecond range⁵⁷ and once formed will react and insert themselves into C-H or C-C bonds.

As with nitrenes, the generation of two types of carbenes occurs during the photolysis of diazirines, namely singlet carbenes and triplet carbenes each existing in a sp^2 hybridized system. Singlet carbenes contain two electrons in the same sp^2 hybrid orbital with antiparallel spins whereas triplet carbenes have two electrons occupying different orbitals with parallel spins; one occupying the sp^2 orbital and the other occupying the p orbital (Figure 7)⁵⁸. In accordance with Hund's rule, the triplet is the more stable ground state of the carbene while the singlet is the reactive excited state of the species. The difference in energy between the two energy states is 8-10 kcal/mol⁵⁹.

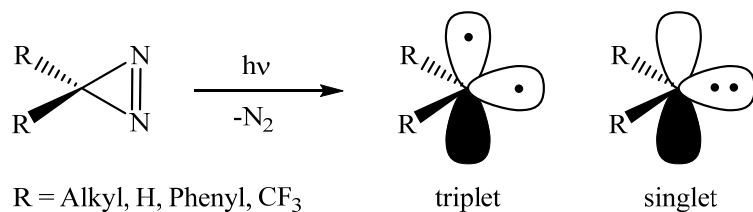


Figure 7: Generation of singlet and triplet carbenes from a diazirine

Various substituents such as aromatics or other groups that donate electron pairs can stabilize the singlet state. The non-bonding pair of electrons are delocalized into an empty *p*-orbital thus reducing their energy.

Once irradiated with UV light, rearrangements in the excited state (RIES) can occur. Diazirines can isomerize to form the linear diazo compound which itself can undergo photolysis to generate the carbene, but can also form carbocations and undergo rearrangements (Figure 8). A useful modification of the aromatic diazirine was developed with the addition of a trifluoromethyl group in 1980⁶⁰. By introducing the trifluoromethyl group, unwanted rearrangements are prevented by stabilizing the carbene intermediate.

The UV-Vis absorption spectra showed that about 65% of 3-trifluoromethyl-3-phenyldiazirine photolysis products are carbenes while the other 35% was converted to the corresponding diazomethane 1-phenyl-2,2,2-trifluoromethyl-3-diazomethane. Photolysis of aliphatic diazirines in general results in a lower yield of carbene compared with aromatic diazirines.

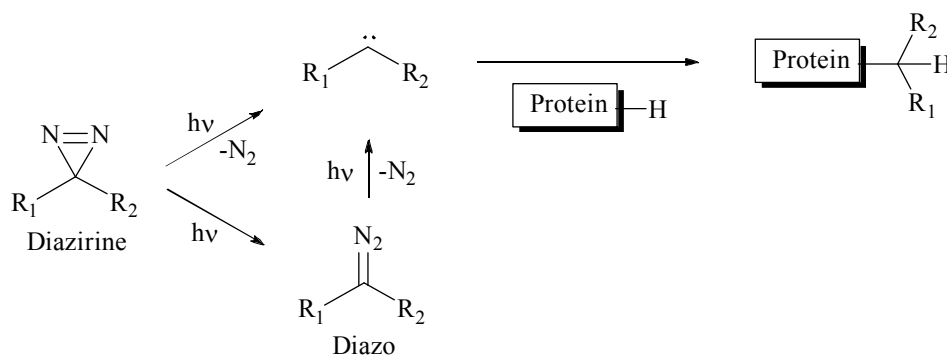


Figure 8: Photolysis of diazirines to yield carbenes and covalent insertion into C-H bonds

1.14 General Synthesis of Diazirines

The diazirine functional group is generated upon oxidation of the corresponding diaziridine. Diaziridines can be formed from ketones or aldehydes. Treating a carbonyl groups with hydroxyl amine followed by a tosylation reaction with tosyl chloride yields the tosylated oxime. Treatment of this tosyl oxime with liquid ammonia under pressure or at -78°C provides the diaziridine ring⁶¹ (Figure 9).

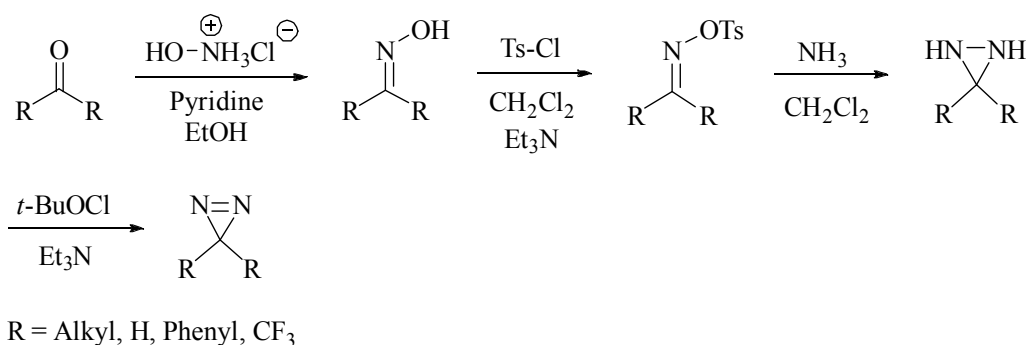


Figure 9: General synthesis of a diazirine ring from a carbonyl

Synthesis of the 3-aryl-3-(trifluoromethyl)diazirine begins with the acylation of bromo-benzene with (trifluoromethyl)piperidine (TFAP) after formation of the Grignard or through a lithium-halogen exchange using *n*-BuLi. This reaction yields (trifluoromethyl)acetophenone which may be converted to the diazirine through the route outlined in Figure 10.

Functionality can be introduced by starting with substituted bromobenzenes or through alternate synthetic methods such as electrophilic aromatic substitution. These functional groups are used to link these photophores to various ligands.

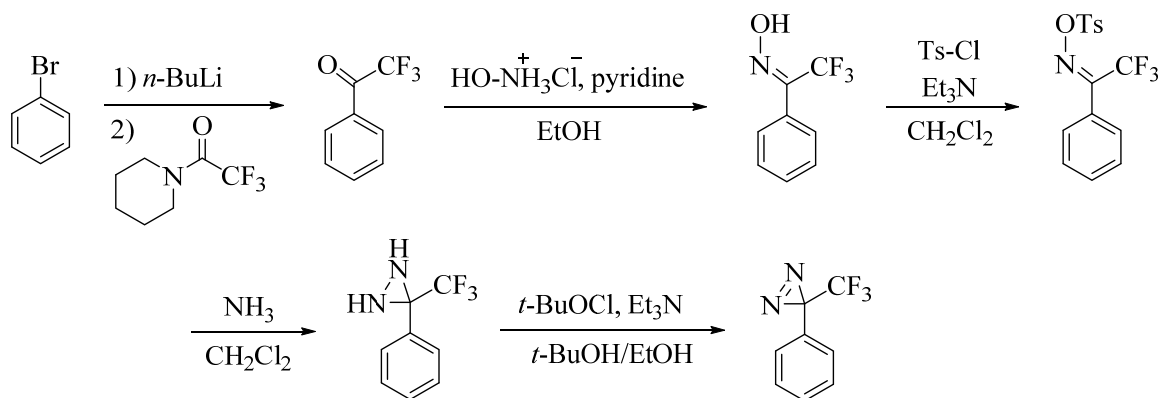


Figure 10: Synthesis of 3-aryl-3-(trifluoromethyl)diazirine from bromobenzene

1.15 Biotin

Biotin is a water soluble B-vitamin necessary for cell growth and it assists in various metabolic reactions including essential roles in carboxylation as a coenzyme⁶². Biotin is used extensively in molecular and cellular assays and is extremely useful for protein purification and detection. Streptavidin is a protein obtained from the bacterium *Streptomyces avidinii*. The protein streptavidin binds with extraordinarily high affinity and specificity to biotin. Exploiting this fact allows biotinylated proteins of interest to be isolated and purified. Immobilizing streptavidin on a solid matrix and subsequent packing onto a column provides a means to selectively isolate proteins that are biotinylated. This type of purification is termed affinity chromatography and takes advantage of these receptor/ligand interactions that are extremely specific. The protein ligand interaction between streptavidin and biotin is one of the strongest non-covalent interactions known⁶³ with the dissociation constant, K_d , between the two on the order of 4×10^{-14} .

Commercial sources of biotin with polyethylene linkers (Figure 11) and various side chain functional groups are available and can be linked to a moiety of interest while

avidin or streptavidin, the latter being more frequently used, is usually coupled to a solid support. Proteins coupled to either biotin or photophors containing a linkage to biotin can be flushed through this solid support and selectively removed from a mixture. Subsequent recovery of the captured protein is then possible.

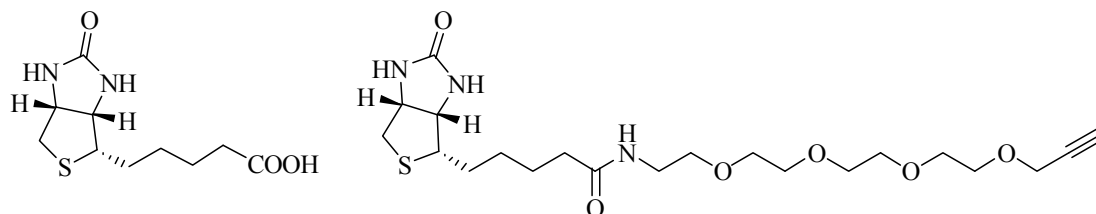


Figure 11: Biotin and modified biotin with a terminal alkyne

1.16 Click Chemistry

1, 3-dipolar cycloadditions are reactions between a 1, 3-dipole and a dipolarophile which provide five-membered rings (Figure 12). These reactions proceed through a concerted pericyclic mechanism. Typical 1,3-dipoles include (amongst a host of others) the azide, nitro, diazo and even imine functional groups and typical dipolarophiles are alkenes and alkynes.

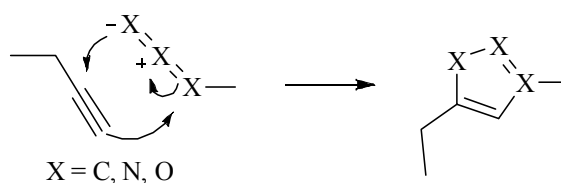


Figure 12: General dipolar cycloaddition between 1, 3-dipoles and a dipolarophile

A 1,3-dipolar cycloaddition reaction between a terminal alkyne and an azide to provide 1,2,3-triazoles (Figure 13) has been termed azide-alkyne Huisgen cycloadditions⁶⁴. The triazole product is effectively chemically inert⁶⁵.

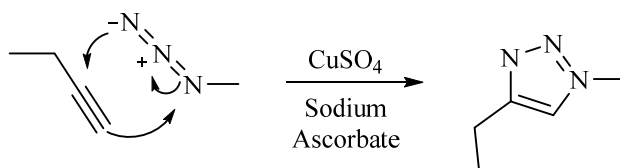


Figure 13: Huisgen cycloaddition between an azide and terminal alkyne “click reaction”

These non-reversible reactions are generally referred to simply as “click” reactions. These click reactions are not sensitive to reaction conditions and may be performed in aqueous or organic solvents. Click reactions typically are conducted in the presence of a copper(I) catalyst. The Cu-alkyne-azide cycloaddition (CuAAC) is the most popular, efficient and wide spread within the category of click chemistry with the term being almost synonymous with the reaction. Before the discovery of these salts as effective catalyst, which was done nearly simultaneously by Medal⁶⁶ and Sharpless⁶⁷, much harsher reaction conditions were needed.

Copper catalysts have the benefit of being inexpensive and easy to handle. They usually involve Cu(II) salts such as sodium sulfate that are reduced *in situ* to provide the Cu(I) species. The use of copper(II) sulfate in the presence of a reducing reagent such as sodium ascorbate usually gives high yields and has grown in popularity to be the most favored. Other catalyst include the halides of copper such as CuBr and CuI but require higher temperatures.

1.17 Cyanobacteria and their toxins

Cyanobacteria are a collective family of single-celled photosynthetic bacteria, previously known as blue-green algae. Cyanobacteria are prolific producers of secondary metabolites. Several genera of cyanobacteria such as *Microcystis*, *Planktothrix*, *Anabaena*, *Aphanizomenon*, *Cylindrospermopsis*, *Lyngbya*, *Nostoc*, and *Oscillatoria* are known to produce a group of toxins known as microcystins.

Blooms of these cyanobacteria occur in freshwater bodies such as lakes, ponds, and slow moving rivers and have contaminated drinking water sources and reservoirs worldwide⁶⁸. *Microcystis aeruginosa* is the species most generally associated with microcystin production though other species abound. There are over 80 variants of the microcystin toxins that have been identified with Microcystin LR (Figure 14) being the most common⁶⁹. They all share a cyclic heptapeptide structure with structural diversity resulting from amino acid substitution⁷⁰ at the variable L-amino acids. The most studied variant has the leucine (L) and arginine (R) amino acids incorporated into structure of the toxin which is how the suffix in the toxin name is derived⁷¹.

Also present in the toxin is the unusual β -amino acid (2*S*,3*S*,8*S*,9*S*)-3-amino-9-methoxy-2,6,8-trimethyl-10-phenyldeca-4,6-dienoic acid (Adda). These hepatotoxins are extremely stable and can persist for years after the algae dies; even boiling water is not enough to destroy them. The environmental factors that prompt production within the cell and the functional role of these toxins have remained mysterious. An intracellular role within the organism has been assumed as toxin production responds to oxidative stress, light, and iron limitation⁷². Fairly recently a group was able to localize microcystin within the cell using immunogold labeling and found specifically within the nucleoplasm and

specially associated with the thylakoid and around polyphosphate bodies⁷³. Theories suggest that the microcystins may play a process in photosynthesis or other light dependent processes within the cell. Light adaptive processes or photoregulatory processes have been suggested as well as a possible role in the structural support for the thylakoids through an association of the microcystins with the membrane. None of these theories though explain the high concentration of microcystins found around the polyphosphate bodies.

The biosynthesis of microcystins has also been shown through other studies to be regulated by light with in an increase in photosynthetically active radiation causing an increase in the toxin production and intracellular content⁷⁴. Once maximum growth rate was reached though, an increase in the light intensity actually caused a decrease in toxin production. An additional study also showed that the transcription of the microcystin synthetase genes *mcyB* and *mcyD*, was increased in response to light. The increased transcription was shown to be initiated at particular threshold intensities and ultimately influenced by the quality of light⁷⁵.

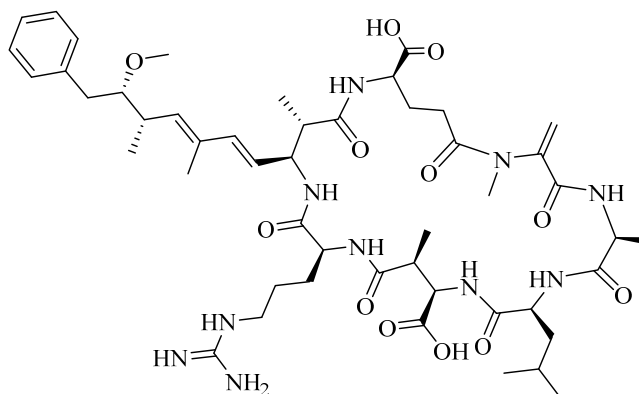


Figure 14: Structure of microcystin LR

Nodularin (Figure 15) is another hepatotoxic compound produced by the cyanobacterium *Nodularia spumigena* which blooms in brackish waters around the world⁷⁶. The potent toxin is a cyclic pentapeptide containing several non-proteinogenic amino acids including the Adda β -amino acid which is seen in the microcystins. The inhibition of protein phosphatases is associated with toxicity with both the microcystins and nodularins affecting hepatocytes in the liver which promotes liver cancer and the destruction of the hepatocytoskeleton⁷⁷. It was shown that a covalent adduct is formed as a result of a nucleophilic addition of the thiol in a cysteine residue of the enzyme at the α , β -unsaturated carbonyl of the toxin though the adduct formed from this Michael addition is not directly responsible for the inhibition of the enzyme but a secondary results of interaction between the two⁷⁸.

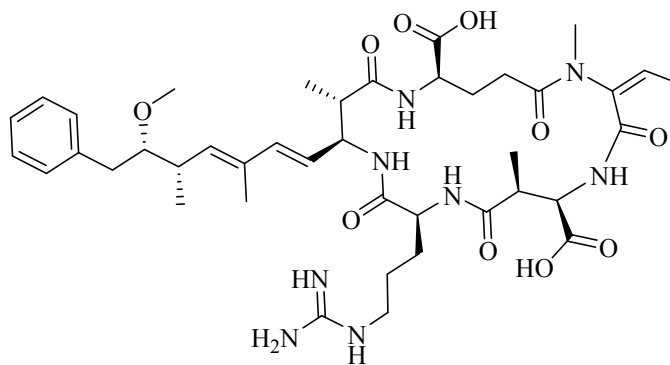


Figure 15: Structure of nodularin

1.18 Fluorescent dyes

The first fluorescent compounds used in biological research were organic dyes like fluorescein and rhodamine (Figure 16). Derivatives of these compounds have been

created to improve in their properties such as photodegradation/photostability, solubility and pH sensitivity.

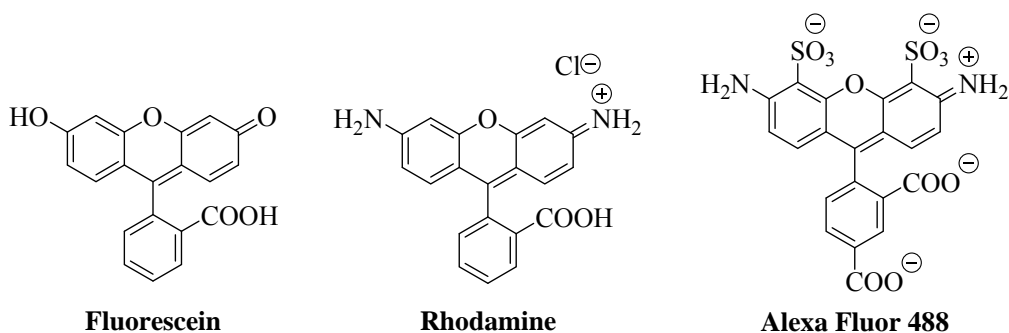


Figure 16: Fluorescein, Rhodamine, and Alexa Fluor 488

A molecule that is capable of fluorescence is a fluorophore. After absorbing radiation, a fluorophore will become excited and then upon relaxing it will re-emit light of a slightly longer wavelength. These types of molecules have been extensively used in the field of microscopy. Typical fluorophores are dyes containing multiple aromatic groups and π bonds. Fluorescent labeling uses fluorophores by attaching them covalently to biologically active compounds.

Alexa fluor 488 alkyne green-fluorescent has nearly identical spectral properties and quantum yield as fluorescein isothiocyanate (FITC). Additionally, the Alexa fluor 488 dye is pH-insensitive in the 4-10 range and more photostable and fluorescent than its spectral analogue. The high degree of sensitivity and selectivity allows the detection of low abundance samples⁷⁹. The number in the Alexa fluor 488 alkyne refers to the approximate excitation maxima of the dye in nm.

1.19 Objectives

Identifying the principal function of brevetoxin within *K. brevis* and determining if there is an endogenous function to the production of brevetoxin is the long term goal of this research. The localization of the toxin to an organelle and the identification of a native receptor would provide insight into its role. The purpose of the work described herein was to synthesize the molecular probes which could be used for localization and identification of a native receptor.

Objectives:

1. To prepare a fluorescent derivative of brevetoxin which may be used to detect the localization of the toxin to an organelle.
2. To prepare a bioorthogonal brevetoxin probe which will covalently link to a brevetoxin receptor and facilitate purification of the receptor.
3. Explore the general utility of synthesized photoaffinity label with other toxins having similar functionality

Localization of brevetoxin and identification of a native receptor may provide insight into the native role of brevetoxins and other polyether ladder type toxins. In higher organisms these polyether ladder type molecules bind to transmembrane proteins with affinities in the nanomolar to picomolar range⁸⁰. At the outset of this work, we anticipated that the native brevetoxin receptor will also be a transmembrane protein, possibly a sodium channel.

2. Experimental design of PbTx-2 photoaffinity probes

2.1. Photoaffinity labels 1 and 2 and placement on PbTx-2

Compound **1** and **2** (Figure 17) were the initially planned photoaffinity labels which were to be linked to the A, H, and K rings of PbTx-2 (Figure 18).

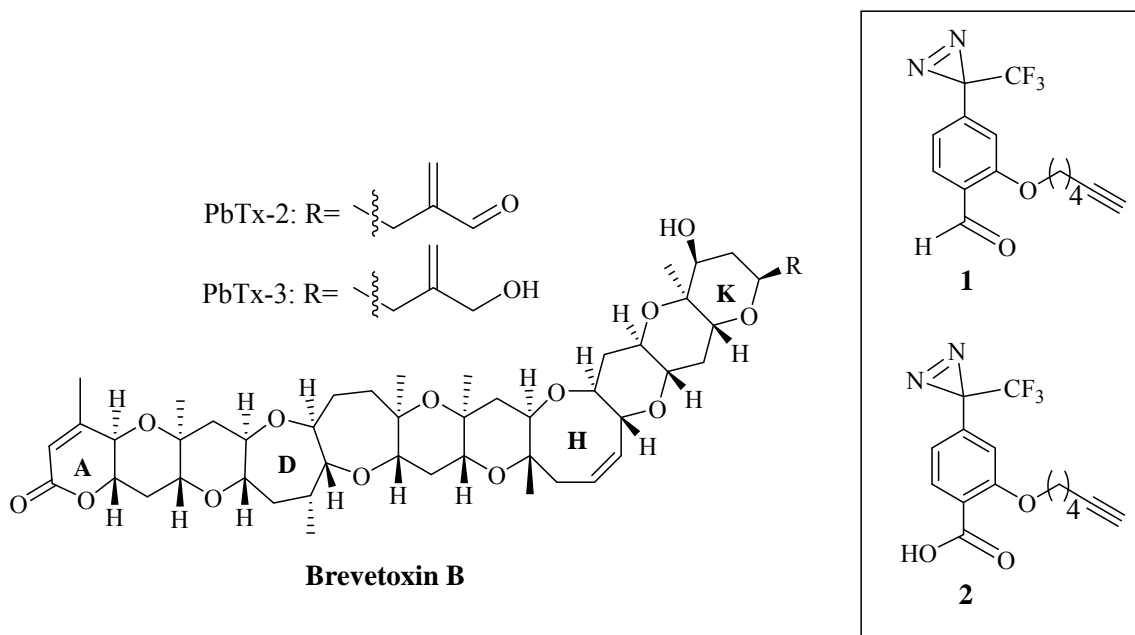


Figure 17: Photoaffinity labels 1 & 2 and brevetoxin PbTx-2 & PbTx-3

The alkyne moiety on each derivative would then be used in a click reaction with an azide modified biotin. Figure 18 shows the three probes attached at the A-ring lactone, H-ring double bond, and the K-ring side-chain of brevetoxin with the terminal alkyne ready for the biotin attachment.

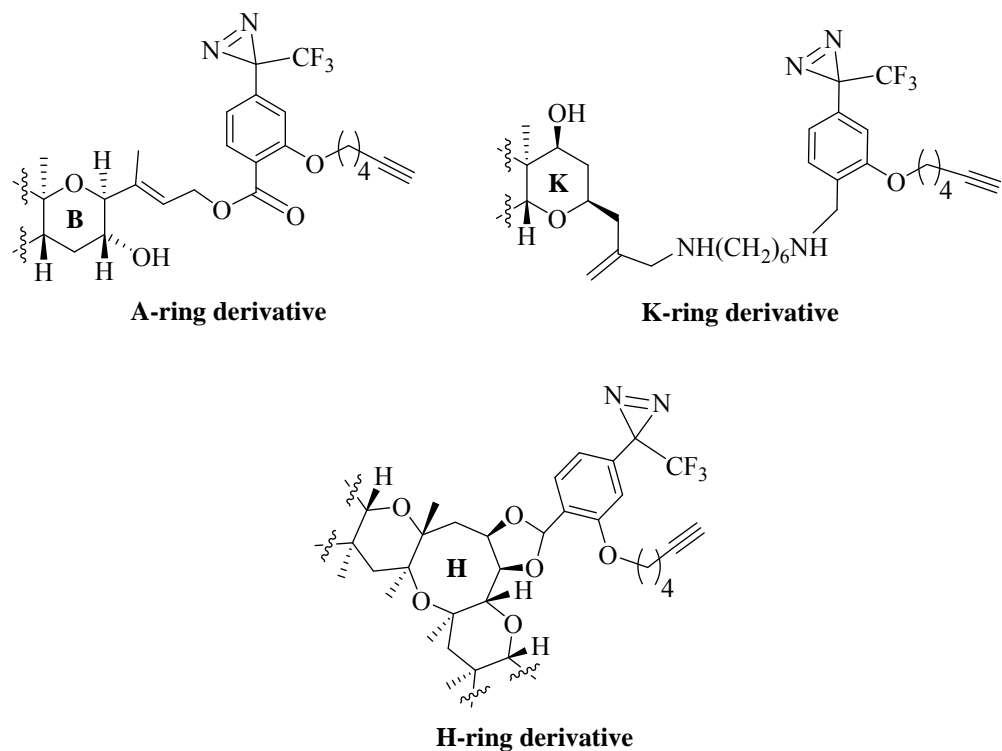
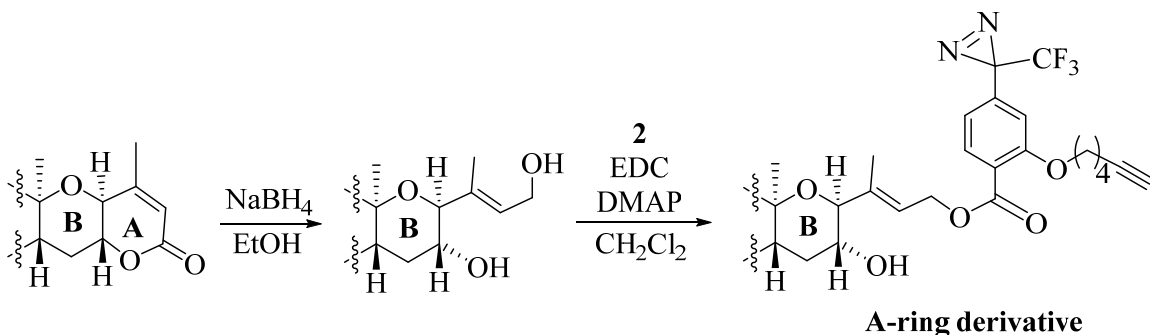


Figure 18: Proposed photoaffinity probes attached to brevetoxin rings A, K, and H

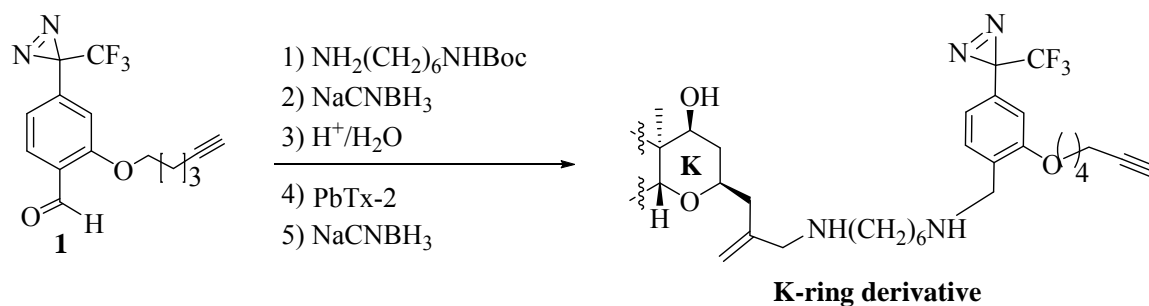
2.2 Synthetic schemes for attachment of **1** and **2** to the A, H, and K rings

The synthesis of **1** and **2** must be completed before coupling to PbTx-2. The coupling reactions would take advantage of functional groups present in PbTx-2 as well as other derivatives of PbTx-2 that have been previously synthesized.



Scheme 1: PbTx-2 A-ring reduction and attachment to photoaffinity label 2

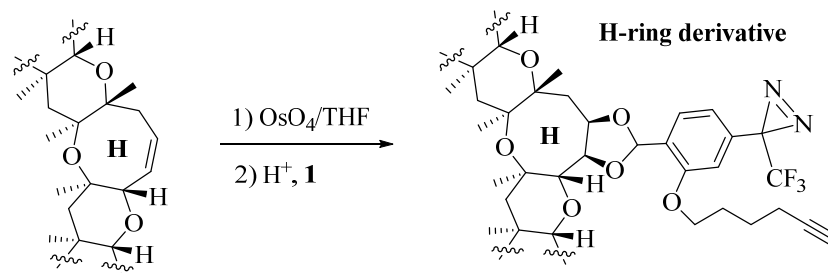
The reductive cleavage of the A-ring lactone to the diol has been reported using sodium borohydride in ethanol⁸¹. The primary alcohol of this derivative can then be coupled to **2** using a suitable coupling reagent such as EDC. A protection of the aldehyde side chain must occur before the A-ring reduction is performed. Reductions using NaBH₄ will reduce the aldehyde and the A-ring which would provide two primary alcohols capable of coupling with **2**.



Scheme 2: PbTx-2 K-ring side chain attachment to photoaffinity label 1

The K-ring derivative can be made by first performing a reductive amination between **1** and Boc protected hexamethylenediamine, followed by a deprotection and another reductive amination to the aldehyde of PbTx-2 to afford the derivative (Scheme 2). Hexamethylenediamine could also be coupled to PbTx-2 first, followed by the deprotection and subsequent coupling to **1**.

The H-ring derivative can be made by converting the H-ring to the diol using OsO₄ following previously reported methods⁸² followed by conversion to the acetonide using the aldehyde of **1** (Scheme 3). Epoxidation of the H-ring using DMDO in acetone has been performed⁸² but if hydrolysis occurred, it would provide the *trans*-diol which would render acetonide formation impossible.

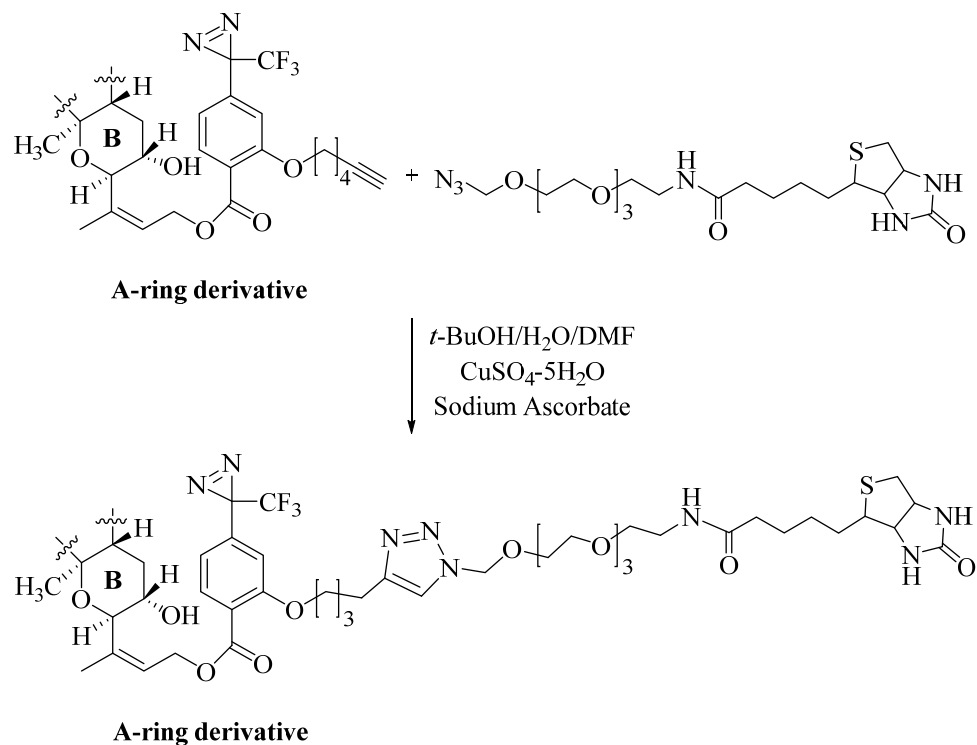


Scheme 3: PbTx-2 H-ring diol formation and attachment to photoaffinity label 1

The biotin moiety can be attached after the photoaffinity label has been coupled to PbTx-2 or before the coupling. The order of attachment can be varied with the only necessity being that the final PbTx-2 photoaffinity probes contain the diazirine photolabel covalently linked to biotin.

2.3 Attachment of azide-biotin to the alkyne of PbTx-2 photoaffinity label derivatives

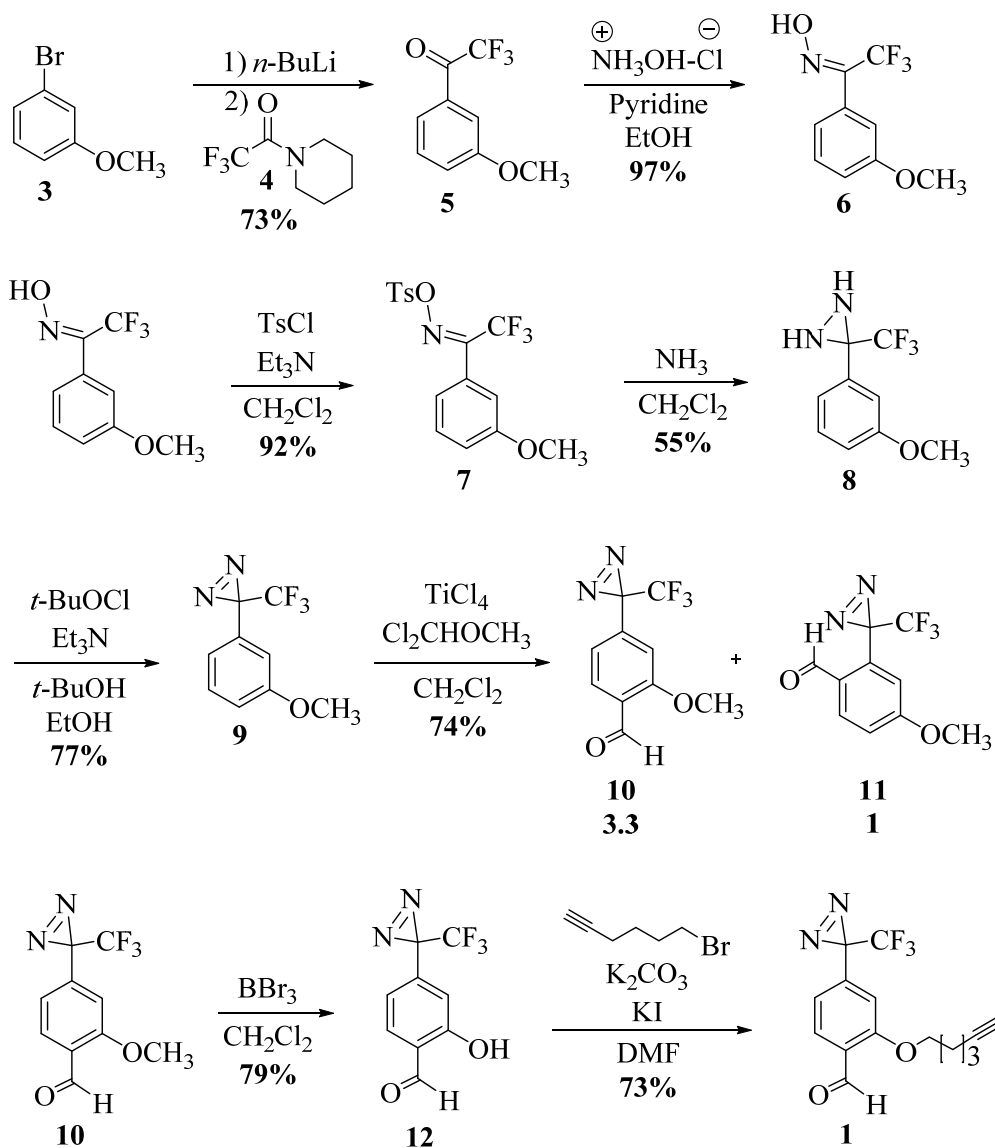
“Click” chemistry will be utilized to couple the biotin moiety to each brevetoxin derivative. Scheme 4 shows the A-ring derivative as an example of this attachment. The alkyne and azide could be interchanged between the two molecules to give similar results. Both the azide and alkyne biotin derivatives containing a polyglycol linker between the two are commercially available. With biotin attached, the photoaffinity probes will be ready to be used to identify a native brevetoxin receptor.



Scheme 4: Example of biotin attachment to the PbTx-2 A-ring derivative

2.4 Synthesis of Photoaffinity label 1 and 2.

Synthesis of compounds **1** and **2** was accomplished following published protocols with slight modifications (Scheme 5). The synthesis begins with an acylation of bromoanisole **3** to give acetophenone **5**. This acylation reaction, which is typically performed via a Grignard reagent, was performed via a lithium-halogen exchange between the bromo-anisole and *n*-BuLi in anhydrous THF. The organolithium formed was then treated with trifluoroacetic piperidine (TFAP) (**4**) which was prepared using established procedures⁸³. The oxime was next generated by treating **5** with hydroxylamine hydrochloride in the presence of pyridine. After 18 hrs of reflux, the reaction was stopped and the oxime **6** purified in high yields.



Scheme 5: Synthesis of photoaffinity label 1

This oxime was tosylated with tosyl chloride in the presence of triethylamine. Formation of the 3-membered diaziridine ring **8**, is carried out by treating the tosyl oxime with liquid NH_3 at -78°C in a pressure tube. The tosyl oxime was dissolved in CH_2Cl_2 and brought to -78°C followed by the addition of ammonia until a liquid layer was observed on top of the CH_2Cl_2 . At this point, the pressure tube is capped and allowed to warm to

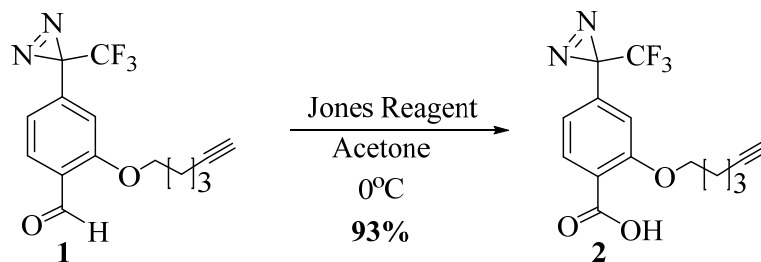
room temperature and allowed to stir for a minimum of 18 hours. Yields of this diaziridine step varied with scale and this particular step turned into a bottle neck for the synthesis of **1**. Reported yields for diaziridine synthesis through this route are variable with the process being described as time-consuming⁸⁴. Small scale synthesis gave larger yields than larger scale reactions. The use of diethyl ether as the solvent did not improve the yield.

Oxidation to the diazirine ring to give **9** was initially performed with *tert*-butyl hypochlorite but was also successfully carried out using Jones reagent. The *tert*-butyl hypochlorite was freshly prepared from normal household bleach, *t*-butyl alcohol, and glacial acetic acid following a published preparation⁸⁵. Other groups have performed this diaziridine oxidation step using iodine in the presence of triethylamine⁸⁶, silver oxide⁸⁷ and even oxalyl chloride⁸⁸.

Following the diazirine formation, a formylation was carried out which provided the *ortho* and *para* aldehyde diazirine products **10** and **11**. The *ortho* aldehyde is undesired because of the need to limit potential intramolecular insertions of the carbene that will ultimately be generated from the diazirine. Dichloromethyl methyl ether is used as the formylating reagent in the presence of TiCl₄ or a Rieche formylation after Alfred Rieche, a German chemist who first discovered and developed the process in the 1960's⁸⁹.

Final steps to give compound **1** included a demethylation to provide the phenol **12** followed by a final alkylation with 6-bromohexyne. The demethylation was carried out with the use of BBr₃ to provide the phenol. Boron tribromide is a strong Lewis acid and its use as a demethylating agent is well documented⁹⁰. Other Lewis acids such as AlCl₃

and BCl_3 have been used also to demethylate phenyl methyl ethers to the corresponding phenol. Treating the phenol with K_2CO_3 in the presence of KI followed by 6-bromo-hexyne in DMF gave the final alkylated diazirine **1**. The acid derivative **2**, was generated by treating aldehyde **1** with Jones reagent (Scheme 6).



Scheme 6: Oxidation of photoaffinity label 1 to 2 using Jones reagent

2.5 Undesirable formation of a geminal dibromo diazirine

A drawback was encountered while demethylating the methyl ester of **10** to produce **12**. The use of older bottles of BBr_3 yielded a geminal dibromide **13** as a byproduct (Scheme 7). This geminal dibromide could be readily converted back to the aldehyde by refluxing in a $\text{MeOH}/\text{H}_2\text{O}/\text{Et}_2\text{NH}$ mixture but with a reduced overall yield.

3. Synthesis of photoaffinity probes and a fluorescent probe

3.1 Brevetoxin Photoaffinity Probes

Three brevetoxin photoaffinity probes were envisioned with the hopes of retaining endogenous activity and more importantly the binding affinity with the goal of isolating the native protein that binds the toxin. All brevetoxin derivatives examined thus far have reduced toxicity so it is reasonable to assume a possible reduction in native activity could occur by alteration of the natural toxin; but maintaining its binding affinity was a much greater concern. The concern during the design of the photoaffinity probes was that endogenous binding affinity would be eliminated or greatly reduced and would lead to non-specific binding of brevetoxin. Activity and binding affinity do not always correlate. The PbTx-3 benzoyl and naphthoyl derivatives synthesized by Parker et al. were shown to have enhanced binding to site 5 on sodium channels although they did not maintain typical activity²². In fact, one of the derivatives were shown to be a brevetoxin antagonist. The increased binding suggest that binding to its receptor site is not altered by K-ring derivatizations.

Out of the three photoaffinity probes designed, the K-ring side chain derivative seemed the most promising because of both ease of attachment and the potential to retain binding affinity for the native receptor. The hydroxyl group located in the K-ring is unreactive as a result of its axial orientation. Some K-ring derivatives have been synthesized previously which did not significantly interfere with the binding to its receptor²² in VGSC studies and even was shown to be enhanced in two of the cases. A

competitive displacement assay was used in these studies to assess the binding affinities with displacement demonstrated to have nanomolar affinity.

An ester linkage was originally envisioned for the A-ring derivative of brevetoxin. Because of the potential presence of esterases in *K. brevis* homogenates, this derivative was not the first choice for the photoaffinity label attachment. In addition, the lactone functional group is also important for binding in voltage gated sodium channels (VGSC) with the toxicity and binding completely eliminated by the reduction of the lactone. This elimination of binding in VGSC after the lactone reduction raised concerns that the same would be true with respect to any native receptor(s).

The H-ring diol formation was also not the first choice for ideal attachment of the label. Reduction of the alkene of the H-ring was also shown to strongly reduce binding in VGSC studies. It is unknown how attachment of a large molecule would affect the endogenous binding of brevetoxin.

3.2 Synthesis of K-ring photoaffinity label

The synthesis of the K-ring derivative (Scheme 2) was met with some initial difficulty when the reductive amination between the *Boc*-protected hexamethylenediamine and **1** was originally attempted. The reductive amination was performed with very high yields, but the removal of the N-Boc protecting group was unsuccessful. The unsuccessful deprotection of the N-Boc protecting group led to an alternative approach involving the attachment of the photoaffinity label to the side chain aldehyde of the K-ring.

3.3 Thiol-Michael addition at the α , β -unsaturated aldehyde side chain of PbTx-2

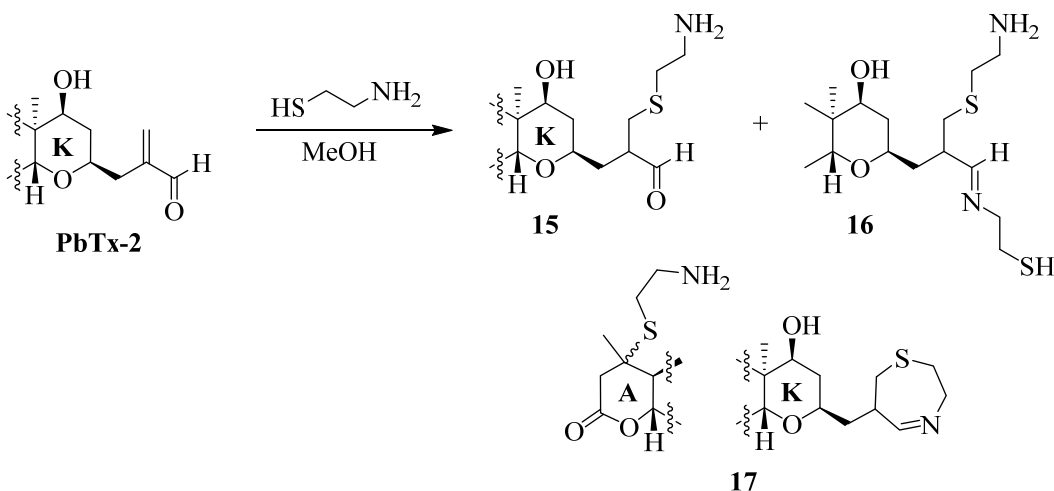
A major detoxification pathway of brevetoxin in shellfish and animals involves reactions at the α , β -unsaturated carbonyl on the side chain of the molecule. Cysteine and glutathione conjugates which add to the α , β -unsaturated carbonyl in a Michael fashion have been identified⁹¹. The Michael addition at the α , β -unsaturated carbonyl in PbTx-2 appears to be spontaneous as it does not require catalysis by glutathione-S-transferase.

As originally defined in the 1880's by Arthur Michael, the Michael addition was the addition of an enolate to the β -carbon of an α , β -unsaturated carbonyl. A more recent and broader definition includes any nucleophilic attack on the β -carbon of an α , β -unsaturated carbonyl. Following the nucleophilic attack at the β -carbon, a negatively charged enolate is subsequently formed that may be protonated or quenched with another electrophile to provide the addition product.

The reaction between a thiol and an α , β -unsaturated carbonyl is termed a thiol-Michael addition and has generated considerable interest recently in materials chemistry being used to engineer adhesives and laminates, block polymer conjugation, bimolecular synthesis and surface modification⁹². The reaction possesses the characteristic traits of an ideal "click" reaction and has been termed such because of the exceedingly quick quantitative yields observed at ambient conditions. The base-catalyzed thiol-Michael addition has been well documented and typically involves the use of an amine base⁹³ such as triethylamine. Reaction rates depend on the acidity of the thiol, the basicity of the catalyst used, and the electrophilicity of the β -carbon.

3.4 Model studies on the thiol Michael addition to PbTx-2

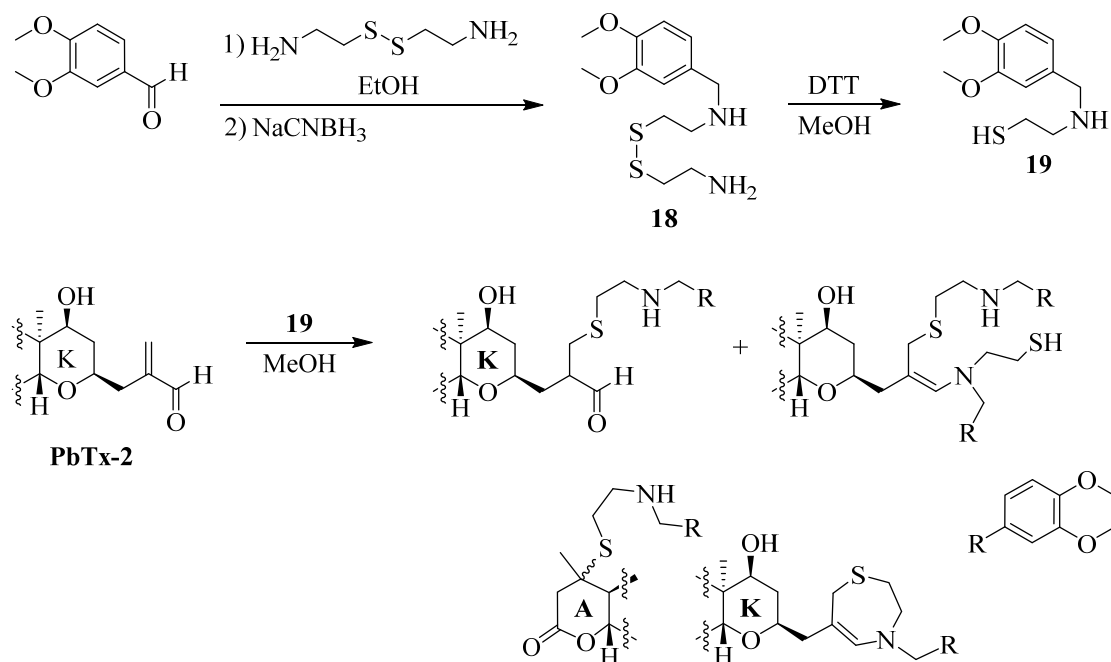
Because cysteine readily adds to PbTx-2 via a Michael addition, we envisioned using a thiol linker to attach the photoaffinity label to the K-ring. A model study was performed between cysteamine and PbTx-2 to demonstrate that a thiol would add in a Michael fashion. Cysteamine (5 and 50 mol excess) was reacted with PbTx-2 at room temperature and the mixture analyzed using LC-MS. Unreacted brevetoxin was still present but new products were observed. One product was shown to have the expected ion peak ($m/z = 972$) for the Michael adduct. Two other products were observed to elute at different rates but with the same m/z of 1031 which corresponds to the addition of two cysteamine molecules plus the loss of water. Considering that cysteamine contains a primary amine, it seemed likely that the loss of water was consistent with the formation of an imine. Proposed products are shown below (Scheme 9).



Scheme 9: Proposed products for thiol-Michael addition between cysteamine and PbTx-2

It is possible to have a thiol-Michael addition, the formation of an imine, or a thiol-Michael addition followed by the imine formation to give the seven membered thiazepine ring. Also possible is a thiol-Michael addition to the A-ring of PbTx-2 which contains an α , β -unsaturated lactone. Formation of a thiazepine ring seemed very likely because of the ease of imine formation between a primary amine and aldehyde. Compound **17** shows both the thiazepine ring formation plus an addition at the A-ring of PbTx-2. Proposed product **16** seemed unlikely as the sulfhydryl group would eventually form a disulfide dimer or a disulfide with unreacted cysteamine. Dimers were not observed in the mass spectra between PbTx-2 and cysteamine.

Following the reaction of PbTx-2 with cysteamine, a second model study was performed (Scheme 10) which used a bulkier substrate containing a benzyl amine. Disulfide **18** was first synthesized by a reductive amination between 3, 4-dimethoxybenzaldehyde and cystamine. The disulfide **18** was then reduced using DTT to yield the thiol **19** which was then added to PbTx-2.

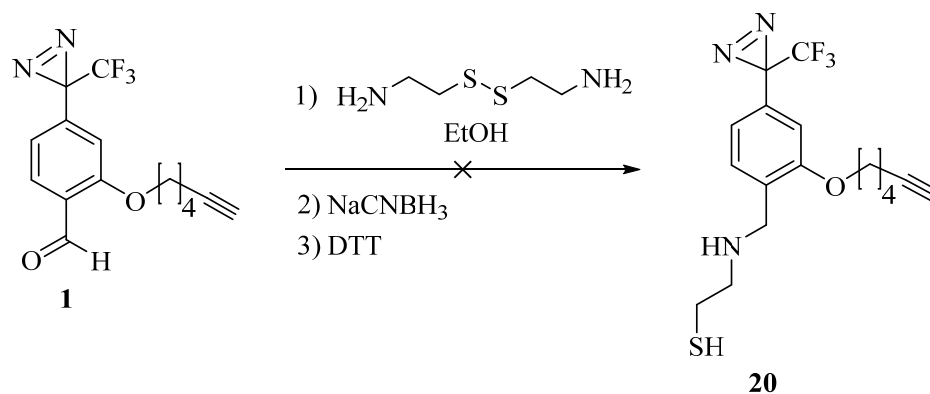


Scheme 10: Thiol-Michael click reaction between **19 and **PbTx-2****

Analysis of the mixture was performed with LC-MS. An ion peak ($m/z = 1122$) corresponding to the Michael adduct was observed as well as an ion peak (m/z of 1331) corresponding to the addition of two molecules of **19** plus a loss of water. Notable in the chromatogram of this reaction was that **PbTx-2** was no longer detectable.

*3.5 Thiol incorporation into photoprobe **1** and the attachment of biotin through a click reaction*

Synthesis of compound **20** (Scheme 11) was planned by way of a reductive amination of aldehyde **1** with cystamine followed by a disulfide reduction using DTT to reduce the disulfide to the thiol. The reductive amination was completed. However, the DTT reduction step was complicated by a competing thiol-yne (Figure 19) reaction between the terminal alkyne linker, DTT and the resulting thiol⁹⁴.



Scheme 11: Unsuccessful synthesis of thiol 1 due to the competing thiol-yne reaction

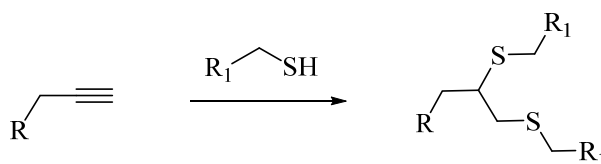
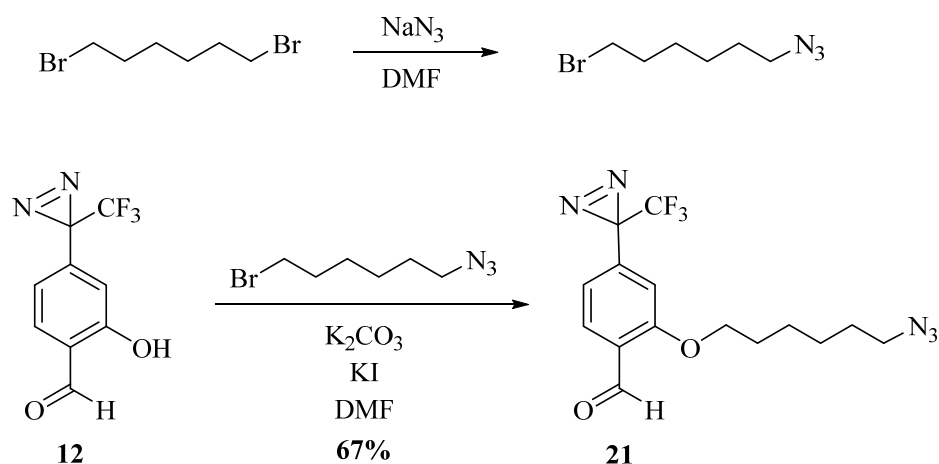


Figure 19: General thiol-yne reaction

Terminal alkynes are as reactive as α , β -unsaturated carbonyls towards thiol addition. This thiol-yne reaction is utilized to produce dendrimers and hyperbranched polymers in material science.

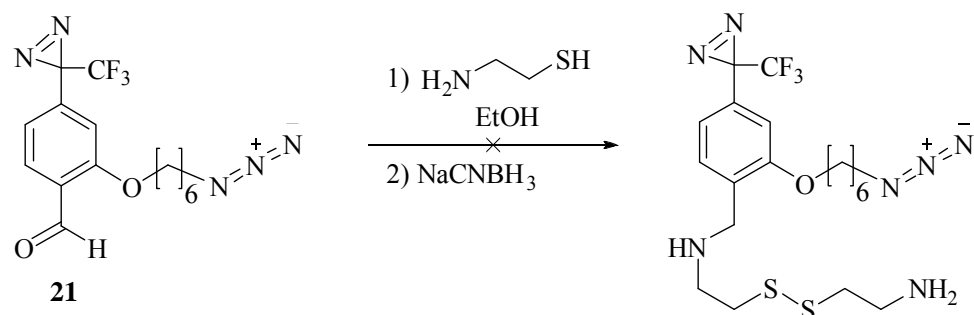
The realization that the thiol-yne reaction would disallow the synthesis of a mercapto alkyne lead to a reassessment of the synthetic design. It was decided to prepare a mercapto azide. This approach would require switching the functional groups (alkyne and azide) on the coupling partners in the click reaction. Because both alkyne and azide derivatives of biotin are commercially available, this was straightforward. Ultimately, the azido aldehyde **21** was synthesized. This synthesis was performed by the alkylation of phenol **12** with 1-azido-6-bromo-hexane using the same procedure use for the alkylation with 6-bromohexyne. The 1-azido-6-bromo-hexane, a known compound⁹⁵ was

synthesized from dibromohexane and sodium azide in DMF (Scheme 12). The mono-substitution of the azide was achieved by using a large molar excess of dibromohexane in the reaction.



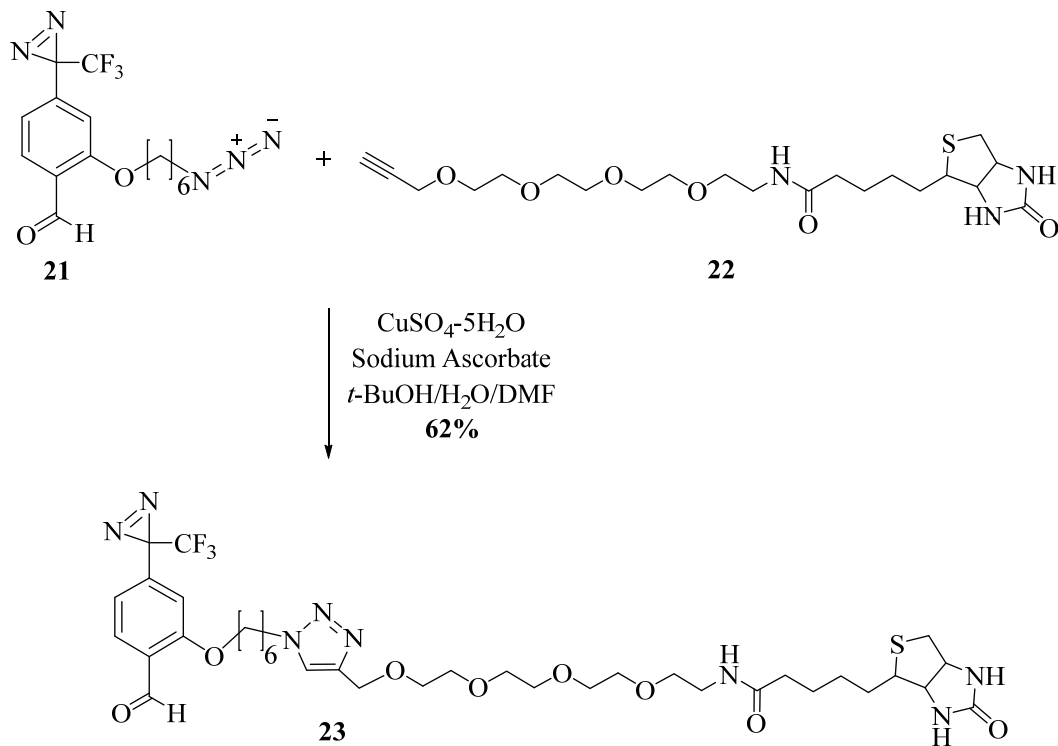
Scheme 12: Synthesis of diazirine 21 with azide linker

From the azido diazirine **21**, a few choices had to be made with respect to the sequence of steps for the attachment of this diazirine to the side chain of PbTx-2. Though initially envisioned was the reductive amination with cysteamine and **21** to form the disulfide, followed by the click reaction with biotin alkyne, it was ultimately decided to perform the reductive amination after the click reaction. A noted point is that using cysteamine in excess in place of cystamine will yield the disulfide as thiols oxidize readily to the disulfide in the presence of oxygen. An attempt to perform the reductive amination between aldehyde **21** and cysteamine gave an intractable mixture.



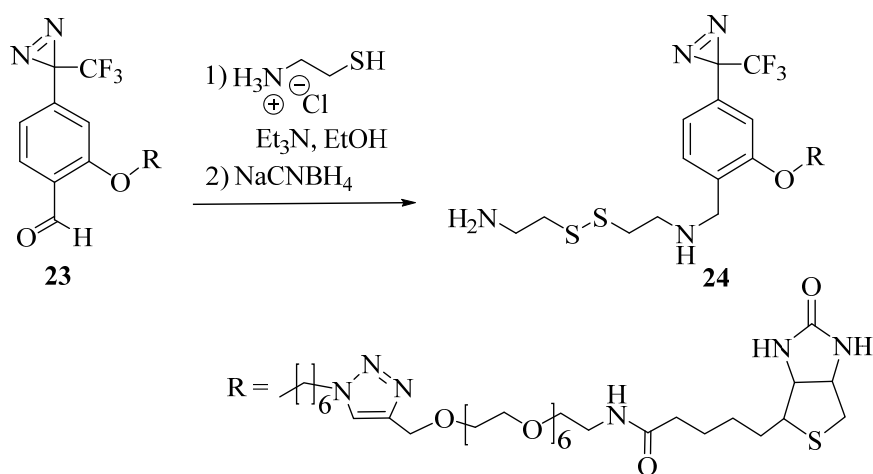
Scheme 13: Attempted reductive amination between 21 and cysteamine

It was decided that the generation of the disulfide followed by reduction to the thiol should be the last step before the addition to PbTx-2. With this reasoning, the azido diazirine **21** was coupled (Scheme 14) to the alkyne linked biotin **22** in a click reaction to produce **23**. The click reaction was performed under standard conditions as described throughout the literature⁹⁶ and provided the biotin aldehyde **23** in 62% yield.



Scheme 14: Synthesis of biotin linked diazirine, 23

The aldehyde **23** was then placed in absolute ethanol with cysteamine (Scheme 15) in a large molar excess and allowed to stir for 5 hours. Electrospray ionization (ESI) quadrupole in positive ion mode was used to monitor imine formation (m/z 947) and the subsequent reduction (m/z 949) in order to ensure complete conversion to the Schiff base prior to reduction to the desired product. Excess sodium cyanoborohydride was necessary to push the reduction to completion.

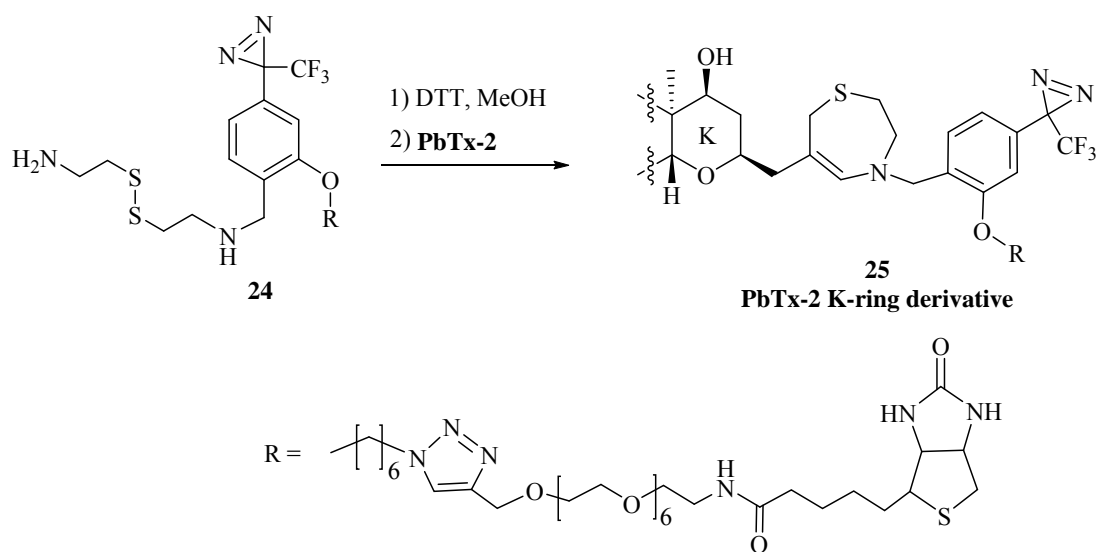


Scheme 15: Reductive amination of 23 with cysteamine to yield disulfide 24

3.6 Reduction of **24** with DTT and subsequent Michael addition to K-ring side chain of *PbTx-2*

Dithiothreitol (DTT) was employed to generate the free thiol (Scheme 16) before addition to *PbTx-2*. This reduction was also monitored by ESI mass spectroscopy and quenched once the disulfide was no longer detectable. The free thiol was taken up in CH_2Cl_2 and washed with H_2O to remove DTT. The free thiol was then immediately added to brevetoxin in methanol, flushed with nitrogen and allowed to stir. The reaction

mixture showed the disappearance of both PbTx-2 and the thiol diazirine though unfortunately no product was able to be detected with ESI MS. Samples submitted for HRMS also failed in the detection of the product. Interestingly, had the reaction completely failed, one would expect to see the disulfide of the oxidized thiol diazirine eventually form, but this was also absent in ESI MS spectra.



Scheme 16: Disulfide reduction of 24 with DTT and Michael addition to PbTx-2

Though a diagnostic HRMS signal of the final product was not observed, ^1NMR provided information that led to the conclusion the reaction was successful. The ^1H NMR of the crude reaction mixture showed the disappearance of the distinctive aldehyde proton from the side chain of PbTx-2 and the appearance of what is believed to be the enamine proton which would both be expected if the thiazepine ring was formed. Also notable in the spectra was the disappearance of the vinyl protons of PbTx-2 (Figure 20). These vinyl protons would not be present if the thiol-Michael addition was successful.

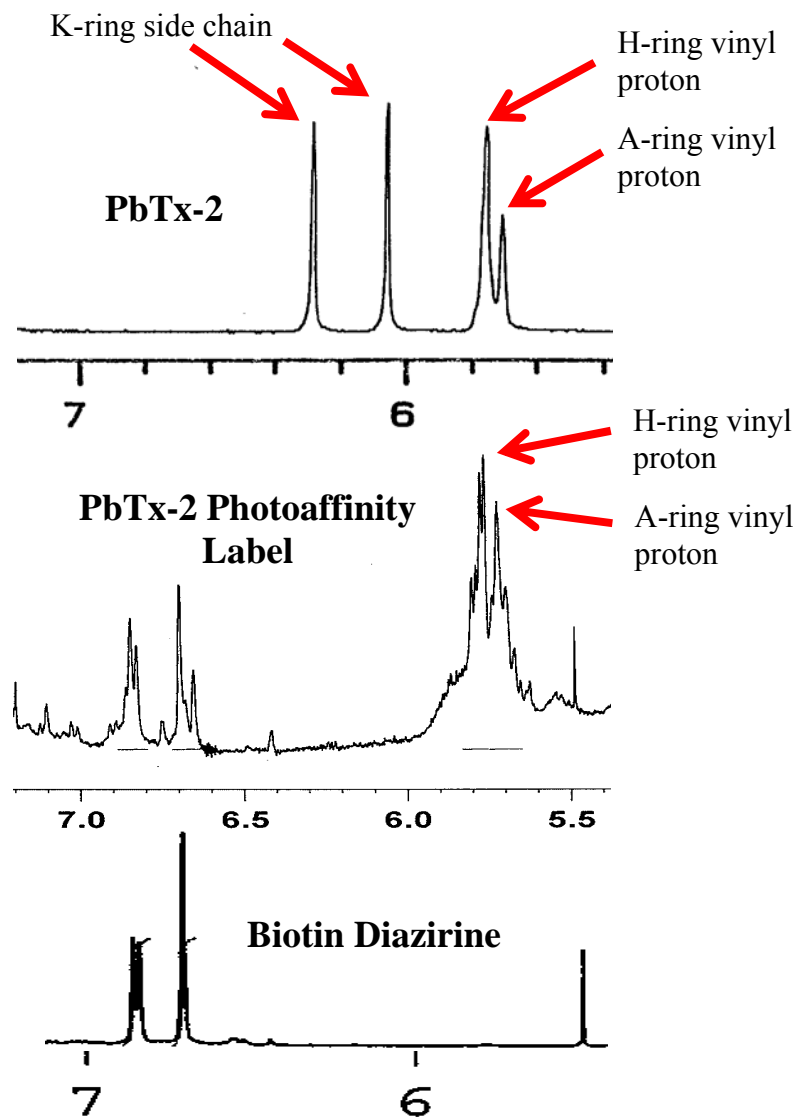


Figure 20: ^1H NMR comparisons of PbTx-2, 23, and PbTx-2 photoaffinity probe 25

3.7 Attachment of Alexa fluor 488 to PbTx-2

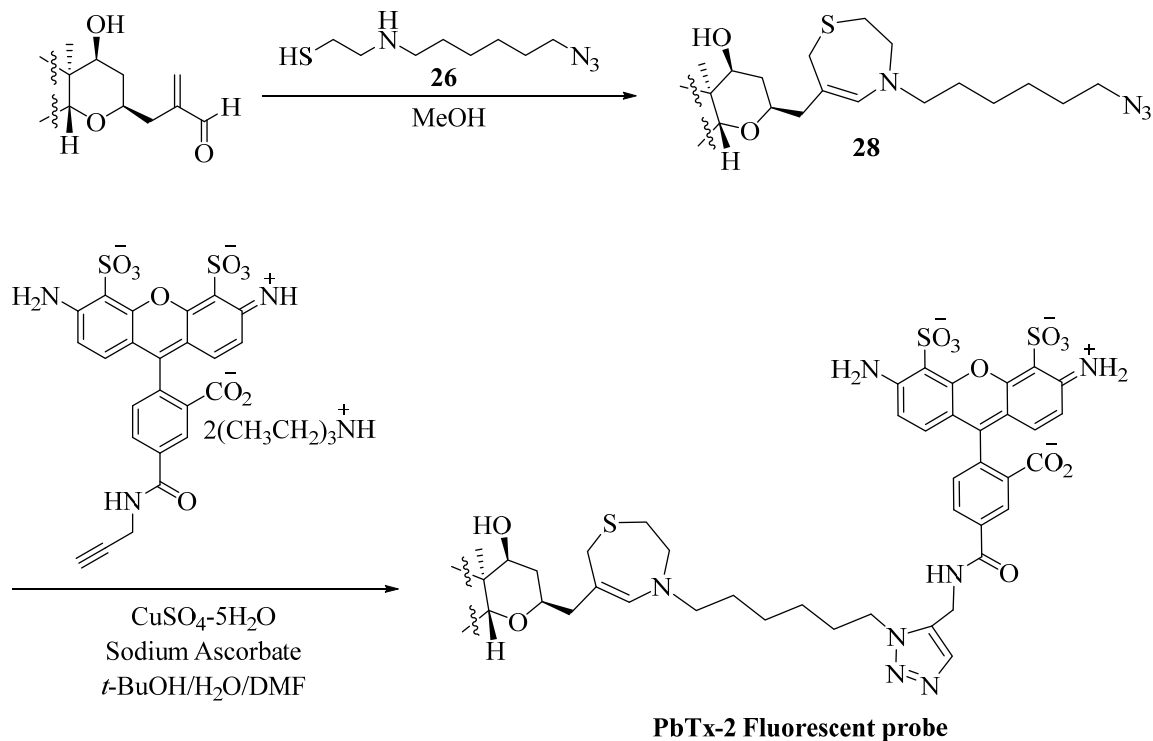
The mono and di-alkylated thiol-azide amines **26** and **27** were synthesized by the alkylation of cystamine with 1-azido-6-bromo-hexane. The alkylation reaction was performed in DMF. To ensure that the mono alkylated secondary amine major product

over the dialkylated tertiary amine, a large excess (10:1 molar ratio) of cystamine was used relative to the 1-azido-6-bromo-hexane.



Scheme 17: Synthesis of thiol linkers 26 and 27

Linker **26** was used in the reaction with PbTx-2 to form **28** (Scheme 18). The thiol **26** would easily oxidize to the disulfide product so it was necessary to use it in the Michael addition with PbTx-2 immediately following the reduction with DTT.



Scheme 18: Synthesis of PbTx-2 fluorescent probe using Alexa Fluor 488 and 28

The azide thiol **26** was reacted with the PbTx-2 aldehyde side chain to give **28** as the major product. This result was determined on the basis of ESI quadrupole MS which showed the product with an m/z ion peak of 1079 in the positive mode which is consistent with a seven membered thiazepine ring formed from the Michael addition between the thiol and the α , β -unsaturated aldehyde followed by formation of an enamine from the reaction between the aldehyde and secondary amine. The reaction product **28** was purified by HPLC and a high resolution mass spectra of the product obtained which showed the m/z ratio of 1079.6007 corresponding to the Michael adduct minus one water molecule. The Alexa Fluor 488 was covalently linked to the azide linked brevetoxin **28** through the use of click chemistry. The reaction was performed in the dark and used to localize brevetoxin within the cells of *K. brevis*. The reaction mixture was not purified though a new product was observed on the HPLC.

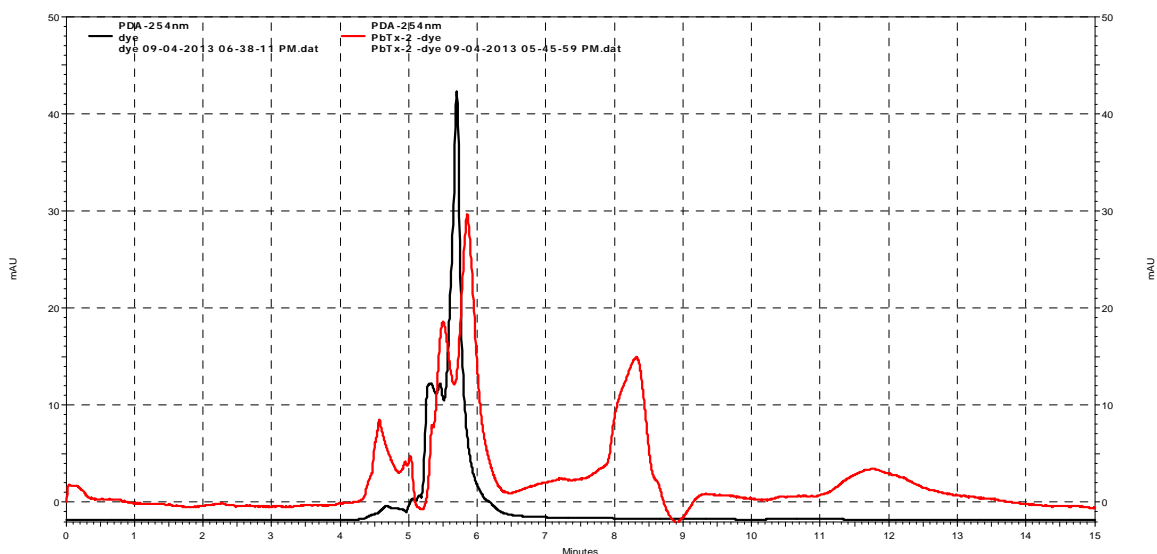


Figure 21: HPLC trace of PbTx-2 fluorescent probe (red) vs Alexa fluor 488 (black)

3.8 Incubation of K. brevis cells with PbTx-2 fluorescent probe and PbTx-2 photoaffinity probe

Wei Chen, another graduate student in our research group performed incubation studies using the PbTx-2 fluorescent probe to localize PbTx-2 within live *K. brevis* cells. Wei used the reaction mixture between **28** and Alexa Fluor 488 for the incubation. The image (Figure 19) shows the probe (yellow) localizing within the chloroplast (red). A control experiment using the fluorescent dye alone shows only the chloroplast in red with no dye being localized.

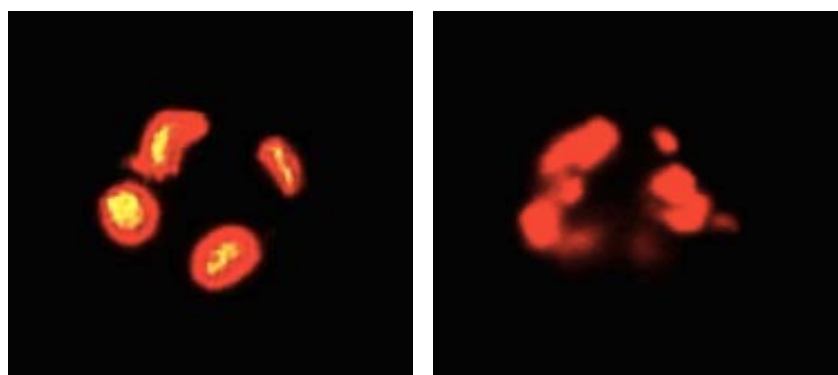


Figure 22: *K. brevis* cells incubated with PbTx-2 fluorescent probe (left) and Alexa fluor 488 (right)

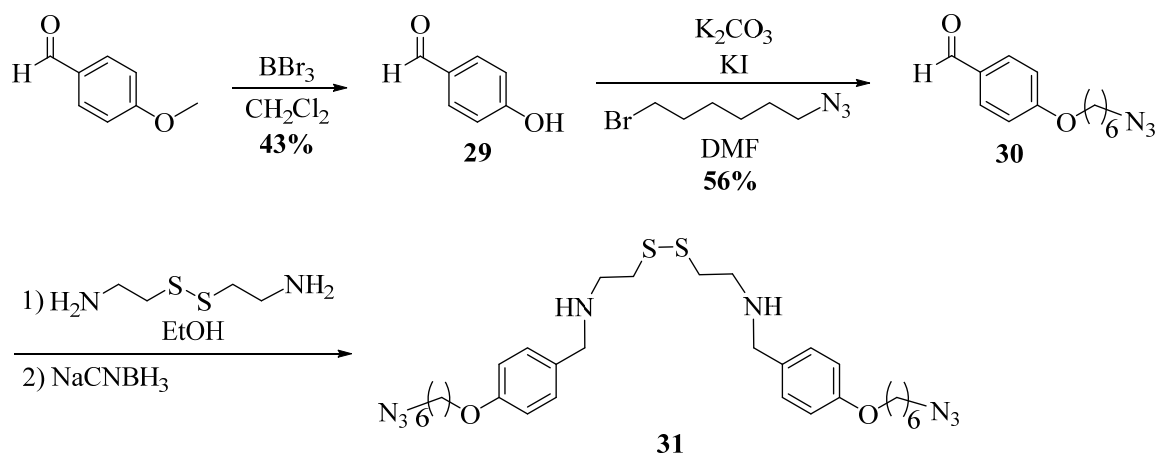
Wei was able to identify a brevetoxin receptor within *K. brevis* using the brevetoxin photoaffinity probe. *K. brevis* cells were incubated with the probe for 1 hour at pH 7.0 and the photolysis of the diazirine ring performed with 350 nm light. Purification was carried out using streptavidin beads and a band around 25 kDa was isolated from an SDS PAGE gel. The excised band was analyzed by ESI LC-MS followed by BLAST analysis of the obtained amino acid sequence which indicated that

the protein was the light harvesting complex II (LHCII) of the photosynthetic apparatus, which is a transmembrane protein approximately 27 kDa.

3.9 Synthesis of alternative thiol azide linker

Though successfully used to make **28**, complete characterization of the thiol azide linker **26** proved difficult. The crude mixture containing **26** and **27** would oxidize to give a collection of disulfides that proved very time consuming and problematic to purify. This prompted the design of a different thiol azide linker that would be easier to purify and handle.

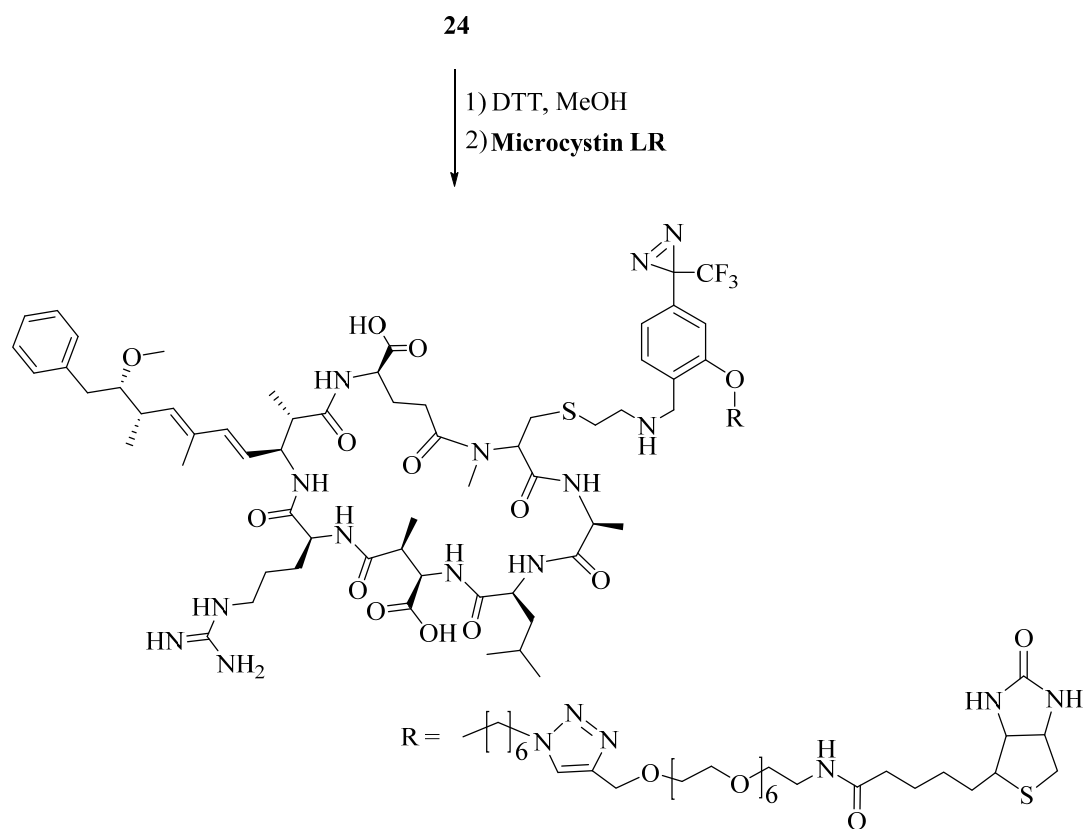
Demethylating *p*-methoxy benzaldehyde using BBr₃ afforded **29**, which was alkylated using 1-azido-6-bromo-hexane to provide **30** (Scheme 20). Compound **30** was taken through a reductive amination using cystamine to give the disulfide **31**. This route was improved due to the lack of side products, and the fact that the product is UV active which greatly aids in the purification.



Scheme 19: Synthesis of alternative thiol azide linker

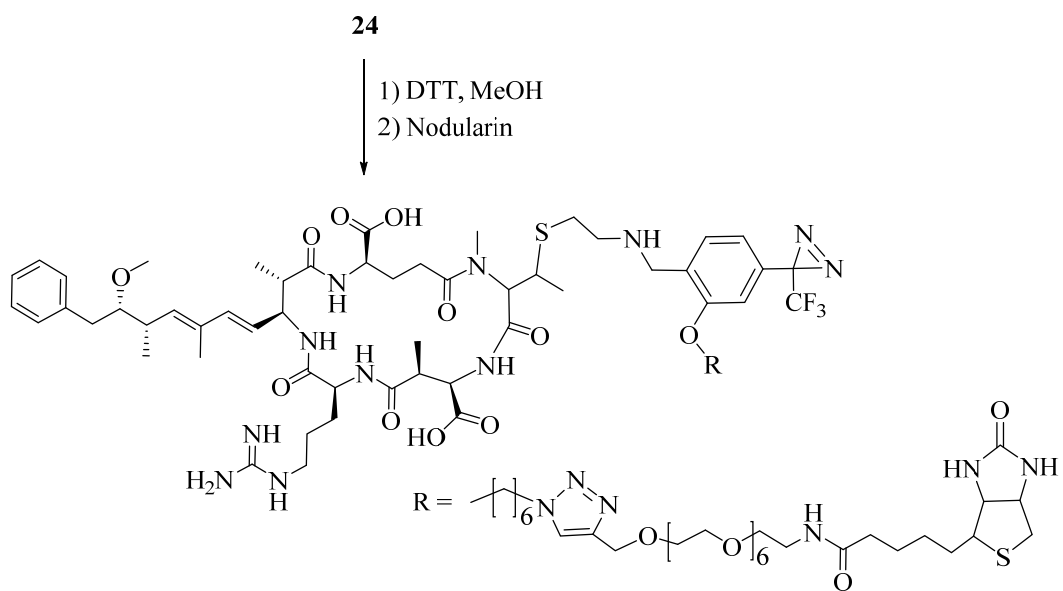
3.10 Synthesis of Microcystin LR photoaffinity probes

Having successfully prepared a brevetoxin photoaffinity probe via a Michael addition to the α , β -unsaturated carbonyl of PbTx-2, we turned our attention to other toxins having similar functionality. As mentioned in chapter 1, both microcystin-LR and nodularin possess an α , β -unsaturated carbonyl which potentially could undergo a thiol-Michael addition in a similar manner as was performed with PbTx-2.



Scheme 20: Synthesis of microcystin-LR photoaffinity probe

3.11 Synthesis of nodularin photoaffinity probe



Scheme 21: Synthesis of nodularin photoaffinity probe

4: Alternative synthetic route to photoaffinity labels

4.1 Proposed alternate synthesis to desired photoaffinity labels

Because the synthesis of photoaffinity probe was hampered by two problematic steps which resulted in low yields overall, an alternative synthesis to the desired photoaffinity label with multiple functionality was envisioned (Figure 22). The commercially available 4-bromo-2-(hydroxymethyl)phenol was chosen because the benzyl alcohol may be oxidized to the aldehyde and the phenol can be readily alkylated after introduction of the diazirine functional group to provide a linker to biotin. In order to introduce the diazirine, both the benzyl alcohol and the phenol would have to be protected during the acylation with TFAP which requires the use of *n*-BuLi. Fortunately a 1, 3-diol protection of **32** via acetonide formation to give **33** had been previously reported and the synthetic procedure available in the literature⁹⁷. It was envisioned that following formation of the acetonide, the acylation with TFAP could be performed to provide **34**. Compound **34** could then be taken through the typical steps needed to construct the diazirine functional group to give **38**. Once the diazirine is in place, the acetonide may be removed, followed by an oxidation of the benzyl alcohol to an aldehyde to provide photoaffinity label **40** capable of being attached to the desired linkers.

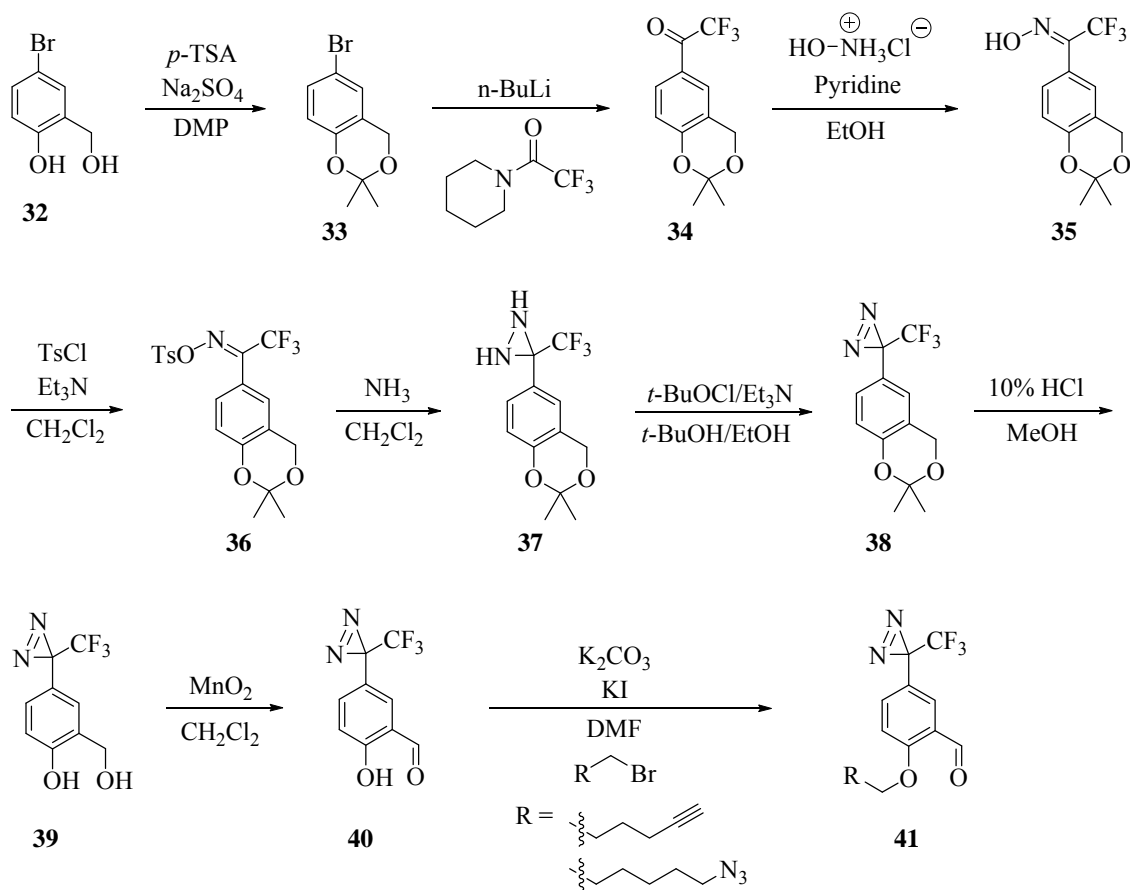


Figure 23: Proposed alternative synthesis to photoaffinity labels

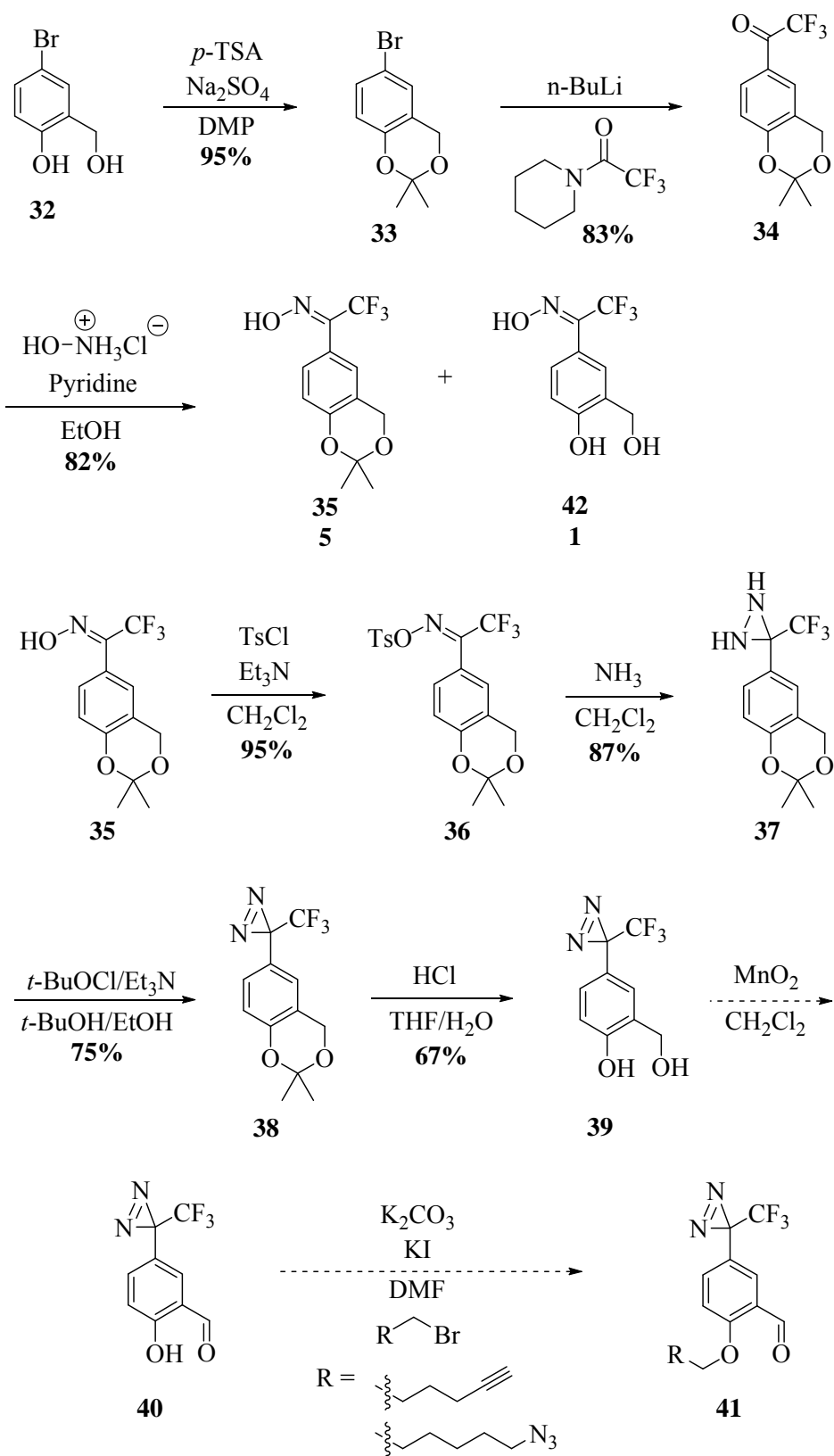
This alternate synthesis would avoid the formylation step, which produces the undesired *ortho* product, and the demethylation of the methyl ether which can produce the geminal dibromide as a byproduct (Scheme 7). The alternate synthesis requires a protection and deprotection step which makes this synthetic route one step longer than that shown in (Scheme 5) but the hopes were that the overall yields of the final product and ease of purification at each step would be increased. This alternative synthesis would also avoid the use of toxic BBr_3 and dichloromethyl methyl ether. Depending on the linker chosen for attachment, the final diazirine **41** would be very similar to **1** and **21** but with the substituents at the *meta* and *para* positions switched.

4.2 Alternate synthesis of photoaffinity labels

Formation of the acetonide from **32** (Scheme 23) was first performed in order to protect the primary alcohol and the phenol. The acetonide formation was performed using 2,2-dimethoxypropane with *p*-toluene sulfonic acid as the catalyst and Na₂SO₄ to remove water that is generated during the course of the reaction.

Acylation yields using **33** were higher and may be due to the electronic donating properties of the *para* alkoxy group. The synthesis of the oxime followed similar conditions as before to provide the oxime **35** but resulted in lower yields than expected due to the loss of the acetonide protection group to also give **42**. Formation of the oxime is typically performed overnight in refluxing ethanol but in order to control the acetonide deprotection, it was necessary to only mildly heat the solution and to monitor the reaction progress by TLC. Formation of the oxime would not occur at room temperature with no product being detected by TLC. Nevertheless, the unprotected diol oxime **42** could still be useful and further synthesis with it was explored.

The tosyl oxime **36** was then synthesized using tosyl chloride in the presence of Et₃N to give the diol protected tosyl oxime in nearly quantitative yields. With this reaction taking place on ice, no deprotection products from the loss of the acetonide group was observed during the formation of the tosyl oxime. The diaziridine **37** was synthesized using liquid ammonia and methylene chloride in a pressure tube. A slight adjustment in the reaction procedure to form **37** was that ammonia was flushed through the pressure tube while on a dry ice/acetone bath to condense the ammonia to a liquid to which the starting material, dissolved in CH₂Cl₂, was added dropwise before the tube was sealed, brought to room temperature, and allowed to stir for 48 hours.



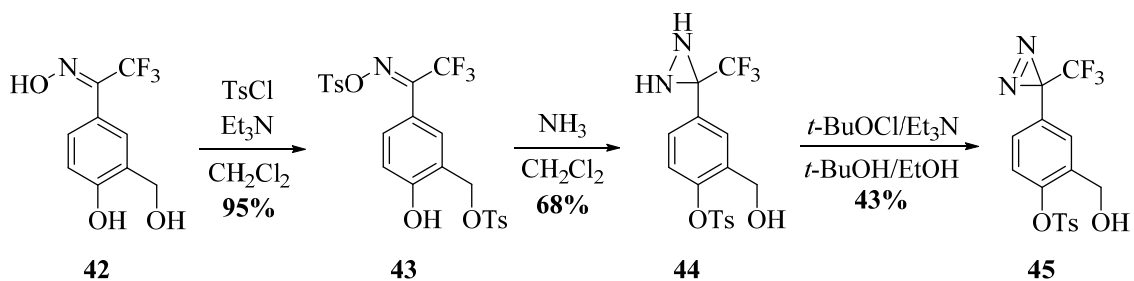
Scheme 22: Alternative synthesis to photoaffinity label with multiple functionality

Much higher yields of the diaziridine were observed using this method. In the previous method, ammonia was always used in a very large excess to the tosyl oxime, but with this alternate method, the ammonia is the solvent with the methylene chloride present in order to transfer the tosyl oxime to the pressure tube. The diaziridine was easily converted to diazirine **38** under similar conditions using *tert*-butyl hypochlorite as the oxidizing agent. Removing the acetonide protecting group of **38** to yield the diol diazirine **39** was performed using HCl in a THF/H₂O mixture. Oxidizing the benzyl alcohol of **39** to yield **40** was met with difficulty and a suitable procedure is still being explored. Once a suitable oxidation procedure is found, the final alkylation step using either 6-bromo-hex-1-yne or 1-azido-6-bromo-hexane should proceed smoothly to yield **41** containing either a terminal alkyne or azide, depending on the linker chosen for attachment.

4.3 Exploring photoaffinity label synthesis with compound 42

The unprotected oxime **42** formed by loss of the acetonide group still seemed to have some potential use and was not discarded as it was only three synthetic steps away from a diazirine that could be of use. It was decided to protect both the oxime and the benzyl alcohol as tosyl alcohols by treatment with tosyl chloride to give **43**. This di-tosyl phenol was treated with liquid ammonia under pressure to provide the diaziridine **44**. An interesting rearrangement occurred during this reaction with ammonia where the tosyl group migrated from the benzyl alcohol to the phenol. Treatment with *tert*-butyl hypochlorite under similar conditions as the other diaziridine oxidations yielded the

diazirine **45**. Compound **45** can be oxidized to its diazirine followed by deprotection of the tosyl alcohol and an oxidation to give **14**.



Scheme 23: Diazirine synthesis using unprotected oxime 42

Future Synthetic Plans:

The A-ring and H-ring brevetoxin photoaffinity probes are still of interest and would be of benefit if synthesized. One of the drawbacks of working with brevetoxin is the availability which makes optimizing reactions somewhat difficult. If purchased commercially it can cost as much as \$5000/mg. The growth of the culture followed by brevetoxin extraction and purification is lengthy and by no means an insignificant task to undertake. With these considerations at the forefront of all synthetic work involving brevetoxin, most reactions are desired to be high yielding with purification mainly done via HPLC or liquid-liquid partition.

Another immediate goal would be to characterize the microcystin LR and nodularin photoaffinity probes that were synthesized. The synthesis of microcystin LR and nodularin fluorescent probes are also of interest and would be of great use and would serve to localize these toxins within their cell as done with PbTx-2. The synthesis of these fluorescent probes could be carried out in a similar manner as with PbTx-2 by use of the

thiol azide linkers. The thiol-Michael addition of the linkers to the α , β -unsaturated carbonyls would be performed followed by a click reaction between the azide of the linker and the alkyne of Alexa fluor 488.

The endogenous role of other polyether ladder toxins such as yessotoxin and ciguatoxin is still unknown. The synthesis of a photoaffinity probe and a fluorescent probe of both yessotoxins and ciguatoxin would provide insight into their functional role. The functionality of the biotin attached photoaffinity probe already synthesized would only need to be adjusted to enable the attachment. Yessotoxin contains a terminal alkene in its side chain which could be utilized and ciguatoxin contains a primary alcohol in its respective side chain. Both of the side chains in these toxins could be utilized to attach a photoaffinity probe. A suitable linker containing an azide would be attached to yessotoxins and ciguatoxin to enable the click reaction with Alexa fluor 488 to provide the fluorescent probes of each.

If a yessotoxin and ciguatoxin photoaffinity and fluorescent probes were successfully synthesized they would be used to localize each toxin within their cells and subsequently isolate their respective receptors. These results would be compared to what was found using the PbTx-2 probes and could offer a theory to the general endogenous role of polyether ladder toxins.

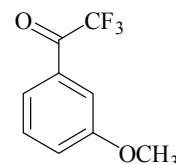
5. Experimental procedures

^1H and ^{13}C NMR spectra were acquired on a Bruker AVANCE 400 MHz spectrometer. Coupling abbreviations are as follows: s, singlet; b, broad; d, doublet; t, triplet; q, quartet; and m, multiplet. Thin layer chromatography (TLC) analyses were performed on 0.25 mm Analtech silica gel GHLF plates. Radial chromatography was performed using 1 mm, 2 mm, and 4 mm plates prepared with silica gel 60 PF₂₅₄ containing gypsum. All air and moisture sensitive reactions were conducted under nitrogen. Glassware for anhydrous reactions was either flame-dried or oven dried for a minimum of two hours before use. All reagents and solvents were purchased from Sigma-Aldrich or Acros chemicals and used without further purification unless otherwise specified.

Solvents were dried by stirring overnight under CaH_2 followed by distillation under a nitrogen environment using dry glassware. Liquid reagents were dried in a similar manner when necessary but distilled by kugelrohr short path distillation after overnight stirring over CaH_2 .

Preparation of 2,2,2-Trifluoro-1-(3-methoxy-phenyl)-ethanone (5)

3-Bromo-anisole **3** (3.0 g, 0.016 mol) was placed into a flame dried round-bottom flask that was partially cooled by flushing with nitrogen. Anhydrous THF (25 ml) was transferred via syringe to the round-bottom flask. The flask was cooled under nitrogen to -78°C in a dry ice/acetone bath. *n*-BuLi (6.74 ml, 2.5 M, 0.017 mol) was transferred dropwise via syringe and the solution was allowed to stir for 5 minutes. *N*-trifluoroacetylpiperidine **4** (2.36 ml, 0.016 mol) was

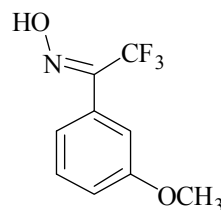


transferred by syringe to the solution and allowed to stir for an hour in the dry ice bath. The solution was brought to room temperature and allowed to stir until a precipitate was observed. The reaction was diluted by the addition of saturated aqueous NH_4Cl (20 ml) and extracted with diethyl ether (3 x 40 ml). The aqueous layer was washed with diethyl ether and dried over Na_2SO_4 , filtered and evaporated in vacuo to give a crude yellow oil. This crude oil was purified by column chromatography (7:3 hexane/ CH_2Cl_2) to provide the product (2.38 g, 73%) as an oil. Spectroscopic data was consistent with literature⁴⁴.

$^1\text{H-NMR}$ (CD_3Cl): δ 3.88 (s, 3H), 7.25 (dd, $J = 2.8, 8.4$ Hz, 1H), 7.45 (t, $J = 8.0$ Hz, 1H), 7.57 (s, 1H), 7.66 (d, $J = 7.8$ Hz, 1H) ppm; **$^{13}\text{C-NMR}$** (CDCl_3): δ 55.5, 114.0, 116.7 (q, $J = 289$ Hz), 122.2, 122.7, 130.1, 131.1, 160.0, 180.4 (q, $J = 35$ Hz) ppm; **$^{19}\text{F-NMR}$** (CDCl_3): δ -71.7 (s) ppm;

Preparation of 2, 2, 2-Trifluoro-1-(3-methoxy-phenyl)-ethanone oxime (6)

A solution of **5** (5.12 g, 0.0251 mol) and hydroxylamine hydrochloride (2.62 g, 0.0376 mol) in absolute ethanol (30 ml) and dry pyridine (15 ml) was heated to 60°C for 18 h. After evaporation of the solvents, the residue was partitioned between water (40 ml) and ether (75 ml). The organic layer was washed with 10% HCl (5 x 20 ml) solution and dried over Na_2SO_4 . After filtration and evaporation of the solvent, the crude oxime was purified using column chromatography (15:1 CH_2Cl_2 :MeOH) to give **6** (5.3 g, 97%) as a colorless oil:



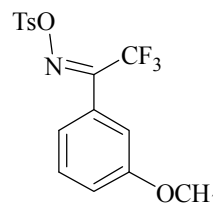
Spectroscopic data was consistent with literature⁴⁴.

$^1\text{H-NMR}$ (CDCl_3): Mixture of *cis* and *trans* isomers δ 3.84 (s, 3H), 7.04-7.10 (m, 3H), 7.34-7.44 (m, 1H), 8.40 (broad, 0.2 H), 8.64 (broad, 0.8H) ppm; **$^{13}\text{C-NMR}$** (CDCl_3): δ

55.37, 55.39, 113.9, 114.3, 116.2, 116.3, 120.6 (q, $J = 273$ Hz), 120.8, 127.2, 129.6, 129.7, 131.2, 147.8 (q, $J = 25$ Hz), 159.5 ppm;

Preparation of *O*-Tosyl-2,2,2-trifluoro-1-(3-Methoxy-phenyl)-ethanone oxime (**7**)

A CH₂Cl₂ solution containing oxime **6** (6.05 g, 0.027 mol), triethylamine (6 ml, 0.043 mol), and (*N,N*-dimethylamino)pyridine (150 mg, 1.2 mmol) was cooled to 0°C. To this solution, *p*-toluenesulfonyl chloride (5.8 g, 0.030 mol) was added in portions and stirred until the triethylamine HCl salts precipitated out of solution (typically within an hour). The reaction mixture was diluted with water (25 ml) and aqueous NaHCO₃ (25 ml) and allowed to stir for another hour. The organic phase was separated and washed with saturated aqueous NaHCO₃ solution (3 x 25 ml). The CH₂Cl₂ was dried over Na₂SO₄, filtered and concentrated in vacuo. The product was purified using column chromatography (1:1 hexane/CH₂Cl₂) to give **7** (9.48 g, 92%) as white crystals.



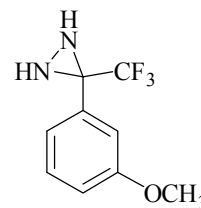
Spectroscopic data was consistent with literature⁴⁴.

¹H-NMR (CDCl₃): δ 2.47 (s, 3H), 3.81 (s, 3H), 6.87 (s, 1H), 6.93 (d, $J = 7.6$ Hz, 1H), 7.04 (dd, $J = 1.9, 8.5$ Hz, 1H), 7.37 (t, $J = 7.3$ Hz, 3H), 7.87 (d, $J = 8.3$ Hz, 2H) ppm;

¹³C-NMR (CDCl₃): δ 21.7, 55.4, 113.9, 117.1, 119.5 (q, $J = 277$ Hz); 120.4, 125.6, 129.2, 129.9, 130.0, 131.1, 146.1, 153.9 (q, $J = 35$ Hz), 159.5 ppm;

Preparation of 3-(3-Methoxy-phenyl)-3-(trifluoromethyl)-diaziridine (**8**)

The tosyl-oxime **7** (1.10 g, 0.003 mol) was dissolved in CH₂Cl₂ (10 ml) and the solution was cooled to -78°C in a glass pressure tube. While at -

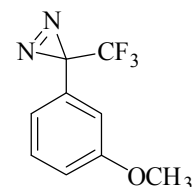


78°C, liquid ammonia was added until a layer was observed on the surface of the CH₂Cl₂. The pressure tube was sealed, brought to room temperature and allowed to stir for 18 hours. The pressure was slowly released over a period of one hour allowing excess ammonia to evaporate. The mixture was diluted with water (30 ml) and CH₂Cl₂ (50 ml). The CH₂Cl₂ layer was dried over Na₂SO₄ and concentrated in vacuo. The crude residue was purified using radial chromatography (4 mm plate, 1:1 hexane/CH₂Cl₂) to give **8** as a pale yellow oil (353 mg, 55 %): Spectroscopic data was consistent with literature⁴⁴.

¹H-NMR (CDCl₃): δ 2.24 (d, *J* = 8.8 Hz, 1H), 2.78 (d, *J* = 8.8 Hz, 1H), 3.83 (s, 3H), 7.03 (dd *J* = 1.6, 8.0 Hz, 1H), 7.15 (s, 1H), 7.20 (d, *J* = 7.6 Hz, 1H), 7.34 (t, *J* = 8.0 Hz, 1H) ppm; ¹³C-NMR (CDCl₃): δ 55.3, 57.9 (q, *J* = 36 Hz), 113.5, 115.7, 120.2, 123.4 (q, *J* = 278 Hz), 129.8, 132.9, 159.8 ppm;

Preparation of 3-(3-Methoxy-phenyl)-3-(trifluoromethyl)-diazirine (**9**)

A solution of freshly prepared *tert*-butyl hypochlorite⁸⁵ (560 mg, 0.0052 mol) and 5 ml of a 1:1 2-methyl-2-propanol/ethanol mixture was prepared. This mixture was added dropwise to a solution of **8** (375 mg,



0.0017 mol) and triethylamine (658 mg, 0.0065 mol) in 2-methyl-2-propanol/ethanol (15 mL/15 mL) while at 0°C with vigorous stirring. Cl₂ gas is produced and flushed with nitrogen from the flask. After stirring at room temperature for 2 h, the reaction was

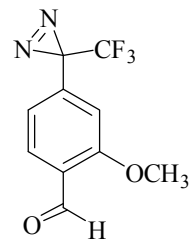
quenched by the addition of a 10% aqueous solution of Na₂S₂O₅ (25 ml). The reaction mixture was extracted with ether (3 x 25 ml) and the organic layers were combined and dried over Na₂SO₄. Evaporation of the solvent, gave a crude yellow oil which was purified by radial chromatography (2 mm plate, 2:1 hexane/CH₂Cl₂) to give **9** (286 mg, 77%) as a pale yellow oil: Spectroscopic data was consistent with literature⁴⁴.

¹H-NMR (CDCl₃): δ 3.81 (s, 3H), 6.69 (s, 1H), 6.77 (d, *J* = 7.8 Hz, 1H), 6.94 (dd, *J* = 2.2, 8.3 Hz, 1H), 7.31 (t, *J* = 7.9 Hz, 1H) ppm;

¹³C-NMR (CDCl₃): δ 28.4 (q, *J* = 40 Hz), 55.3, 112.3, 115.2, 118.7, 122.1 (q, *J* = 273 Hz), 130.0, 130.6, 159.8 ppm; **¹⁹F-NMR** (CDCl₃): -65.6 ppm;

Preparation of 2-Methoxy-4-(3-trifluoromethyl-diazirine)-benzaldehyde (**10**)

Diazirine **9** (502 mg, 2.3 mmol) was dissolved in CH₂Cl₂ and placed on ice. TiCl₄ (0.28 ml, 2.5 mmol) was added dropwise to the solution via syringe followed by dichloromethyl methyl ether (288 mg, 2.3 mmol) dissolved in CH₂Cl₂ (25 ml). The reaction was allowed to stir on ice for



3 h and was quenched by the slow addition of water and diluted with CH₂Cl₂ (25 ml). The CH₂Cl₂ was washed multiple times with saturated aqueous NaHCO₃ solution (5 x 20 ml) and dried over Na₂SO₄. After evaporation of the solvent in vacuo, the residue was purified by radial chromatography (2 mm plate, 5:1 hexane/EtOAc) to provide **10** as a pale amber oil (322 mg, 57%). The *para* (in relation to the diazirine ring) product elutes first.

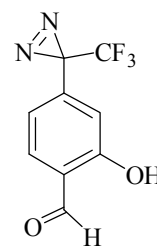
Spectroscopic data was consistent with literature⁴³. *Para* to diazirine ring: **¹H-NMR** (CDCl₃): δ = 3.92 (s, 3H), 6.68 (s, 1H), 6.83 (d, *J* = 8.1 Hz, 1 H), 7.82 (d, *J* = 8.1 Hz, 1

H), 10.42 (s, 1 H) ppm; $^{13}\text{C-NMR}$ (CDCl_3): δ = 28.6 (q, J = 40.3 Hz), 55.8, 109.5, 118.6, 121.8 (q, J = 274.4 Hz), 125.4, 129.0, 136.6, 161.5, 188.7 ppm;

Ortho to diazirine ring: $^1\text{H-NMR}$ (CDCl_3): δ 3.88 (s, 3H), 7.05 (dd, J = 8.7, 2.2 Hz, 1H), 7.16 (s, 1H), 7.89 d, J = 8.6 Hz, 1H), 10.38 (s, 1H) ppm; $^{13}\text{C-NMR}$ (CDCl_3): δ 27.2 (q, J = 43 Hz), 55.8, 116.2, 116.8, 121.6 (q, J = 275 Hz), 129.1, 130.8, 133.8, 164.6, 188.2 ppm;

Preparation of 2-Hydroxy-4-(3-trifluoromethyl-3-diazirine)-benzaldehyde (**12**)

BBr_3 (0.07 mL, 0.7 mmol) was added dropwise via syringe to a solution of **10** (170 mg, 0.7 mmol) in CH_2Cl_2 (3 mL) while on an ice bath at 0°C . The reaction was stirred for 30-45 min and monitored by TLC until the starting material was consumed. The reaction was quenched by the slow addition

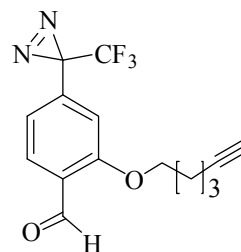


of H_2O (5 ml) followed by the addition of CH_2Cl_2 (25 ml). The CH_2Cl_2 layer was removed and washed with saturated aqueous NaHCO_3 solution (3 x 15 ml), and dried over Na_2SO_4 . After evaporation of the solvent, the crude residue was purified by radial chromatography (2 mm plate, 3:1 hexane/ CH_2Cl_2) to give **12** (127 mg, 79%) as a white solid. Spectroscopic data was consistent with literature.

$^1\text{H-NMR}$ (CDCl_3): δ 6.75–6.80 (m, 2H), 7.59 (d, J = 7.8 Hz, 1H), 9.91 (s, 1H), 11.04 (s, 1H) ppm; $^{13}\text{C-NMR}$ (CDCl_3): δ 28.4 (q, J = 41 Hz), 115.8, 117.3, 120.8, 121.6 (q, J = 275 Hz), 133.9, 138.0, 161.3, 195.9 ppm;

Preparation of 2-(Hex-5-ynyloxy)-4-(3-trifluoromethyl-diazirine)-benzaldehyde (1)

The diazirine-phenol **12** (203 mg, 0.88 mmol) was dissolved in DMF followed by the addition of K₂CO₃ (365 mg, 2.64 mmol) and KI (20 mg, 0.120 mmol). 6-Bromo-hex-1-yne (156 mg, 0.97 mmol) was added and the reaction mixture was allowed to stir for 18 h at



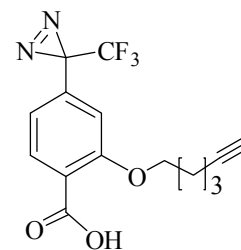
room temperature. The solution was diluted with ether (30 ml) and water (20 ml) and adjusted to neutral pH using 10% HCl solution. The aqueous layer was washed with ether multiple times and the combined ether layers dried over Na₂SO₄ and concentrated in vacuo. The residue was purified using radial chromatography (2 mm plate, 4:1 petroleum ether/diethyl ether) to give the product (200 mg, 73%) as a pale yellow oil:

¹H-NMR (CDCl₃): δ 1.74 (m, 2H), 1.97-2.04 (m, 3H), 2.30 (td, *J* = 4.3, 2.6 Hz, 2H), 4.11 (t, *J* = 6.2 Hz, 2H), 6.68 (s, 1H), 6.83 (d, *J* = 8.2 Hz, 1H), 7.83 (d, *J* = 8.2 Hz, 1H), 10.46 (s, 1H) ppm; **¹³C-NMR** (CDCl₃): δ 18.1, 24.9, 27.9, 28.6 (q, *J* = 41 Hz), 68.3, 69.0, 83.6, 110.3, 118.5, 121.8 (q, *J* = 273 Hz), 125.5, 128.9, 136.5, 161.0, 188.6 ppm; **¹⁹F-NMR** (CDCl₃): -64.76 (s) ppm;

HRMS-(ESI-TOF): calculated for C₁₅H₁₃N₂O₂F₃Na = 333.0821 [M + Na⁺]; observed 333.0830;

Preparation of 2-(Hex-5-ynyloxy)-4-(3-trifluoromethyl-diazirine)-benzoic acid (2)

Compound **1** (26 mg, 0.08 mmol) was dissolved in acetone, cooled to 0°C and allowed to stir. Jones reagent was added dropwise and the reaction allowed to stir for 15 min. The reaction was monitored by TLC and additional Jones reagent was added in 0.5 ml portions until

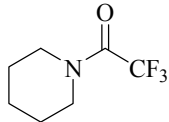


the starting material disappeared. The reaction was filtered to remove the green chromium precipitate by-product and water was added to the filtrate. The filtrate was washed with CH_2Cl_2 (3 x 20 ml). The CH_2Cl_2 layers were combined and washed with saturated NaHCO_3 solution (3 x 25 ml). The NaHCO_3 washes were combined and the pH adjusted to 2 using 10% HCl solution and washed with CH_2Cl_2 (3 x 25 ml). The organic extracts were combined, dried over Na_2SO_4 , and concentrated in vacuo to provide the product as a white solid (25 mg, 93%).

$^1\text{H-NMR}$ (CDCl_3): δ 1.71-1.80 (m, 2H), 2.01 (t, $J = 2.4$ Hz, 1H), 2.06-2.13 (m, 2H), 2.33 (td, $J = 4.0, 2.8$ Hz, 2H), 4.29 (t, $J = 6.4$ Hz, 2H) 6.77 (s, 1H), 6.95 (d, $J = 8.4$ Hz, 1H), 8.21 (d, $J = 8.4$ Hz, 1H) ppm; **$^{13}\text{C-NMR}$** (CDCl_3): δ 18.1, 24.9, 27.9, 28.4 (q, $J = 41$ Hz), 68.3, 69.0, 83.6, 110.3, 118.5, 121.6 (q, $J = 273$ Hz), 125.5, 128.9, 136.5, 164.6 ppm;

HRMS-(ESI-TOF): calculated for $\text{C}_{15}\text{H}_{13}\text{N}_2\text{O}_3\text{F}_3\text{Na} = 349.0770$ [$\text{M} + \text{Na}^+$]; observed 349.0773;

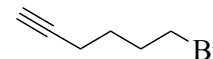
Preparation of N-(Trifluoroacetyl)piperidine

Piperidine (9.03 g, 0.11 mol) and triethylamine (8.71 g, 0.085 mol) were placed in a round bottom flask and diethyl ether (100 ml) was added. The  solution was cooled on ice and trifluoroacetic anhydride (12 ml, 0.086 mol) was added dropwise over 10 min. The reaction was flushed with nitrogen and allowed to stir for 2 h before dilution with water (50 ml) and additional diethyl ether (50 ml). The aqueous phase was discarded and the ether washed with 10% HCl (6 x 30 ml) and concentrated to give a pale yellow oil. This oil was stirred over CaH_2 overnight and kugelrohr distilled to provide a clear oil. (14.3 g, 92%).

¹H-NMR (CDCl₃): δ 1.60-1.74 (m, 6H), 3.55 (t, *J* = 5.2 Hz, 2H), 3.64 (t, *J* = 5.6 Hz, 2H) ppm; **¹³C-NMR** (CDCl₃): δ 24.1, 25.3, 26.3, 44.5, 46.8, 116.6 (q, *J* = 287 Hz), 155.2 (q, *J* = 36 Hz) ppm;

Preparation of 6-bromo-hex-1-yne

Hex-5-yne-1-ol (1.00 g, 0.01 mol) was dissolved in diethyl ether (30 ml) and placed in an ice bath. PBr₃ (0.97 ml, 0.01 mol) was slowly added with a syringe to the mixture and the solution allowed to stir for 3 h while on ice. The reaction was quenched by the slow, dropwise addition of NaHCO₃ (25 ml). The ether was washed with NaHCO₃ solution (5 x 30 ml) and dried with Na₂SO₄. The ether was concentrated and the residue purified by flash chromatography using hexane to yield 6-bromo-hex-1-yne as a colorless oil (1.06 g, 66%).

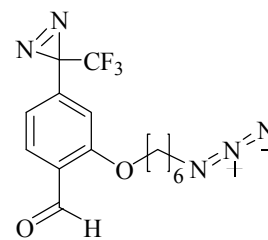


¹H-NMR (CDCl₃): δ 1.73 (p, *J* = 6.6 Hz, 2H), 1.96 (t, *J* = 1.9 Hz, 1H), 2.02 (p, *J* = 6.6 Hz, 2H), 2.30 (dt, *J* = 6.6, 1.9 Hz, 2H), 3.50 (t, *J* = 6.6 Hz, 2H) ppm;

Preparation of 2-(6-Azido-hexyloxy)-4-(3-trifluoromethyl-diazirine)-benzaldehyde (21)

The diazirine-phenol (127 mg, 0.55 mmol), K₂CO₃ (228 mg, 1.65 mmol) and KI (20 mg, 0.12 mmol) were combined in DMF (5 ml).

1-Azido-6-bromo-hexane⁹⁵ (227 mg, 1.10 mmol) was added dropwise and the reaction mixture was allowed to stir for 14 h at



room temperature. The solution was diluted with water (25 ml) and ether (25 ml) and the ether layer was removed. The aqueous layer was washed with ether (2 x 30 ml) and the combined ether layers were dried over Na₂SO₄ and concentrated in vacuo. The residue

was purified by radial chromatography (2 mm plate, 4:1 petroleum ether/diethyl ether) to provide **21** as a pale yellow oil (131 mg, 67%).

¹H-NMR (CDCl₃): δ 1.47-1.54 (m, 4H) 1.64 (dt, *J* = 6.6, 8.2 Hz, 2H), 1.88 (quint, *J* = 6.5 Hz, 2H), 3.30 (t, *J* = 6.8 Hz, 2H), 4.07 (t, *J* = 6.3 Hz, 2H), 6.68 (s, 1H) 6.83 (d, *J* = 8.2 Hz, 1H) 7.83 (d, *J* = 8.2 Hz, 1H) 10.46 (s, 1H) ppm; **¹³C-NMR** (CDCl₃): δ 25.6, 26.4, 28.6 (q, *J* = 40 Hz), 28.7, 28.8, 51.3, 68.6, 110.4, 118.6, 121.8 (q, *J* = 273 Hz) 125.5, 128.9, 136.6, 161.1, 188.7 ppm; **HRMS-(ESI-TOF)**: calculated for C₁₅H₁₆N₅O₂F₃Na = 378.1154 [M + Na⁺]; observed 378.1156;

Preparation of diazirine-PEG4-biotin, (23)

The diazirine azide **21** (51 mg, 0.14 mmol) and biotin-PEG4-alkyne (50 mg, 0.11 mmol) (purchased from Click Chemistry Tools) were dissolved in *t*-butyl alcohol:H₂O (5 ml, 4:1) followed by the addition of CuSO₄·H₂O (18 mg, 0.07 mmol) and sodium ascorbate (14 mg, 0.07 mmol). The mixture was allowed to stir for 18 h at room temperature. The solution was diluted with water and washed with CH₂Cl₂ (2 x 15 ml), dried over Na₂SO₄, filtered, and concentrated in vacuo. The residue was purified by column chromatography using (1:1 hexane/CH₂Cl₂) to remove unreacted starting materials and the product eluted with methanol to yield **23** as an amber oil (55 mg, 62%).

¹H-NMR (CDCl₃): δ 1.26-1.36 (m, 4H), 1.41-1.55 (m, 6H), 1.71-1.88 (m, 6H), 2.07 (m, 2H), 2.68 (d, *J* = 12.4 Hz, 2H), 2.81 (dd, *J* = 5.2 Hz, 12.4 Hz, 2H) 3.05-3.12 (m, 1H), 3.19 (t, *J* = 5.6 Hz, 2H), 3.34-3.40 (m, 2H), 3.40-3.56 (m, 12H), 4.11 (t, *J* = 6.4 Hz, 2H), 4.21 (dd, *J* = 4.4, 8.0 Hz 1H), 4.31 (t, *J* = 7.2 Hz, 2H), 4.37 (ddd, *J* = 0.8, 2.4, 2.8 Hz, 1H), 4.47 (s, 2H), 6.77 (s, 1H), 6.93 (dd, *J* = 8.0, 1.0 Hz, 1H), 7.71 (d, *J* = 8.0 Hz, 1H),

7.82 (s, 1H), 10.34 (d, $J = 1$ Hz, 1H) ppm; $^{13}\text{C-NMR}$ (CDCl_3): δ 25.5, 26.3, 28.0, 28.1, 28.4, 28.5 (q, $J = 40.4$ Hz), 28.8, 30.1, 30.1, 35.8, 39.2, 68.6, 69.8, 70.0, 70.1, 70.5, 70.5, 76.7, 110.4, 118.6, 120.4, 121.8 (q, $J = 273$ Hz) 123.1, 125.5, 129.0, 136.6, 161.1, 173.4, 188.7 ppm; **HRMS-(ESI-TOF)**: calculated for $\text{C}_{36}\text{H}_{51}\text{N}_8\text{O}_8\text{F}_3\text{SNa} = 835.3400$ [$\text{M} + \text{Na}^+$]; observed 835.3413;

Preparation of diazirine disulfide-PEG4-biotin, (24)

Aldehyde **23** (3 mg, 3.7 μmol), triethylamine (30 mg, 0.30 mmol) and cysteamine hydrochloride (20 mg, 0.18 mmol) were combined in 3 ml of EtOH and stirred at room temperature. ESI MS (positive ion mode) was used to monitor the disappearance of the aldehyde ($m/z = 813$) and the appearance of the Schiff base ($m/z = 947$) as a disulfide with cysteamine. When the aldehyde was no longer detectable, NaCNBH_4 (15 mg, 0.24 mmol) was added and the reaction was monitored by ESI MS (positive ion mode) until the Schiff base was fully reduced to the corresponding amine ($m/z = 949$). Water (5 ml) and CH_2Cl_2 (5 ml) were added and 10% HCl solution was added dropwise until all of the NaBH_4 had been quenched (approximately 20 drops). 10 ml of saturated aqueous NaHCO_3 solution was added to the reaction mixture. The phases were separated and the aqueous layer washed with CH_2Cl_2 (2 x 10 ml). The organic layers were combined, dried over Na_2SO_4 and concentrated in vacuo to provide the crude disulfide **24**.

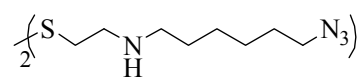
HRMS-(ESI-TOF): calculated for $\text{C}_{40}\text{H}_{63}\text{O}_7\text{N}_{10}\text{S}_3\text{F}_3 = 949.4068$ [$\text{M} + 1$]; found 949.4051;

Reduction of diazirine disulfide-PEG4-biotin, **24** with DTT:

The crude disulfide **24** was dissolved in 3 ml of MeOH and DTT (10 mg, 0.06 mmol) was added. The reaction mixture was stirred for 2 h at ambient temperature. This reaction was monitored ESI MS (positive ion mode) and stopped once the disulfide ($m/z = 949$) was completely reduced to the thiol ($m/z = 874$). The reaction was diluted with water (10 ml) and washed with diethyl ether (2 x 10 ml). The combined ether washes were dried over MgSO₄ and concentrated in vacuo. This thiol product was not purified but used immediately for thiol-Michael additions. ESI MS (positive ion mode) of the thiol product showed that no remaining DTT was present.

Preparation of N, N'-(disulfanediylobis(ethane-2,1-diyl))bis(6-azidohexan-1-amine)

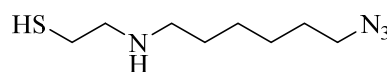
K₂CO₃ (3 g, 0.022 mol) was placed in a round bottom flask with cystamine dihydrochloride (2.20 g, 0.01 mol) and dissolved in DMF (30 ml). After stirring at room temperature for 30 min, 1-azido-6-bromo-hexane⁹⁷ (200 mg, 0.98 mmol) was added to the flask and the reaction allowed to stir overnight at room temperature. The reaction was diluted with water (65 ml) and washed with CH₂Cl₂ (3 x 30 ml). The combined organic phases were washed with water (5 x 15 ml) to remove DMF and concentrated in vacuo to provide crude disulfide (93 mg, 24% yield).



HRMS-(ESI-TOF): calculated for C₁₆H₃₅N₈S₂ = 403.2421 [M + 1]; observed 403.2435;

Preparation of 2-(6-azido-hexylamino)-ethanethiol (**26**)

This crude disulfide (93 mg, 0.23 mmol) was dissolved



in MeOH (5 ml) and DTT (93 mg, 0.60 mmol) was added. The mixture was stirred at room temperature. The reaction was monitored by ESI MS (positive ion mode) for the disappearance of the disulfide ($m/z = 403$) and the appearance of the thiol ($m/z = 203$). After 1.5 h the reaction mixture was diluted with water (20 ml) and washed with CH₂Cl₂ (2 x 25 ml). The combined CH₂Cl₂ layers were washed with water (15 ml), and dried over Na₂SO₄, filtered and evaporated in vacuo. The crude thiol was used immediately in the next step.

Preparation of azide thiazepene PbTx-2 (28)

Brevetoxin (250 µg, 0.28 µmol) was dissolved in MeOH (1 ml). 2-(6-Azido-hexylamino)-ethanethiol (10 mg, 0.05 mmol) was added and the mixture stirred for 3 hours. PbTx-2 was no longer detectable using ESI MS (positive ion mode). Purification was performed using HPLC. Conditions: Column 5 µm C₁₈, 250 mm X 4.6 mm Discovery column (Supelco, Bellefonte, PA). Mobile phase, A: MeOH. B: 0.2 % formic acid (aq.). Gradient: A:B, 10:90 to 30:70 at 10 min, to 40:60 at 15 min, to 90:10 at 30 min, flow rate: 0.5 ml/min.

HRMS-(ESI-TOF): calculated for C₅₈H₈₇O₁₃N₄S = 1079.5985 [M+1]; observed 1079.6007;

Click reaction between brevetoxin-azide linker 28 and alkyne fluorophor 488

A solution of CuSO₄·5H₂O (6.9 µl, 40 mM in DMF or 0.28 µmol) and sodium ascorbate (5.5 µl, 50.5 mM in DMF or 0.28 µmol) were added to the brevetoxin azide derivative **28** (300 µg, 0.28 µmol) in a *t*-butyl alcohol/H₂O solution (1 ml, 4:1). A solution of Alexa

fluor 488 alkyne (215 μg , 0.28 μmol) in DMF (215 μl) was added to the brevetoxin solution. The mixture was stirred in the dark for 18 h at room temperature.

Preparation of Microcystin-LR photoaffinity probe

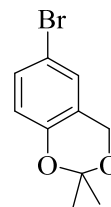
Microcystin-LR (1.0 mg, 1.0 μmol) was dissolved in MeOH (1 ml) and the crude thiol from the reduction of photoaffinity label **24** (1 mg) was added to this solution. The mixture was allowed to stir at room temperature. ESI MS of the solution showed the disappearance of the thiol though no product was able to be detected.

Preparation of Nodularin photoaffinity probe

Nodularin (1 mg, 1.2 μmol) was dissolved in MeOH (1 ml) and the crude thiol from the reduction of photoaffinity label **24** (1 mg) was added to this solution. The mixture was allowed to stir at room temperature. ESI MS of the solution showed the disappearance of the thiol though no product was able to be detected.

Preparation of 6-Bromo-2,2-dimethyl-4*H*-benzo[1,3]dioxine (**33**)

5-Bromo-2-hydroxybenzyl alcohol **32** (6 g, 0.030 mol), *p*-toluenesulfonic acid monohydrate (600 mg, 0.003 mol), and anhydrous sodium sulfate (25 g) was

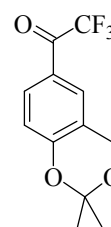


dissolved in DMP (70 ml) and the suspension allowed to stir at room temperature for 4 h. The reaction was diluted with EtOAc (80 ml) and filtered to remove the sodium sulfate. The organic mixture was washed with 5% NaOH (5 x 20 ml), dried with MgSO_4 and concentrated to provide **33** (6.96 g, 97% yield) as an oil. Spectroscopic data was consistent with literature⁹⁸.

¹H-NMR (Acetone-*d*₆): δ 1.49 (s, 6H), 4.85 (s, 2H), 6.73 (d, 1H), 7.24 (t, 1H), 7.30 (dd, 1H) ppm; **¹³C-NMR** (Acetone-*d*₆): δ 24.9, 60.8, 100.6, 112.7, 119.7, 123.1, 128.6, 131.6, 151.6 ppm;

Preparation of 1-(2,2-Dimethyl-4*H*-benzo[1,3]dioxin-6-yl)-2,2,2-trifluoro-ethanone (34)

6-Bromo-2,2-dimethyl-4*H*-benzo[1,3]dioxine **33** (3.0 g, 0.0123 mol) was placed in a flame dried round-bottom flask and dried under vacuum for 1 h. Anhydrous THF (30 mL) was transferred via syringe to the capped round-bottom flask. With a positive flow of nitrogen, the flask was cooled to -78°C in a dry ice/acetone bath. *n*-BuLi (7.72 ml, 1.6 M, 0.0123 mol) was transferred dropwise via syringe and the solution was allowed to stir for 7 min. *N*-trifluoroacetyl piperidine **4** (1.82 ml, 0.0123 mol) which had been kugelrohr distilled from CaH₂, was transferred by syringe to the reaction flask and the solution allowed to stir for 45 min at -78°C. The solution was brought to room temperature and allowed to stir for another 1.5 h. The reaction was diluted by the addition of H₂O (30 ml), saturated aqueous NH₄Cl (10 mL), and THF (30 ml). The aqueous layer was washed with THF (3 x 20 ml) and the combined THF layers dried over Na₂SO₄ and evaporated in vacuo to give a crude yellowish oil. This crude oil was purified by column chromatography (6:4 hexane/CH₂Cl₂) to provide **34** (2.54 g, 79%) as a colorless oil.

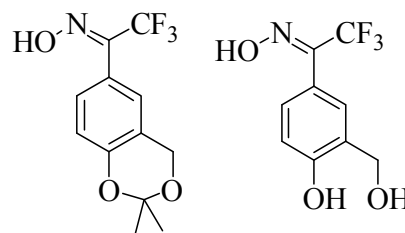


¹H-NMR (CDCl₃): δ 1.58 (s, 6H), 4.91 (s, 2H), 6.93 (d, *J* = 8.8 Hz, 1H), 7.76 (s, 1H), 7.92 (d, *J* = 8.8 Hz, 1H) ppm; **¹³C-NMR** (CDCl₃): δ 24.8, 60.5, 101.3, 116.9 (q, *J* = 290

Hz), 117.9, 119.9, 122.2, 128.0, 130.9, 157.9, 178.9 (q, $J = 35$ Hz) ppm; $^{19}\text{F-NMF}$ (CDCl_3): -70.91 (s) ppm;

Preparation of 1-(2,2-Dimethyl-4*H*-benzo[1,3]dioxin-6-yl)-2,2,2-trifluoro-ethanone oxime (35) and (42)

A solution of **34** (2.33 g, 0.0090 mol), hydroxylamine hydrochloride (778 mg, 0.0112 mol) in absolute ethanol (25 ml) and pyridine (2.66 g, 0.0336 mol) was heated to 35°C for five hours while monitoring the reaction using



TLC. The reaction was cooled and diluted with ether (50 ml) and H_2O (30 ml). The ether was washed with 10% HCl solution (5 x 25 ml), dried over Na_2SO_4 , filtered and concentrated in vacuo. The crude mixture was purified by column chromatography (15:1 CH_2Cl_2 :MeOH) to provide **35** as a yellow oil (2.02 g, 82%) and **42** as a white solid (371 mg, 18%).

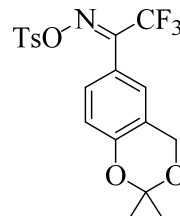
$^1\text{H-NMR}$ (Acetone- d_6): Mixture of *cis* and *trans* isomers of **35** - δ 1.52,1.53 (s,s, total = 6H), 4.90,4.92 (s,s, total = 2H), 6.85 (d, $J = 8.6$ Hz, 0.22H), 6.90 (d, $J = 8.6$ Hz, 0.82H), 7.23 (s, 0.22H), 7.31,7.33 (bs, bs, total = 1H), 7.38 (d, $J = 8.5$ Hz, 0.79H), 11.64 (bs, 0.62H) and 11.89 (bs, 0.15H) ppm; $^{13}\text{C-NMR}$ (Acetone- d_6): Mixture of *cis* and *trans* isomers of **35** - δ 25.0, 25.4, 61.1, 100.9, 101.0, 117.6, 117.7, 119.5, 120.8, 120.9, 122.3 (q, $J = 272$ Hz), 126.2,126.7, 129.0, 129.7, 146.3 (q, $J = 31$ Hz), 153.7, 153.8 ppm;

$^1\text{H-NMR}$ (Acetone- d_6): Mixture of *cis* and *trans* isomers of **42** - δ 4.51 (t, $J = 5.3$ Hz, 1H), 4.77,4.78 (s,s total = 2H), 6.93 (d, $J = 8.4$ Hz, 1H), 7.35 (dd, $J = 8.4, 1.8$ Hz, 1H), 7.55 (d, $J = 1.1$ Hz, 1H), 8.96 (s, 0.94H), 11.52 (s, 0.97H);

¹³C-NMR (Acetone-d₆): Mixture of *cis* and *trans* isomers of **42** - δ 60.93, 115.73, 118.75, 122.41 (q, *J* = 272 Hz), 128.90, 128.96, 129.69, 146.7 (q, *J* = 30 Hz), 157.36;

Preparation of (E & Z)-O-Tosyl-2,2,2-trifluoro-1-(3-Methoxy-phenyl)-ethanone oxime (36)

Oxime **35** (100 mg, 0.364 mmol), triethylamine (51 mg, 0.50 mmol), and (*N,N'*-dimethylamino)pyridine (20 mg, 0.164 mmol) was added to CH₂Cl₂ (20 ml) and allowed to stir at 0°C. To this solution, *p*-toluenesulfonyl chloride (76 mg, 0.399 mmol) was added in one portion and allowed to stir until triethylamine HCl salts precipitated out of the solution (typically within an hour). The reaction mixture was diluted with water (10 ml) and aqueous NaHCO₃ solution (10 ml) and allowed to stir for another hour. The two phases were separated and the CH₂Cl₂ washed with NaHCO₃ solution (2 x 10 ml). The CH₂Cl₂ was dried over Na₂SO₄, filtered and concentrated in vacuo. The product was purified by radial chromatography (2 mm plate, 1:1 hexane/CH₂Cl₂) to give **36** (144 mg, 92%) as pure white crystals (M.P. = 120-122°C).

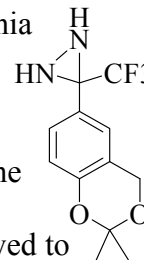


¹H-NMR (Acetone-d₆): Mixture of *cis* and *trans* isomers - δ 1.52, 1.54 (s,s, total = 6H), 2.45, 2.48 (s,s, total = 3H), 4.91, 4.93 (s,s, total = 2H), 6.90, 6.96 (dd *J* = 8.6 Hz, total = 1H), 7.28-7.40 (m, 2H), 7.52-7.55 (m, 2H), 7.90-7.94 (m, 2H) ppm; ¹³C-NMR (CDCl₃): δ 21.69, 24.69, 24.76, 60.47, 100.57, 100.63, 116.04, 117.56, 117.59, 119.80, 119.81 (q, *J* = 276 Hz), 119.83, 125.85, 125.99, 129.04, 129.12, 129.24, 129.88, 129.90, 131.18, 131.53, 146.02, 146.19, 153.06 (q, *J* = 33 Hz), 153.62 (q, *J* = 32 Hz), 154.30, 154.71 ppm; ¹⁹F-NMR (CDCl₃): -66.00 (s, 1F), -61.38 (s, 0.38F) ppm;

HRMS-(ESI-TOF): calculated for $C_{19}H_{19}N_1O_5S_1F_3 = 430.0931$ [$M + 1$]; observed 430.0957;

Preparation of 3-(2,2-dimethyl-4H-benzo[d][1,3]dioxin-6-yl)-3-(trifluoromethyl) diaziridine (37)

Ammonia gas was flushed into a pressure tube at $-78^{\circ}C$ until liquid ammonia (10 ml) was condensed. The tosyl oxime, **36** (2.03 g, 0.0047 mol) was dissolved in CH_2Cl_2 and the solution added to the pressure tube. Following the addition, the pressure tube was sealed, brought to room temperature and allowed to stir for 48 hours. The pressure tube was slowly opened over a period of an hour allowing excess ammonia to evaporate. The mixture was diluted with water (30 ml) and the CH_2Cl_2 layer removed. The water layer was washed with CH_2Cl_2 (2 x 15 ml) and the CH_2Cl_2 layers combined, dried over Na_2SO_4 , filtered and concentrated in vacuo. The crude residue was purified using radial chromatography (4 mm plate, 1:2 hexane/ CH_2Cl_2) to give **37** (1.13 g, 87%) as a white solid (M.P. = $104-106^{\circ}C$).

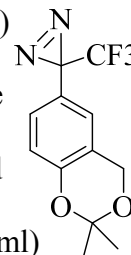


1H -NMR (Acetone- d_6): δ 1.50 (s, 6H), 3.15 (d, $J = 8.4$ Hz, 1H), 3.53 (d, $J = 8.4$ Hz, 1H), 4.88 (s, 2H), 6.83 (d, $J = 8.5$ Hz, 1H), 7.33 (s, 1H), 7.41 (d, $J = 8.5$ Hz, 1H) ppm;

^{13}C -NMR ($CDCl_3$): δ 24.9, 25.1, 58.2 (q, $J = 36$ Hz), 61.2, 100.7, 117.6, 120.7, 125.1, 125.3 (q, $J = 276$ Hz), 126.2, 129.1 153.4 ppm; **HRMS-(ESI-TOF):** calculated for $C_{12}H_{14}N_2O_2F_3 = 275.1002$ [$M + 1$]; observed 275.0997;

Preparation of 3-(2,2-dimethyl-4H-benzo[d][1,3]dioxin-6-yl)-3-(trifluoromethyl)-3H-diazirine (38)

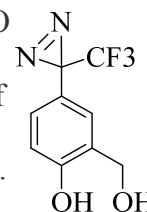
A solution of freshly prepared *tert*-butyl hypochlorite⁸⁵ (776 mg, 0.0071 mol) and a 1:1 2-methyl-2-propanol/ethanol (5 ml) mixture was made. This mixture was added dropwise to a solution of **37** (653 mg, 0.0024 mol) and triethylamine (1.08 g, 0.0107 mol) in a 1:1 2-methyl-2-propanol/ethanol (20 ml) mixture while at 0°C with vigorous stirring. After stirring at room temperature for 3 h, the reaction was quenched by the addition of a 10% aqueous solution of Na₂S₂O₅ (15 ml). The reaction mixture was extracted with ether (5 x 20 ml), and these organic extracts combined and dried over MgSO₄. Evaporation of the solvent, gave a crude yellow oil which was purified by column chromatography on silica gel (hexane/CH₂Cl₂ = 2:1) to give **38** (427 mg, 66%) as a pale yellow oil:



¹H-NMR (CDCl₃): δ 1.53 (s, 6H), 4.82 (s, 2H), 6.82-6.84 (3H), 7.02 (dd, *J* = 1.6, 8.6 Hz, 1H) ppm; ¹³C-NMR (CDCl₃): δ 24.6, 28.2 (q, *J* = 40 Hz), 60.6, 100.2, 117.7, 120.0, 120.7, 122.2 (q, *J* = 273 Hz), 123.3, 126.6, 152.6 ppm; ¹⁹F-NMR (CDCl₃): δ -65.6 (s) ppm; HRMS-(ESI-TOF): calculated for C₁₂H₁₃N₂O₃F₃ = 289.0806 [M + H₂O - 1]; observed 289.1057;

Preparation of 2-(hydroxymethyl)-4-(3-(trifluoromethyl)-3H-diazirin-3-yl)phenol (39)

Compound **38** (255 mg, 0.938 mmol) was dissolved into a methanol/H₂O solution (6 ml, 5:1) and allowed to stir at room temperature. Five drops of concentrated HCl was added to the solution and the mixture allowed to stir.

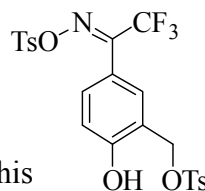


The reaction mixture was monitored by TLC until the starting material was no longer detectable by TLC (36-48 h). The reaction was quenched by the addition of saturated aqueous NaHCO₃ (5 ml). The aqueous layer was partitioned and extracted with THF (2 x 10 ml). The THF extracts were combined, dried over Na₂SO₄, filtered and concentrated in vacuo. The product was purified by radial chromatography (2 mm plate, CH₂Cl₂) to give **39** (146 mg, 67%) as a white solid.

¹H-NMR (CDCl₃): δ 4.87 (s, 2H), 6.88 (s, 1H), 6.90 (d, *J* = 8.6 Hz, 1H), 7.08 (dd, *J* = 2.2, 8.5 Hz, 1H); **¹³C-NMR** (CDCl₃): δ 28.1 (q, *J* = 40 Hz), 64.1, 117.1, 120.4, 122.2 (q, *J* = 273 Hz), 125.2, 126.3, 128.0, 157.3 ppm; **HRMS-(ESI-LIFDI)**: calculated for C₁₅H₁₆N₅O₂F₃Na = 232.0454 [M + 1]; observed 232.0451;

Preparation of (E & Z)-2-hydroxy-5-(2,2,2-trifluoro-1-((tosyloxy)imino)ethyl)benzyl 4-methylbenzenesulfonate (**43**)

Oxime **42** (79 mg, 0.336 mmol), triethylamine (89 mg, 0.882 mmol), and (*N,N'*-dimethylamino)pyridine (20 mg, 0.164 mmol) was added to a 1:1 ACN:CH₂Cl₂ solution (15 ml) and allowed to stir at 0°C. To this solution, *p*-toluenesulfonyl chloride (135 mg, 0.706 mmol) was added in one portion and allowed to stir for two h. During that time, triethylamine HCl salts precipitated out. The reaction mixture was diluted with water (5 ml) and saturated NaHCO₃ solution (5 ml) and allowed to stir for another hour. The organic layer was removed and the aqueous layer washed with CH₂Cl₂ (3 x 15 ml). The CH₂Cl₂ layers were combined and dried over Na₂SO₄, filtered and concentrated in vacuo. The product was purified by radial



chromatography (2 mm plate, 1:1 hexane/CH₂Cl₂) to give **43** (175 mg, 96%) as pure white crystals.

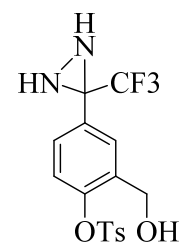
¹H-NMR (CDCl₃): Mixture of *cis* and *trans* isomers - δ 2.48, 2.49 (s,s, total = 6.91H), 4.58 (s, 0.32H), 4.61 (s, 2H), 6.93 (d, *J* = 8.6 Hz, 0.17H), 7.05 (d, *J* = 8.5 Hz, 1H), 7.28 (dd, *J* = 8.5, 2.2 Hz, total = 1.21 Hz), 7.39 (d, *J* = 7.5 Hz, total = 4.8H), 7.57 (d, *J* = 1.9 Hz, 1H), 7.79 (d, *J* = 8.4 Hz, total = 2.47H), 7.88 (d, *J* = 8.4 Hz, total = 2.20H) ppm;

¹³C-NMR (CDCl₃): Mixture of *cis* and *trans* isomers - δ 21.8, 59.2, 59.3, 119.4 (q, *J* = 276 Hz), 122.9, 122.9, 123.7, 128.5, 129.2, 129.3, 129.9, 130.0, 130.2, 130.2, 130.9, 132.1, 135.8, 146.4, 146.4, 148.8, 152.8 (q, *J* = 34 Hz) ppm;

¹⁹F-NMR (CD₃Cl): Mixture of *cis* and *trans* isomers - δ -65.15 (s, 0.15H), -66.64 (s, 1H) ppm;

Preparation of 2-(hydroxymethyl)-4-(3-(trifluoromethyl)diaziridin-3-yl)phenyl 4-methylbenzenesulfonate (**44**)

Ammonia gas was flushed through a pressure tube at -78°C until liquid ammonia (10 ml) was condensed. The oxime-tosylate **43** (175 mg, 0.322 mmol) was dissolved in CH₂Cl₂ and the solution added to the pressure tube. The pressure tube was sealed and brought to room temperature and



allowed to stir for 48 h. The pressure tube was slowly opened over a period of an hour allowing excess ammonia to evaporate. The mixture was diluted with water (30 ml) and the CH₂Cl₂ layer removed. The water layer was washed with CH₂Cl₂ (2 x 15 ml) and the CH₂Cl₂ layers combined, dried over Na₂SO₄, filtered and concentrated in vacuo. The

crude residue was purified using radial chromatography (1 mm plate, 20:1 CH₂Cl₂/MeOH) to give **44** as a very pale yellow oil (89 mg, 68%):

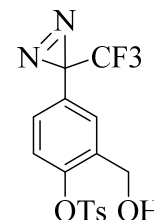
¹H-NMR (Acetone-d₆): δ 2.49 (s, 3H), 3.41 (d, *J* = 8.4 Hz, 1H), 3.69 (d, *J* = 8.5 Hz, 1H), 4.44 (t, *J* = 5.6 Hz, 1H), 4.56 (d, *J* = 5.3 Hz, 2H), 7.12 (d, *J* = 8.5, 1H), 7.53 (m, 3H), 7.82 (d, *J* = 8.4 Hz, 2H), 7.88 (s, 1H) ppm;

¹³C-NMR (Acetone-d₆): δ 21.6, 58.3 (q, *J* = 35 Hz), 58.9, 122.7, 125.1 (q, *J* = 276 Hz), 129.0, 129.1, 129.5, 131.1, 132.3, 133.8, 137.1, 147.1, 148.2 ppm;

HRMS-(ESI-TOF): calculated for C₁₆H₁₅N₂S₁O₄F₃ = 411.0597 [M + Na⁺]; observed 411.0600;

Preparation of 2-(hydroxymethyl)-4-(3-(trifluoromethyl)-3H-diazirin-3-yl)phenyl 4-methylbenzenesulfonate (45)

A solution of **44** (56 mg, 0.144 mmol) in 1:1 2-methyl-2-propanol/ethanol (10 ml) and triethylamine (150 mg, 1.482 mmol) was prepared and allowed to stir at 0°C. Freshly prepared *tert*-butyl hypochlorite (50 mg, 0.461 mmol) in 1:1 2-methyl-2-propanol/ethanol (2 ml) mixture was added dropwise to



the reaction mixture and allowed to stir for 1.5 h. The reaction was quenched by the addition of a 10% aqueous solution of Na₂S₂O₅ (10 ml). The reaction mixture was extracted with CH₂Cl₂, and the organic layer dried over MgSO₄. Evaporation of the solvent, gave a crude yellow oil which was purified by radial chromatography (1 mm plate, 20:1 CH₂Cl₂/MeOH) to give **45** (24 mg, 43%) as a pale yellow oil:

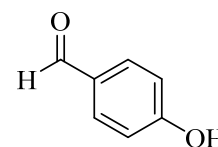
¹H-NMR (CDCl₃): δ 2.48 (s, 3H), 4.58 (s, 2H), 6.93 (d, *J* = 8.6, 1H), 7.09 (dd, *J* = 8.5, 2.2 Hz, 1H), 7.34 (d, *J* = 2.2 Hz, 1H), 7.38 (d, *J* = 8.0 Hz, 2H), 7.76 (d, *J* = 8.4 Hz, 2H)

ppm; **HRMS-(ESI-TOF)**: calculated for $C_{16}H_{13}N_2S_1O_4F_3 = 409.0440$ [$M + Na^+$];

observed 409.0450;

Preparation of 4-hydroxybenzaldehyde

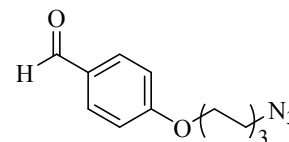
p-Methoxy benzaldehyde (1 g, 0.0074 mol) was placed in a round bottom flask with CH_2Cl_2 (20 ml) and placed on ice. BBr_3 (0.7 ml, 0.0078 mol) was added dropwise and the solution was allowed to stir for two hours. The reaction was brought to room temperature and allowed to stir for an additional two hours before being quenched with concentrated $NaHCO_3$ solution (20 ml). The CH_2Cl_2 layer was removed and washed with 10% $NaOH$ solution (5 x 15 ml). The $NaOH$ washings were combined and the pH adjusted to neutral using 10% HCl solution and washed with CH_2Cl_2 (2 x 20 ml). The CH_2Cl_2 layers were combined, dried over Na_2SO_4 and concentrated in vacuo to give the product as a yellow solid (385 mg, 43% yield). Spectroscopic data was consistent with literature⁹⁸.



1H -NMR ($CDCl_3$): δ 6.25 (s, 1H), 6.97 (d, $J = 8.4$ Hz, 2H), 7.81 (d, $J = 8.4$ Hz, 2H), 9.86 (s, 1H) ppm;

Preparation of 4-((6-azidohexyl)oxy)benzaldehyde

4-Hydroxybenzaldehyde (285 mg, 0.0023 mol), K_2CO_3 (969 mg, 0.007 mol), KI (25 mg, 0.12 mmol) and 1-azido-6-bromohexane⁹⁷ (722 mg, 0.0035 mol) were combined in DMF (15 ml) and allowed to stir for 3 d at room temperature. The solution was diluted with water (25 ml) and ethyl acetate (75 ml) and the ethyl acetate layer removed and washed with water (5 x 20 ml). The ethyl acetate was dried over Na_2SO_4 and concentrated in vacuo. The crude residue was purified



using radial chromatography (2 mm plate, 8:1-1:2 hexane/ethyl acetate) to yield a pale yellow oil (326 mg, 56% yield).

¹H-NMR (CDCl₃): δ 1.48 (m, 4H), 1.64 (q, *J* = 7.1 Hz, 2H), 1.83 (q, *J* = 6.5 Hz, 2H), 3.29 (t, *J* = 6.8 Hz, 2H), 4.04 (t, *J* = 6.4 Hz, 2H), 6.98 (d, *J* = 8.7 Hz, 2H), 7.82 (d, *J* = 8.7 Hz, 2H), 9.87 (s, 1H) ppm; **¹³C-NMR** (CDCl₃): δ 25.6, 26.5, 28.8, 28.9, 51.4, 68.1, 114.7, 129.8, 132.0, 164.2, 190.9 ppm;

References:

-
- ¹ Glibert, P.; Anderson, D.; Gentien, P.; Graneli, E.; Sellner, K. The global complex phenomena of harmful algae blooms. *Oceanography*, **2005**, *18*, 130-141.
- ² Pierce, R.H.; Henry, M.S. Harmful algal toxins of the Florida red tide (*Karenia brevis*): natural chemical stressors in South Florida coastal ecosystems. *Ecotoxicology*, **2008**, *17*, 623-631.
- ³ Fleming, L.E.; Kirkpatrick, B.; Backer, L.C.; Walsh, C.J.; Nierenberg, K.; Clark, J.; Reich, A.; Hollenbeck, J.; Benson, J.; Cheng, Y.S.; Naar, J.; Pierce, R.; Bourdelais, A.J.; Abraham, W.M.; Kirkpatrick, G.; Zaias, J.; Wanner, A.; Mendes, E.; Shalat, S.; Hoagland, P.; Stephan, W.; Bean, J.; Watkins, S.; Clarke, T.; Byrne, M.; Baden, D.G. Review of Florida red tide and human health effects. *Harmful Algae*, **2011**, *10*, 224-233.
- ⁴ Backer, L.C. Impacts of Florida red tides on coastal communities. *Harmful Algae*, **2009**, *8*, 618-622.
- ⁵ Heil, D.C. *Karenia brevis* monitoring, management, and mitigation for Florida molluscan shellfish harvesting areas. *Harmful Algae*, **2009**, *8*, 608-610.
- ⁶ Flewelling, L.; Naar, J.; Abbott, J.; Baden, D.G.; Barros, N.B.; Bossart, G.D.; Bottein, M.; Hammond, D.G.; Haubold, E.M.; Heil, C.A.; Henry, M.S.; Jacocks, H.M.; Leighfield, T.A.; Pierce, R.H.; Pitchford, T.D.; Rommel, S.; Scott, P.S.; Steidinger, K.A.; Truby, E.W.; Van Dolah, F.M.; Landsberg, J.H. Brevetoxicosis: Red tides and marine mammal mortalities. *Nature*, **2005**, *435*, 755-756.
- ⁷ Watkins, S.M.; Reich, A.; Fleming, L.E.; Hammond, R. Neurotoxic shellfish poisoning. *Marine Drugs*, **2008**, *6*, 431-455.
- ⁸ Kirkpatrick, B.; Fleming, L.E.; Squicciarini, D.; Backer, L.C.; Clark, R.; Abraham, W.; Benson, J.; Cheng, Y.S.; Johnson, D.; Pierce, R.; Zaias, J.; Bossart, G.D.; Baden, D.G. Literature review of Florida red tide: implications for human health effects. *Harmful Algae*, **2004**, *3*, 99-115.
- ⁹ Bossart, G.D.; Baden, D.; Ewing, R.; Roberts, B.; Wright, S. Brevetoxicosis in Manatees from the 1996 epizootic: Gross, histologic, and immunohistochemical features. *Toxicol. Pathol.*, **1998**, *26*, 276-282.
- ¹⁰ Baden, D.G.; Bourdelais, A.J.; Jacocks, H.; Michelliza, S.; Naar, J. Natural and derivative brevetoxins: Historical background, multiplicity, and effects. *Environ. Health Persp.*, **2005**, *113*, 621-625.
- ¹¹ Lombet, A.; Bidard, J.; Lazdunski, M. Ciguatoxin and brevetoxins share a common receptor site on the neuronal voltage-dependent Na⁺ channel. *FEBS Lett.*, **1987**, *219*, 355-359.

-
- ¹² Nicolaou, K.C.; Aversa, R. Maitotoxin: An inspiration for synthesis. *Isr. J. Chem.*, **2011**, *51*, 359-377.
- ¹³ Wang, D. Neurotoxins from marine *dinoflagellates*: A brief review. *Marine Drugs*, **2008**, *6*, 349-371.
- ¹⁴ Tubaro, A.; Dell'Ovo, V.; Sosa, S.; Florio, C. Yessotoxins: A toxicological review. *Toxicon*, **2010**, *56*, 163-172.
- ¹⁵ Miles, C.O.; Samdal, I.A.; Aasen, J.A.G.; Jensen, D.J.; Quilliam, M.A.; Petersen, D.; Briggs, L.M.; Wilkins, A.L.; Rise, F.; Cooney, J.M.; MacKenzie, A.L. Evidence of numerous analogs of yessotoxins in *Protoceratium reticulatum*. *Harmful Algae*, **2005**, *4*, 1075-1091.
- ¹⁶ Andresen, B.M.; Du Bois, J. De novo synthesis of modified saxitoxins for sodium ion channel study. *J. Am. Chem. Soc.*, **2009**, *131*, 12524-12525.
- ¹⁷ Cestele, S.; Catterall, W. Molecular mechanisms of neurotoxin action on voltage-gated sodium channels. *Biochimie*, **2000**, *82*, 883-892.
- ¹⁸ Flewelling, L.J.; Naar, J.P.; Abbott, J.P.; Baden, D.G.; Barros, N.B.; Bossart, G.D.; Bottein, M.Y.; Hammond, D.G.; Haubold, E.M.; Heil, C.A.; Henry, M.S.; Jacocks, H.M.; Leighfield, T.A.; Pierce, R.H.; Pitchford, T.D.; Rommel, S.A.; Scott, P.S.; Steidinger, K.A.; Truby, E.W.; Van Dolah, F.M.; Landsberg, J.H. Brevetoxins: Red tides and marine mammal mortalities. *Nature*, **2005**, *435*, 755-756.
- ¹⁹ LePage, K.T.; Baden, D.G.; Murray, T.F. Brevetoxin derivatives act as partial agonist at neurotoxin site 5 on the voltage-gated Na⁺ channel. *Brain Res.*, **2003**, *959*, 120-127.
- ²⁰ Gawley, R.; Rein, K.; Jeglitsch, G.; Adams, D.; Theodorakis, E.; Tiebes, J.; Nicolaou, K.; Baden, D. The relationship of brevetoxin 'length' and A-ring functionality to binding and activity in neuronal sodium channels. *Chem. Biol.*, **1995**, *2*, 533-541.
- ²¹ Steidinger, K.A. Historical perspective on *Karenia brevis* red tide research in the Gulf of Mexico. *Harmful Algae*, **2009**, *8*, 549-561.
- ²² Purkerson-Parker, S.; Fieber, L.; Rein, K.; Podona, T.; Baden, D.G. Brevetoxin derivatives that inhibit toxin activity. *Chem. Biol.*, **2000**, *7*, 385-393.
- ²³ Bourdelais, A.J.; Campbell, S.; Jacocks, H.; Naar, J.; Wright, J.L.; Carsi, J.; Baden, D.G. Brevenal is a natural inhibitor of brevetoxin action in sodium channel receptor binding assays. *Cell. Mol. Neurobiol.* **2004**, *24*, 553-563.

-
- ²⁴ Gold, E.; Jacocks, H.; Bourdelais, A.; Baden, D. Brevenal, a brevetoxin antagonist from *Karenia brevis*, binds to a previously unreported site on mammalian sodium channels. *Harmful Algae*, **2013**, *26*, 12-19.
- ²⁵ Potera, C.; Florida red tide brews up drug lead for cystic fibrosis. *Science*, **2007**, *316*, 1561-1562.
- ²⁶ Ebine, M.; Fuwa, H.; Sasaki, M. Total synthesis of (-)-brevenal: A concise synthetic entry to the pentacyclic polyether core. *Org. Lett.*, **2008**, *10*, 2275-2278.
- ²⁷ Takamura, H.; Kukuchi, S.; Nakamura, Y.; Yamagami, Y.; Kishi, T.; Kadota, L.; Yamamoto, Y. Total synthesis of brevenal. *Org. Lett.*, **2009**, *11*, 2531-2534.
- ²⁸ Zhang, Y.; Rohanna, J.; Zhou, J.; Iyer, K.; Rainier, J. Total synthesis of brevenal. *J. Am. Chem. Soc.*, **2011**, *133*, 3208-3216.
- ²⁹ Errera, R.; Bourdelais, A.; Drennan, M.A.; Dodd, E.B.; Henrichs, D.W.; Campbell, L. Variation in brevetoxin and brevenal content among clonal cultures of *Karenia brevis* may influence bloom toxicity. *Toxicon*, **2010**, *55*, 195-203.
- ³⁰ Kirst, G.O. Salinity tolerance of eukaryotic marine algae. *Annu. Rev. Plant Physiol. Plant Mol. Biol.*, **1989**, *40*, 21-53.
- ³¹ Taylor, A.R. A fast Na⁺/Ca²⁺ based action potential in a marine diatom. *PLoS ONE*, **2009**, *4*, e4966.
- ³² Errera, R.M.; Campbell, L. Osmotic stress triggers toxin production by the dinoflagellate *Karenia brevis*. *PNAS*, **2011**, *108*, 10597-10601.
- ³³ Sunda, W.; Burleson, C.; Hardison, R.; Morey, J.; Wang, Z.; Wolny, J.; Corcoran, A.; Flewelling, L.; Van Dolah, F. Osmotic stress does not trigger brevetoxin production in the dinoflagellate *Karenia brevis*. *PNAS*, **2013**, *110*, 10223-10228.
- ³⁴ Errera, R.M.; Campbell, L. Osmotic stress does trigger brevetoxin production in the dinoflagellate *Karenia brevis*. *PNAS*, **2013**, *110*, E2255.
- ³⁵ Sunda, W.G.; Burleson, C.; Hardison, R.D.; Morey, J.S.; Wang, Z.; Wolny, J.; Corcoran, A.A.; Flewelling, L.J.; Van Dolah, F.M. Reply to Errera and Campbell: No, low salinity shock does not increase brevetoxins in *Karenia brevis*. *PNAS*, **2013**, *110*, e2256.
- ³⁶ Cohen, J.; Tester, P.; Forward, R. Sublethal effects of the toxic dinoflagellate *Karenia brevis* on marine copepod behavior. *J. Plankton Res.*, **2007**, *29*, 301-315.
- ³⁷ Van Dolah, F.M.; Lidie, K.B.; Monroe, E.A.; Bhattacharya, D.; Campbell, L.; Doucette, G.J.; Kamykowski, D. The Florida red tide dinoflagellate *Karenia brevis*: New

insights into cellular and molecular processes underlying bloom dynamics. *Harmful Algae*, **2009**, *8*, 562-572.

³⁸ Bryant J.; Chapin III, F.S.; Klein, D.R. Carbon/nutrient balance of boreal plants in relation to vertebrate herbivory. *Oikos*, **1983**, *40*, 357-368.

³⁹ Hardiness, D.; Sunda, W.; Litaker, W. Nitrogen limitation increases brevetoxins in *Karenia brevis* (dinophyceae): Implications for bloom toxicity. *J. Phycol.*, **2012**, *48*, 844-858.

⁴⁰ Hardison, D.; Sunda, W.; Shea, D.; Litaker, R. Increased toxicity of *Karenia brevis* during phosphate limited growth: ecological and evolutionary implications. *PLoS ONE*, **2013**, *8*, e58545.

⁴¹ Sunda, W.; Graneli, E.; Gobler, C. Positive feedback and the development and persistence of ecosystem disruptive algal blooms. *J. Phycol.*, **2006**, *42*, 963-974.

⁴² Fu, F.X.; Place, A.R.; Garcia, N.S.; Hutchins, D.A. CO₂ and phosphate availability control the toxicity of the harmful bloom dinoflagellate *Karlodinium veneficum*. *Aquat. Microb. Ecol.*, **2010**, *59*, 55-65.

⁴³ Hashimoto, M.; Kanaoka, Y.; Hatanaka, Y. A versatile approach for functionalization of 3-aryl-3-trifluoromethyl-diazirine photophor. *Heterocycles*, **1997**, *46*, 119-122.

⁴⁴ Hatanaka, Y.; Hashimoto, M.; Hiroko, K.; Nakayama, H.; Kanaoka, Y. A novel family of aromatic diazirines for photoaffinity labeling. *J. Org. Chem.*, **1994**, *59*, 383-387.

⁴⁵ Dequierez, G.; Pons, V.; Dauban, P. Nitrene chemistry in organic synthesis: Still in its infancy? *Angew. Chem. Int. Ed.*, **2012**, *51*, 7384-7395.

⁴⁶ Lwowski, W. Nitrenes in photoaffinity labeling: Speculations of an organic chemist. *Ann. N.Y. Acad. Sci.*, **1980**, *346*, 491-500.

⁴⁷ Hashimoto, M.; Hatanaka, Y.; Yang, J.; Dhesi, J.; Holman, G.D. Synthesis of biotinylated bis(D-glucose) derivatives for glucose transporter photoaffinity labeling. *Carbohydr. Res.*, **2001**, *331*, 119-127.

⁴⁸ Konoki K.; Hashimoto, M.; Honda, K.; Tachibana, K.; Tamate, R.; Hasegawa, F.; Oishi, T.; Murata, M. Maitotoxin-photoactive probe binds to membrane proteins in blood cells. *Heterocycles*, **2009**, *79*, 1007-1017.

⁴⁹ Trainer, V.L.; Thomsen, W.J.; Catterall, W.A.; Baden, D.G. Photoaffinity labeling of the brevetoxin receptor on sodium channels in rat brain synaptosomes. *Mol. Pharmacol.*, **1991**, *40*, 988-994.

-
- ⁵⁰ Moss, R.A. Diazirines: Carbene precursors par excellence. *Acc. Chem. Res.*, **2006**, *39*, 267-272.
- ⁵¹ Paulsen, S.R. 3, 3-Dialkyl-diazacyclopropen-(1). *Angew. Chem. Int. Ed. Engl.*, **1960**, *72*, 781-782.
- ⁵² Pierce, L.; Dobyms, V.J. Molecular structure, dipole moment, and quadrupole coupling constants of diazidine. *J. Am. Chem. Soc.*, **1962**, *84*, 2651-2652.
- ⁵³ Richards, F.M.; Lamed, R.; Wynn, R.; Patel, D.; Olack, G. Methylene as a possible universal footprinting reagent that will include hydrophobic surface areas: Overview and feasibility: Properties of diazidine as a precursor. *Protein Sci.*, **2000**, *9*, 2506-2517.
- ⁵⁴ Craig, P.O.; Ureta, D.B.; Delfino, J.M. Probing protein conformation with a minimal photochemical reagent. *Protein Sci.*, **2002**, *11*, 1353-1366.
- ⁵⁵ Smith, R. A. G.; Knowles, J.R. Aryldiazirines. Potential reagents for photolabeling of biological receptor sites. *J. Am. Chem. Soc.*, **1973**, *95*, 5072-5073.
- ⁵⁶ Kerwin, B.; Remmele, R. Protect from light: Photodegradation and protein biologics. *J. Pharm. Sci.*, **2007**, *96*, 1468-1479.
- ⁵⁷ Ford, F. ; Yuzawa, T.; Platz, M.S.; Matzinger, S.; Fulscher, M. Rearrangement of dimethylcarbene to propene: Study by laser flash photolysis and *ab initio* molecular orbital theory. *J. Am. Chem. Soc.*, **1998**, *120*, 4430-4438.
- ⁵⁸ Das, J. Aliphatic diazirines as photoaffinity probes for proteins: recent developments. *Chem. Rev.*, **2011**, *111*, 4405-4417.
- ⁵⁹ Dewar, M.J.S.; Haddon, R.C.; Weiner, P. K. MINDO [modified intermediate neglect of differential overlap]/3 study of the electronic states of methylene. *J. Am. Chem. Soc.*, **1974**, *96*, 253-255.
- ⁶⁰ Brunner, J.; Senn, H.; Richards, F. 3-Trifluoromethyl-3-phenyldiazirine. A new carbene generating group for photolabeling reagents. *J. Biol. Chem.*, **1980**, *225*, 3313-3318.
- ⁶¹ Church, R.F.R.; Weiss, M.J. Diazirines: Synthesis and properties of small functionalized diazidine molecules. Some observations on the reaction of a diazidine with the iodine-iodide ion system. *J. Org. Chem.*, **1970**, *35*, 2465-2471.
- ⁶² De Clercq, P.J. Biotin: A timeless challenge for total synthesis. *Chem. Rev.*, **1997**, *97*, 1755-1792.

-
- ⁶³ Holmberg, A.; Blomstergren, A.; Nord, O.; Lukacs, M.; Lundeberg, J.; Uhlén, M. The biotin-streptavidin interaction can be reversibly broken using water at elevated temperatures. *Electrophoresis*, **2005**, *26*, 501-510.
- ⁶⁴ Huisgen, R. Kinetics and reaction mechanisms: selected examples from the experience of forty years. *Pure Appl. Chem.*, **1989**, *61*, 613-628.
- ⁶⁵ Meldal, M.; Tornøe, C.W. Cu-catalyzed azide-alkyne cycloaddition. *Chem. Rev.*, **2008**, *108*, 2952-3015.
- ⁶⁶ Tornøe, C.W.; Christensen, C.; Meldal, M.J. Peptidotriazoles on solid phase: [1,2,3]-triazoles by regiospecific copper(I)-catalyzed 1,3-dipolar cycloadditions of terminal alkynes to azides. *J. Org. Chem.*, **2002**, *67*, 3057-3064.
- ⁶⁷ Rostovtsev, V.V.; Green, L.G.; Fokin, V.V.; Sharpless, B. A stepwise huisgen cycloaddition process: copper(I)-catalyzed regioselective “ligation” of azides and terminal alkynes. *Angew. Chem., Int. Ed.*, **2002**, *41*, 2596-2599.
- ⁶⁸ Zurawell, R.W.; Chen, H.R.; Burke, J.M.; Prepas, E.E.; Hepatotoxic cyanobacteria: A review of the biological importance of microcystins in freshwater environments. *J. Toxicol. Environ. Health, Part B*, **2005**, *8*, 1-37.
- ⁶⁹ Moore, R.E.; Chen, J.L.; Moore, B.S.; Patterson, G. Biosynthesis of Microcystin-LR. Origin of the carbons in the adda and masp units. *J. Am. Chem. Soc.*, **1991**, *113*, 5083-5084.
- ⁷⁰ Christiansen, G.; Yoshida, W.Y.; Blom, J.F.; Portman, C.; Gademann, K.; Hemscheidt, T.; Kurmayer, R. Isolation and structure determination of two microcystins and sequence comparison of the McyABC adenylation domains *Planktothrix* species. *J. Nat. Prod.*, **2008**, *71*, 1881-1886.
- ⁷¹ De Figueiredo, D.; Azeiteiro, U.; Esteves, S.; Gonçalves, F.; Pereira, M. Microcystin-producing blooms: A serious global public health issue. *Ecotoxicol. Environ. Saf.*, **2004**, *59*, 151-163.
- ⁷² Klein, A.R.; Baldwin, D.S.; Silvester, E. Proton and iron binding by the cyanobacterial toxin Microcystin-LR. *Environ. Sci. Technol.*, **2013**, *47*, 5178-5184.
- ⁷³ Young, F.M.; Thomson, C.; Metcalf J.S.; Lucocq, J.M.; Codd, G.A. Immunogold localization of microcystins in cryosectioned cells of *Microcystis*. *J. Struct. Biol.*, **2005**, *151*, 208-214.
- ⁷⁴ Wiedner, C.; Visser, P.; Fastner, J.; Metcalf, J.; Codd, G.; Mur, L. Effects of light on the microcystin content of *Microcystis* strain PCC 7806. *Appl. Environ. Microbiol.*, **2003**, *69*, 1475-1481.

-
- ⁷⁵ Kaebernick, M.; Neilan, B.; Borner, T.; Dittmann, E. Light and the transcriptional response of the microcystin biosynthesis gene cluster. *Appl. Environ. Microbiol.*, **2000**, *66*, 3387-3392
- ⁷⁶ Imanishi, S.; Kato, H.; Mizuno, M.; Tsuji, K.; Harada, K. Bacterial degradation of microcystins and nodularin. *Chem. Res. Toxicol.*, **2005**, *18*, 591-598.
- ⁷⁷ Saito, K.; Konno, A.; Ishii, H.; Saito, H.; Nishida, F.; Abe, T.; Chen, C. Nodularin-Har: A new nodularin from *Nodularia*. *J. Nat. Prod.*, **2001**, *64*, 139-141.
- ⁷⁸ Runnegar, M.; Berndt, N.; Kong, S.; Lee, E.; Zhang, L. In vivo and in vitro binding of microcystin to protein phosphatases 1 and 2A. *Biochem. Biophys. Res. Commun.*, **1995**, *216*, 162-169.
- ⁷⁹ Panchuk-Voloshina, N.; Haugland, R.; Bishop-Stewart, J.; Bhargat, M.; Millard, P.; Mao, F.; Leung, W.Y.; Haugland, R. Alexa dyes, a series of new fluorescent dyes that yield exceptionally bright, photostable conjugates. *J. Histochem. Cytochem.*, **1999**, *47*, 1179-1188.
- ⁸⁰ Baden, D.G. Brevetoxins: unique polyether dinoflagellate toxins. *FASEB J.*, **1989**, *7*, 1807-1817.
- ⁸¹ Rein, K.; Lynn, B.; Gawley, R.E.; Baden, D.G. Brevetoxin B: Chemical modifications, synaptosome binding, toxicity, and an unexpected conformational effect. *J. Org. Chem.*, **1994**, *59*, 2107-2113.
- ⁸² Lin, Y.Y.; Risk, M.; Ray, S.M.; Van Engen, D.; Clardy, J.; Golik, J.; James, J.C.; Nakanishi, K. Isolation and structure of brevetoxin B from the "red tide" dinoflagellate *Ptychodiscus brevis* (*Gymnodinium breve*). *J. Am. Chem. Soc.*, **1981**, *103*, 6773-6775.
- ⁸³ Schenck, H.A.; Lenkowski, P.W.; Choudhury-Mukherjee, I.; Ko, S.H.; Stables, J.P.; Patel, M.K.; Brown, M.L. Design, synthesis, and evaluation of novel hydroxyamides as orally available anticonvulsants. *Bioorg. Med. Chem.*, **2004**, *12*, 979-993.
- ⁸⁴ Korshunova, G.A.; Sumbatyan, N.V.; Topin, A.N.; Mtchedlidze, M.T. Photoactivatable reagents based on aryl(trifluoromethyl)diazirines: Synthesis and application for studying nucleic acid-protein interactions. *Mol. Biol.*, **2000**, *34*, 823-839.
- ⁸⁵ Teeter, H.M.; Bell, E.W. *Tert*-butyl hypochlorite. *Org. Synth.*, **1952**, *32*, 20.
- ⁸⁶ Burkard, N.; Bender, T.; Westmeier, J.; Nardmann, C.; Huss, M.; Wierczorek, H.; Grond, S.; Von Zezschwitz, P. New fluoros photoaffinity labels (F-PAL) and their application in V-ATPase inhibition studies. *Eur. J. Org. Chem.*, **2010**, *11*, 2176-2181.
- ⁸⁷ Al-Omari, M.; Banert, K.; Hagedorn, M. Bi-3*H*-diazirin-3-yls as precursors of highly strained cycloalkanes. *Angew. Chem., Int. Ed.*, **2006**, *45*, 309-311.

-
- ⁸⁸ Kumar, N.S.; Young, R.N. Design and synthesis of an all-in-one 3-(1,1-difluoroprop-2-ynyl)-3H-diazirin-3-yl functional group for photo-affinity labeling. *Bioorg. Med. Chem.*, **2009**, *17*, 5388-5395.
- ⁸⁹ Gross, H.; Rieche, A.; Matthey, G. Über α -halogenäther, XIII. Neue verfahren zur darstellung von phenolaldehyden. *Chem. Ber.*, **1963**, *96*, 308-319.
- ⁹⁰ Doyaguez, E. Boron Tribromide. *Synlett*, **2005**, *10*, 1636-1637.
- ⁹¹ Abraham, A.; Wang, Y.; El Said, K.R.; Plakas, S.M. Characterization of brevetoxin metabolism in *Karenia brevis* bloom-exposed clams (*Mercenaria* sp.) by LC-MS/MS. *Toxicon*, **2012**, *60*, 1030-1040.
- ⁹² Nair, P.D.; Podgorski, M.; Chatani, S.; Gong, T.; Xi, W.; Fenoli, C.R.; Bowman, C.N. The thiol-Michael addition click reaction: A powerful and widely used tool in materials chemistry. *Chem. Mater.*, **2014**, *26*, 724-744.
- ⁹³ Mather, B.D.; Viswanathan, K.; Miller, K.M.; Long, T.E. Michael addition reactions in macromolecular design for emerging technologies. *Prog. Polym. Sci.*, **2006**, *31*, 487-531.
- ⁹⁴ Hoogenboom Richard. Thiol-yne Chemistry: A powerful tool for creating highly functional materials. *Angew. Chem. Int. Ed.*, **2010**, *49*, 3415-3417.
- ⁹⁵ Lang, A.; Thelakkat, M. Modular synthesis of poly(perylene bisimides) using click chemistry: a comparative study. *Polym. Chem.*, **2011**, *2*, 2213-2221.
- ⁹⁶ Hein, C.; Liu, X.M.; Wang, D. Click chemistry, a powerful tool for pharmaceutical sciences. *Pharm. Res.*, **2008**, *25*, 2216-2230.
- ⁹⁷ Gisch, N.; Balzarini, J.; Meier, C. Enzymatically activated *cycloSal*-d4T-monophosphate: The third generation of *cycloSal*-pronucleotides. *J. Med. Chem.*, **2007**, *50*, 1658-1667.
- ⁹⁸ Xu, H.J.; Liang, Y.F.; Cai, Z.Y.; Qi, H.X.; Yang, C.Y.; Feng, Y.S. CuI-Nanoparticles catalyzed selective synthesis of phenols, anilines, and thiophenols from aryl halides in aqueous solution. *J. Org. Chem.*, **2011**, *76*, 2296-2300.

VITA

RYAN T. CASSELL

Born, Norfolk, Virginia

2006

B.S., Chemistry
Minor in Physics
Florida State University
Tallahassee, Florida

2011

Doctoral Candidate
Florida International University
Miami, Florida